



저작자표시-비영리-변경금지 2.0 대한민국

이용자는 아래의 조건을 따르는 경우에 한하여 자유롭게

- 이 저작물을 복제, 배포, 전송, 전시, 공연 및 방송할 수 있습니다.

다음과 같은 조건을 따라야 합니다:



저작자표시. 귀하는 원저작자를 표시하여야 합니다.



비영리. 귀하는 이 저작물을 영리 목적으로 이용할 수 없습니다.



변경금지. 귀하는 이 저작물을 개작, 변형 또는 가공할 수 없습니다.

- 귀하는, 이 저작물의 재이용이나 배포의 경우, 이 저작물에 적용된 이용허락조건을 명확하게 나타내어야 합니다.
- 저작권자로부터 별도의 허가를 받으면 이러한 조건들은 적용되지 않습니다.

저작권법에 따른 이용자의 권리는 위의 내용에 의하여 영향을 받지 않습니다.

이것은 [이용허락규약\(Legal Code\)](#)을 이해하기 쉽게 요약한 것입니다.

[Disclaimer](#)

A THESIS
FOR THE DEGREE OF MASTER OF SCIENCE

**INNATE IMMUNE RESPONSES AND HOST DEFENSE
MECHANISMS BY TWO THIOREDOXIN LIKE PROTEINS
IN BIG-BELLY SEAHORSE (*Hippocampus abdominalis*)**

AND

**TERMINAL COMPLEMENT COMPLEXES
IN REDLIP MULLET (*Liza haematocheila*)**

DILEEPA SRIPAL LIYANAGE

DEPARTMENT OF MARINE LIFE SCIENCES

GRADUATE SCHOOL

JEJU NATIONAL UNIVERSITY

February 2019

Innate immune responses and host defense mechanisms by two thioredoxin like proteins in big-belly seahorse (*Hippocampus abdominalis*)

and

terminal complement complexes in redlip mullet (*Liza haematocheila*)

Dileepa Sripal Liyanage
(Supervised by Professor Jehee Lee)

A thesis submitted in partial fulfillment of the requirement for the degree of

MASTER OF SCIENCE

February 2019

This thesis has been examined and approved by

.....

Thesis Director, **Qiang Wan (PhD)**, Research professor
Fish Vaccine Research Center, Jeju National University

.....

Thanthrige Thiunuwan Priyathilaka (PhD), Research professor
School of Marine Biomedical Sciences, Jeju National University

.....

Jehee Lee (PhD), Professor of Marine Life Sciences
School of Marine Biomedical Sciences, Jeju National University

2018.11.28

Date

Department of Marine Life Sciences

GRADUATE SCHOOL

JEJU NATIONAL UNIVERSITY

REPUBLIC OF KOREA

~ II ~

CONTENTS

Acknowledgement	III
SUMMARY	V
List of Figures	VII
List of Tables	VIII
CHAPTER 1	1
1. Introduction.....	2
2. Materials and Methods.....	5
2.1. Identification of big-belly seahorse thioredoxin-like sequences.....	5
2.2. In silico analysis of sequences	5
2.3. Tissue distribution and immune challenge/ Rearing of seahorses and tissue collection.....	7
2.4. cDNA library construction.....	8
2.5. Spatial and temporal transcriptional analysis.....	8
2.6. Recombinant plasmid construction.....	9
2.7. Protein expression and purification.....	10
2.8. Functional assays	11
2.8.1. DPPH radical-scavenging assay.....	11
2.8.2. Insulin disulfide reduction assay.....	11
2.8.3. Protective effect on the cultured cells under oxidative stress	12
3. Results.....	13
3.1. Molecular characterization.....	13
3.1.1. Homology and phylogenetic analysis	16
3.1.2. Protein structure	22
3.1.3. Analysis of mRNA expression.....	24
3.1.4. Expression and purification of rHaTXNL1 and rHaTXNDC17	28
3.2. Functional assays	29
3.2.1. DPPH assay.....	29
3.2.2. Insulin disulfide reduction assay.....	31
3.2.3. The protective effect on the cultured cells under oxidative stress	32
4. Discussion.....	33
CHAPTER 2	39
1. Introduction.....	40
2. Materials and Methods.....	42
2.1. Database construction and isolation of the MuC6, MuC7, MuC8 β , and MuC9 sequences.....	42
2.2. Sequence characterization.....	43

2.3. Fish rearing, immune challenge, and collection of tissues.....	44
2.4. RNA isolation and cDNA library construction.....	44
2.5. Tissue distribution and Immune challenge expression analysis of TCC genes	45
3. Results.....	46
3.1. Isolation and sequence analysis of full-length TCC genes from mullet cDNA.....	46
3.2. Alignment of TCC amino acid sequences and phylogenetic analysis	53
3.3. Spatial mRNA expression of TCC.....	55
3.4. Induced expression of TCC genes after infection with LPS, Poly I:C, and <i>L. garvieae</i>	57
4. Discussion.....	59
References.....	64

Acknowledgement

At the first of my thesis I would like to thank to all these people who helped and encouraged me to make this possible.

First, I would like to express my most sincere gratitude to my research supervisor Professor Jehee Lee, who gave me this opportunity to commence my post graduate studies at Marine Molecular Genetics Lab, Jeju National university and supported me throughout my thesis with his patience and knowledge while giving me the room to work my own way. I acknowledge him for the great effort he put into encourage and guide me in scientific field.

Beside my supervisor, I would like to thank my thesis director Dr. Qiang Wan and Dr. Thiunuwan Priyathilaka at Department of Marine Life Sciences, Jeju National University, for being my committee members.

Further, I am especially grateful to Dr. Gelshan Godahewa and Dr. Thiunuwan Priyathilaka, Dr. Seongdo Lee, Dr. Sukkyoung Lee, Mr. Nilojan Jehanathan, Mr. Neranjan Tharuka for their valuable guidance and ideas to improve my laboratory experiments and writings.

I would like to thank all the past and present lab members: Dr. Changnam Jin, Mr. Changyong Lim, Ms. Gabin Kim, Dr. Sang Phil Shin, Dr. Myoung-Jin Kim, Ms. Sumi Jung, Mr. Hyukjae Kwon, Ms. Heyrim Young, Ms. Gayashani Sandamalika, Ms. Jeongeun Kim, Mr. Hanchang Sohn, Mr. Thilina Kasthuriarachchi, Mr. Nimod Dilushan, Mr. Kalana Prabhath, Mr. Kasun Madusanka, Ms. Chaehyeon Lim, Ms. Anushka Samaraweera, Ms. Sarithaa Sellaththurai, Mr. Jaewon Kim, Mr. Sudeera Shanaka, Mr. Srinith Prabhatha for helping me in various ways to complete my laboratory works, studies in Marine Molecular Genetics Lab. I am thankful to my friends in other labs for supporting me to fulfill laboratory works and experiments.

I would like to thank to my wife Malithi Omeka for her love and constant support in lab experiments and always been with me.

My sincere thanks to all the funding authorities (Ministry of Oceans and Fisheries, Jeju National University, Korea) for providing research grants to accomplish the lab experiments.

SUMMARY

Thioredoxin is a highly conserved protein found in both prokaryotes and eukaryotes. Reactive oxygen species (ROS) are produced in response to metabolic processes, radiation, metal oxidation, and pathological infections. High levels of ROS lead to cell death via autophagy. However, thioredoxin acts as an active regulatory enzyme in response to excessive ROS. Here, we performed in-silico analysis, immune challenge experiments, and functional assays of seahorse thioredoxin-like protein 1 (HaTXNL1) and thioredoxin domain-containing protein 17 (HaTXNDC17). Evolutionary identification showed that HaTXNL1 and HaTXNDC17 proteins belongs to the thioredoxin superfamily comprising 289 and 123 amino acids respectively. HaTXNL1 possesses an N-terminal active thioredoxin domain and C-terminal proteasome-interacting thioredoxin domain (PITH) of TXNL1 which is a component of 26S proteasome and binds to the matrix or cell. HaTXNDC17 possesses only thioredoxin domain. Pairwise alignment results showed 99.0 % identity and similarity with *Hippocampus comes*. Similar to the other thioredoxins, conserved thiol-disulfide cysteine residue containing Cys-X-X-Cys motif can be found in TXNL1 and TXNDC17 sequences. HaTXNL1 comprised two N-linked glycosylation sites at 72NISA75 and 139NESD142 and HaTXNDC17 has no sites. According to the quantitative real-time polymerase chain reaction analysis from healthy seahorses, highest *HaTXNL1* mRNA expression was observed in muscle, followed by ovary, brain, gill, and blood tissues. The highest spatial mRNA expressions of *HaTXNDC17* were observed in the muscle, brain, and intestine. Moreover, significant temporal expression of HaTXNL1 and HaTXNDC17 was observed in blood, gill and kidney tissues after bacterial stimuli. The DPPH assay showed that the radical scavenging activity varies in a concentration-dependent manner. The insulin reduction assay demonstrated a significant logarithmic relationship with the concentration of rHaTXNL1 and rHaTXNDC17. Moreover, FHM cells treated with recombinant HaTXNDC17 significantly enhanced cellular viability under oxidative stress.

Together, these results show that HaTXNL1 and HaTXNDC17 function is important for maintaining cellular redox homeostasis and that it is also involved in the immune mechanism in seahorses.

The redlip mullet (*Liza haematocheila*) is one of the most economically important fish in Korea and other East Asian countries; it is susceptible to infections by pathogens such as *Lactococcus garvieae*, *Argulus spp.*, *Trichodina spp.*, and *Vibrio spp.* Learning about the mechanisms of the complement system of the innate immunity of redlip mullet is important for efforts towards eradicating pathogens. Here, we report a comprehensive study of the terminal complement complex (TCC) components that form the membrane attack complex (MAC) through in-silico characterization and comparative spatial and temporal expression profiling. Five conserved domains (TSP1, LDLa, MACPF, CCP, and FIMAC) were detected in the TCC components, but the CCP and FIMAC domains were absent in MuC8 β and MuC9. Expression analysis of four TCC genes from healthy redlip mullets showed the highest expression levels in the liver, whereas limited expression was observed in other tissues; immune-induced expression in the head kidney and spleen revealed significant responses against *Lactococcus garvieae* and poly I:C injection, suggesting their involvement in MAC formation in response to harmful pathogenic infections. Furthermore, the response to poly I:C may suggest the role of TCC components in the breakdown of the membrane of enveloped viruses. These findings may help to elucidate the mechanisms behind the complement system of the teleosts innate immunity.

List of Figures

Figure 1: Sequence analysis figure of HaTXNL1 and HaTXNDC17 from big-belly seahorse and domain arrangement.....	16
Figure 2: Multiple sequence alignment of HaTXNL1 and HaTXNDC17 with different ortholog amino acid sequences.....	20
Figure 3: The phylogenetic tree of HaTXNL1 and HaTXNDC17 with other orthologs.	21
Figure 4: Predicted tertiary structure of HaTXNL1 and HaTXNDC17.....	23
Figure 5: Relative mRNA expression (fold change) of HaTXNL1 and HaTXNDC17.....	25
Figure 6: Temporal expression of HaTXNL1 and HaTXNDC17.....	27
Figure 7: SDS-PAGE analysis of purified HaTXNL1 and HaTXNDC17.....	29
Figure 8: (A) DPPH radical- scavenging activity of rHaTXNL1 at different concentrations.	30
Figure 9: Insulin disulfide reduction activity assay for HaTXNL1 and HaTXNDC17.	32
Figure 10: Effects of rHaTXNDC17 on the viability of fathead minnow epithelial cells	33
Figure 11: Structural representation of the redlip mullet terminal complement components (C6-C9): C6 (MuC6), C7 (MuC7), C8 β (MuC8 β), and C9 (MuC9).....	48
Figure 12: Nucleotide and deduced amino acid sequence of MuC6 (A), MuC7 (B), MuC8 β (C), and MuC9 (D) from redlip mullet.....	52
Figure 13: Phylogenetic tree of Mullet TCC genes.	54
Figure 14: Multiple-sequence alignment of MuC6 (A.); MuC7 (B.); MuC8 β (C.); and MuC9 (D.); and its orthologs from selected organisms.	55
Figure 15: MuC6 (A), MuC7 (B), MuC8 β (C), and MuC9 (D) tissue-specific transcript expression analysis of healthy mullets under normal physiological conditions.	56
Figure 16: Temporal expression profiles of MuC6, MuC7, MuC8 β , and MuC9.	58

List of Tables

Table 1: Primers used in the study	10
Table 2: Pairwise identity and similarity percentages of HaTXNL1 and HaTXNDC17 with its ortholog amino acids.....	18
Table 3: cDNA fragment information, gene length in amino acids, molecular mass, theoretical isoelectric point and domain positions of the redlip mullet C6, C7, C8 β and C9.....	47
Table 4: Percent identity and similarity of C6, C7, C8 β and C9 orthologs from different species compared to MuC6, MuC7, MuC8 β and MuC9	53

CHAPTER 1

**Identification of two thioredoxin like proteins from big-belly seahorse
Hippocampus abdominalis: Molecular insights, immune responses, and
functional characterization**

1. Introduction

Thioredoxins are intracellular proteins ubiquitously found in all the kingdoms of living organisms. The thioredoxin family comprises thioltransferases, including thioredoxins (Txn) and glutaredoxins (Grx) (Aslund et al., 1994; Miranda-Vizueté et al., 1997). The thioredoxin domain possesses a universally conserved redox-active thiol-disulfide CXXC motif with two cysteines called the thioredoxin motif. The thiol active CXXC motif of the thioredoxin domain is also found in the protein disulfide isomerase (PDI) and PDI-D subfamily (Kozlov et al., 2010). Further, the thioredoxin domain can be found in *Escherichia coli* disulfide-bond oxidoreductases (DsbA, DsbC, DsbD, DsbE, and DsbG), which promote the disulfide bond formation in periplasmic proteins (Ren et al., 2009).

Thioredoxin domain-containing proteins and thioredoxin-related proteins are ubiquitously expressed in all the cell organelles. For example, thioredoxin reductase 2 (Txnrd2), Txn, glutaredoxin 2 (Grx2), and peroxiredoxin 3 (Prx3) can be found in the mitochondria, while PDI proteins, calcium binding protein 1 (CaBP1), ERp72, thioredoxin-related transmembrane protein (Tmx), an ER-resident protein disulfide reductase/J-domain-containing PDI-like protein (ERdj5/JPDI) are present in the endoplasmic reticulum [5]. Further, nucleoredoxin and Grx2 are expressed in the nucleus. The cytosol contains a large number of thioredoxin-related proteins including Txnrd1, thioredoxin-related protein 32 (Trp32), thioredoxin-like protein 2 (Txnl2), Grx1, Prx1, Prx2, Prx4, Prx5, and Prx6. Apart from that, plasma cell thioredoxin-related protein (PC-Trp), Txnrd3, Txn1, Txn2, and Txn3 show tissue-specific expression (Nakamura, 2005).

Thioredoxins play multiple functions at the cellular level. They act as reductases and regulate the redox homeostasis, thereby protecting proteins and cellular organelles from oxidative aggregation and inactivation (Gleason and Holmgren, 1988; Holmgren, 1995, 1985; Holmgren and Bjornstedt, 1995). Further, thioredoxins protect the cells from various

environmental stresses such as reactive oxygen species (ROS), arsenate, and peroxyntirite (Landino et al., 2004; Messens and Silver, 2006). Moreover, some thioredoxins promote protein folding (Kern et al., 2003), modulate inflammatory response (Nakamura et al., 2005), and prevent apoptosis (Ravi et al., 2005).

Reactive oxygen species (ROS) may be generated by the different types of biological stimuli, including bacteria, virus, and parasites as well as physical stimuli such as UV rays, environmental temperature, metal ions (Wang et al., 2011), and already formed ROS. ROS are produced as a byproduct of the cellular metabolic processes and may mediate the oxidative modification of macromolecules in the cells, inhibit protein function, and promote cell death (Circu and Aw, 2010). Proteins may be oxidized and malfunctioned, owing to their direct reaction to the ROS or secondary reaction with byproducts produced during the stress conditions (Berlett and Stadtman, 1997). Hence, regulation of oxidative and reductive stress is necessary to protect the cells from ROS. Eukaryotes and prokaryotes have integrated antioxidant systems, which include enzymatic and non-enzymatic antioxidants that are usually effective in blocking the harmful effects of ROS (Birben et al., 2012). In addition, several proteins such as thioredoxin, thioredoxin-like proteins, catalase, superoxide dismutase, peroxiredoxin, glutathione peroxidase, glutathione transferase, and glutaredoxin act as antioxidants (Birben et al., 2012).

Big-belly seahorse (*Hippocampus abdominalis*) is one of the important seahorse species used in oriental medicine as a remedy for treating diseases such as erectile dysfunction, as well as for suppressing neuroinflammatory responses and collagen release (Chang et al., 2013; Vincent et al., 2011). Moreover, it exhibits antitumor and anti-aging properties (Chang et al., 2013). Further, it is used as an ornamental fish species and as food (Chang et al., 2013). However, seahorses are highly susceptible to pathogenic attacks leading to fatal diseases (Balcázar et al., 2010; Vincent and Clifton-Hadley, 1989), and hence

they have been included in the conservation list (“*Hippocampus* spp (Seahorses) | CITES,” n.d.). The big-belly seahorse (*Hippocampus abdominalis*) is one of the largest seahorse species in the world and used as a remedy for several diseases in traditional Chinese medicine. Seahorses also exhibit an antitumor, antiaging, and anti-fatigue properties and suppress neuroinflammatory responses as well as collagen release; seahorses are also used to treat the erectile dysfunction (Chang et al., 2013; Vincent et al., 2011). In addition, seahorses are used as ornamental fish species and consumed by different ethnic groups as a food (Chang et al., 2013). Though seahorses are popular marine aquaculture species worldwide, they are highly vulnerable to pathogenic attacks, leading to fatal diseases (Balcázar et al., 2010; Vincent and Clifton-Hadley, 1989). Because of their high extinction rate, this species has been listed under the Convention on International Trade in Endangered Species of Wild Fauna and Flora (CITES) and its import and export has been controlled. Therefore, it is essential to explore the redox balance mechanisms existing in seahorses to gain an insight into the host antioxidant system at the molecular level.

E. tarda is considered as a severe fish pathogen in aquaculture which can cause edwardsiellosis to cultured and wild fishes. It can produce virulence factors leading to the higher survival of bacteria in the host (Park et al., 2012). Further *S. iniae* is a severe fish pathogen, can cause streptococcal disease that influences the mortality in fish (Weinstein et al., 1997). Therefore, exploring the immune mechanisms prevalent in seahorses related to these pathogens provides insight into host immune system at the molecular level (Jo et al., 2017; Priyathilaka et al., 2017).

In this study, TXNL1 and TXNDC17 cDNA sequences were mined from big-belly seahorse transcriptomic database and characterized to gain a better understanding of thioredoxin mechanisms in teleost fishes. The cDNA and protein sequences of *Hippocampus abdominalis* TXNL1 (HaTXNL1) and TXNDC17 (HaTXNDC17) were characterized using

various bioinformatics tools. The recombinant proteins were produced to endorse its functional aspects using 2,2-diphenylpicrylhydrazyl (DPPH), insulin disulfide reduction, and cell survival assay. Finally, the spatial distribution of the *HaTXNLI*, *HaTXNDC17*, and temporal transcriptional modulations were investigated against bacterial endotoxin lipopolysaccharides (LPS), viral mimic polyinosinic-polycytidylic acid (poly I:C), gram-negative bacteria (*Edwardsiella tarda*) and gram-positive bacteria (*Streptococcus iniae*) as stressors.

2. Materials and Methods

2.1. Identification of big-belly seahorse thioredoxin-like sequences

The cDNA sequences of *HaTXNLI* (Accession number: MG571449) and *HaTXNDC17* (Accession number: MH455283) were identified from the seahorse transcriptomic database established at Marine Molecular Genetics Lab, Jeju National University. The database was established using the Blast2Go sequence annotation software and 454 GS FLX™ sequencing data. The total RNA was isolated from liver, kidney, gill, spleen and blood tissues using 18 seahorses. Extracted RNA was purified using RNeasy Mini kit (Qiagen, USA) and sent for sequencing (Insilicogen, Korea). The method was described as previously mentioned in our previous study (Oh et al., 2016). The collected sequence was cross-checked and confirmed with the NCBI Blast tool with NCBI nucleotide and non-redundant protein databases (Agarwala et al., 2016).

2.2. In silico analysis of sequences

The derived *HaTXNLI* and *HaTXNDC17* cDNA sequences were analyzed using several bioinformatics tools. Initially, the cDNA sequences of *HaTXNLI* and *HaTXNDC17* gene was assessed for the open reading frame (ORF) using the Unipro UGENE bioinformatics software v1.26.1, and the corresponding amino acid sequence was derived according to the best ORF

matches. Further, NCBI conserved domain database (NCBI CDD) (<https://www.ncbi.nlm.nih.gov/Structure/cdd/wrpsb.cgi>), ExPASy Prosite (<http://prosite.expasy.org/>), and EMBL-EBI Pfam domain database (<http://pfam.xfam.org/>) were used to determine the characteristic domain structure, active site motif, and the signature motifs in the amino acid sequence. Moreover, molecular properties were figured out by using ExPASy Protparam (<http://web.expasy.org/protparam/>). Signal peptide and its cleavage site were checked by using SignalP 4.1 online tool (<http://www.cbs.dtu.dk/services/SignalP/>). All known characteristic motifs of the sequence of TXNDC17 were analyzed by using the Motif Scan software (http://myhits.isb-sib.ch/cgi-bin/motif_scan). Potential *N*-linked glycosylation sites were checked by using the NetNGlyc 1.0 server (<http://www.cbs.dtu.dk/services/NetNGlyc/>). SWISS model ExPASy protein modeling workbench (<https://swissmodel.expasy.org/>) was used to draw the predicted tertiary structure of thioredoxin domain and other amino acid residues in the HaTXNDC17. The 3D structure of the proteins was created by using PyMOL v1.3 software. Characteristic motifs and domain structure were illustrated by using IBS 1.0.3 software.

The thioredoxin orthologs were determined from the NCBI public database and compared against each individual sequence using EMBOSS needle software (http://www.ebi.ac.uk/Tools/psa/emboss_needle/) to find their sequence identities and similarities. Online Clustal Omega multiple sequence alignment tool (<http://www.ebi.ac.uk/Tools/msa/clustalo/>) was used to align the species-specific amino acid sequences. Evolutionary relationship and phylogenetic analysis were carried out by using the MEGA7 tool with a neighbor-joining method with 5000 bootstraps (Kumar et al., 2016).

2.3. Tissue distribution and immune challenge/ Rearing of seahorses and tissue collection

Big-belly seahorses were obtained from the Korea Marine Ornamental Fish Breeding Center (Jeju Island, Republic of Korea) and maintained in 300 L tanks at constant temperature 18 ± 2 °C and 34 ± 0.6 ‰ practical salinity units (psu) for 1 week in laboratory conditions. Six healthy seahorses (3 males and 3 females) with an average body weight of 8 g were dissected and fourteen different tissues (ovary, spleen, intestine, gill, liver, testis, skin, muscle, heart, stomach, trunk kidney, pouch, brain and blood) were carefully removed for the tissue distribution analysis. Blood was collected from the tail cutting, and peripheral blood cells were extracted by centrifugation at $3,000 \times g$ for 10 min at 4 °C. All the samples were stored at -80 °C after immediate freezing by liquid nitrogen.

For the temporal expression analysis experiment, juvenile big belly seahorses with an average body weight of 3 g were divided into five groups including 30 individuals per tank and they were acclimatized as mentioned in the previous paragraph. Seahorses were intraperitoneally injected with 100 μ L of LPS (1.25 μ g/ μ L), poly I:C (1.5 μ g/ μ L), *E. tarda*: KCTC12267 (5×10^3 CFU/ μ L), and *S. iniae*: KCTC3657 (10^5 CFU/ μ L) dissolved in phosphate buffered saline (PBS – pH 7.4). Brain heart infusion (BHI) growth media with 1.5% salt was used to grow the bacteria at 37 °C until reaching the OD₆₀₀ 0.5. Then harvest the bacteria by centrifugation at 3500 rpm for 20 mins and resuspended in PBS buffer. The control group was injected with 100 μ L of PBS. Following the immune stimulation, blood and trunk kidney tissues from five seahorses were isolated at 3 h, 6 h, 12 h, 24 h, 48 h, and 72 h post injection (p.i.). Additionally, five seahorses were dissected at 0 h p.i and collected the tissues as a control. During the experiment period, seahorses were not fed.

2.4. cDNA library construction

Total RNA was extracted from isolated tissues using RNAiso plus reagent (TaKaRa, Japan) and clean-up with RNeasy spin column (Qiagen, USA) according to the protocol supplied by the manufacturer. The purity and the concentration of the extracted RNA were measured by the spectrophotometer and subsequently visualized on a 1.5% agarose gel. The cDNA was synthesized from 2.5 µg of RNA by using PrimeScript™ II 1st Strand cDNA Synthesis Kit (TaKaRa, Japan). Finally, constructed cDNA libraries were diluted to 40-fold and stored at -80 °C for longer use.

2.5. Spatial and temporal transcriptional analysis

The mRNA expression of *HaTXNLI* and *HaTXNDC17* genes was measured with quantitative real-time PCR (qPCR) by using the TaKaRa Thermal Cycler Dice Real Time System III. The seahorse *40S ribosomal protein S7* gene (Accession number KP780177) was used as a reference gene in the quantitative real-time polymerase chain reaction (qPCR) experiment which did not observe any significant expressional variation within each tissue under same qPCR profile. The reaction was performed in a 10-µL reaction mixture composed of 50 ng of template cDNA, TaKaRa Ex Taq™ SYBR premix 5 µL with 4 pmol of each primer (Table 1) using a thermal cycler profile of initial denaturation at 95 °C for 10 s and 45 cycles of 95 °C for 5 s, 58 °C for 10 s, and 72 °C for 20 s. The final cycle was set to dissociation analysis using the following cycle: 95 °C for 15 s, 60 °C for 30 s and 95 °C for 15 s.

The Livak ($2^{-\Delta\Delta CT}$) method (Livak and Schmittgen, 2001) was used to calculate the relative mRNA expression in the qPCR experiment. All the experiments were conducted in triplicate. Spatial expression folds of *HaTXNLI* and *HaTXNDC17* transcripts in different tissues were calculated as a fold values relative to the mRNA expression levels of seahorse 40S ribosomal protein *S7* gene. Statistical analysis was performed by ANOVA with posthoc

pairwise comparisons. The tissue showing the lowest mRNA expression was used for the basal level. In the temporal expression analysis, the mRNA expression levels of blood, gill and trunk kidney tissues were represented as fold changes relative to the PBS control. All the data were calculated with standard deviation (SD, n=3) and a value of $P < 0.05$ was considered as statistically significant.

2.6. Recombinant plasmid construction

cDNA encoding mature information of the HaTXNL1 and HaTXNDC17 was amplified using a 50- μ L reaction mixture having 5 units of ExTaq polymerase, 5 μ L of 10 \times ExTaq buffer, 4 μ L of 2.5 mM dNTPs, 0.4 μ L of 10 pmol/ μ L of each primer (Table 1), and 50 ng of template cDNA. The reaction steps consisted of initial denaturation at 94 °C for 3 min, followed by 35 cycles of 94 °C for 30 s, 55 °C for 30 s, 72 °C for 45 s, and a final extension at 72 °C for 10 min. Then PCR product was purified using the AccuPrep® PCR purification Kit (Bioneer Co., Korea). The PCR amplified HaTXNL1 and HaTXNDC17 genes, and the pMAL c5x (BioLabs Inc., USA) cloning vector was subjected to double restriction digestion with *EcoRI*, *EcoRV* and *NdeI*, *EcoRV* respectively. Then, 200 ng of digested PMAL c5x vector and 50 ng of digested insert fragments were ligated by using 5 μ L of Ligation Mighty Mix, (TaKaRa, Japan) followed by a 30-min incubation at 16 °C in a thermal cycler and overnight incubation at 4 °C. The ligated product was transformed into *E. coli* DH5 α competent cells by using the heat-shock method. Recombinant cells carrying the HaTXNL1 and HaTXNDC17 plasmids were isolated using the AccuPrep Plasmid Mini Extraction Kit (Bioneer Co., Korea) from the grown cell cultures and the sequence was confirmed by using capillary sequencing (Macrogen, Korea).

Table 1: Primers used in the study

Primer Sequence 5'-3'	Description	Amplicon size (bp)	Tm (°C)	Accession No
GAGAGAgatatacATGGTCGGTGTAAAGTGATCGGGAG	TXNL1 Cloning F, <i>EcoRV</i>	870 bp	60.3	MG571449
GAGAGAgattcTCAGTGACTCTCTCTTTCTTTCCAACAAC	TXNL1 Cloning R, <i>EcoRI</i>	870 bp	60	MG571449
ACTCTGGAAGTGGCAGAGGAAGAC	TXNL1 qPCR F	187 bp	60	MG571449
TGAAGTCATTCATGTTGGTGGCCTGTA	TXNL1 qPCR R	187 bp	60	MG571449
GAGAGAcataatgATGGCCAGTACGAACAAGTG	TXNDC17 Cloning F, <i>NdeI</i>	372 bp	57.5	MH455283
GAGAGAgatatacTCAATCTTCAGTGAACATCATCCTCAC	TXNDC17 Cloning R, <i>EcoRV</i>	372 bp	56.7	MH455283
CCAGGGCTCGGTCTTCATCTACT	TXNDC17 qPCR F	149 bp	60	MH455283
AGCATTCTCTCCACCAGTTTCT	TXNDC17 qPCR R	149 bp	60	MH455283
GCGGGAAGCATGTGGTCTTCATT	40S ribosomal protein S7, qPCR F	95 bp	60	KP780177
ACTCCTGGGTCGCTTCTGCTTATT	40S ribosomal protein S7, qPCR R	95 bp	60	KP780177

2.7. Protein expression and purification

The recombinant plasmids with confirmed sequence were transformed into *E. coli* ER2523 cells (Novagen, Germany). Then, the transformed cells were grown in Luria-Bertani rich medium (LB + 0.2% glucose) medium supplemented with 100 µg/mL ampicillin. Following incubation at 37 °C and 200 rpm, cell cultures were grown until the absorbance (OD₆₀₀) reached 0.5. Protein production was induced by adding 1 mM isopropyl β-D-1-thiogalactopyranoside (IPTG). The cell culture was further incubated at 25 °C and 200 rpm for 8 h.

Cells were pelleted by centrifugation at 3,000 × g for 30 min at 4 °C, and the pellet was resuspended in 25 mL of column buffer containing 20 mM Tris-HCl, 200 mM sodium chloride (NaCl), and 1 mM ethylenediaminetetraacetic acid (EDTA), pH 7.4. The recombinant proteins (rHaTXNL1 and rHaTXNDC17) was purified as a fusion protein of maltose binding protein (MBP) by PMAL protein fusion and purification system (NEB, USA) according to the manufacturer instructions. Bradford's method (Qi et al., 2017) was used to measure the

concentrations of the purified recombinant proteins, and 12% sodium dodecyl sulfate polyacrylamide gel electrophoresis (SDS-PAGE) was performed to visualize the protein banding patterns at different stages of purification. Eluted proteins were stored at -80 °C for future use.

2.8. Functional assays

2.8.1. DPPH radical-scavenging assay

The 2,2-diphenyl-1-picrylhydrazyl (DPPH) radical scavenging assay (Bajpai et al., 2014) was performed in a 96-well plate to determine the radical scavenging ability of rHaTXNL1 and rHaTXNDC17. First, 0.4 mM DPPH solution was prepared with dimethylsulfoxide (DMSO). Then, 100 μ L of the protein sample at different concentrations (HaTXNDC17 15, 30, 45, 60, and 90 μ g/mL) and (HaTXNL1 45, 60, 90, and 120 μ g/mL) along with 100 μ L of DPPH solution were added into the wells. Ascorbic acid was used as positive control at the above concentrations separately. The absorbance of the mixture was recorded at 517 nm after 30-min incubation at room temperature. Radical scavenging activity (RSA) percentage was calculated for each treatment according to the following equation: $[(\text{Optical density of control} - \text{Optical density of a sample}) / \text{Optical density of control}] \times 100$. The IC₅₀ value of HaTXNL1 and HaTXNDC17 for DPPH was measured as described previously (Sebaugh, 2011).

2.8.2. Insulin disulfide reduction assay

Insulin disulfide reduction assay was performed in a 96-well plate to determine the antioxidant activity of rHaTXNL1 and rHaTXNDC17 (Cintra et al., 2017). Total reaction mixture (200 μ L) was prepared by adding 10 μ L of 2 mM insulin from bovine pancreas, 10 μ L of 0.5 M ethylenediaminetetraacetic acid (EDTA) (pH 8.0), and 175 μ L of recombinant protein

in phosphate buffered saline (PBS) (at 0, 25, 50, 100, and 200 $\mu\text{g/mL}$), and the reaction was initiated by adding 5 μL of 0.1 M dithiothreitol (DTT). Samples were incubated at 25 $^{\circ}\text{C}$ for 120 min, and the absorbance at 650 nm was recorded at 5-min intervals. A negative control was prepared using DTT, without the recombinant protein. In addition, a blank was prepared by adding all the components without DTT. All the samples were prepared in triplicate. The statistical analysis was performed using IBM SPSS statistics 24 software (IBM, USA) and independent student t-test was used to compare the treatments. Standard deviation (SD) was calculated, and significant differences were defined at $P < 0.05$. The IC_{50} value of HaTXNL1 and HaTXNDC17 for insulin reduction assay was measured (Sebaugh, 2011). The specific activity was calculated by using the equation ($\Delta A_{650} \text{ nm} \times \text{min}^{-1} \times \mu\text{M}^{-1} \text{ protein}$) described previously (Holmgren, 1979).

2.8.3. Protective effect on the cultured cells under oxidative stress

Cell viability assay was conducted to investigate the cellular protective ability of rHaTXNDC17 protein. Previous studies had suggested that thioredoxins induce cell survival under oxidative stress (Hirota et al., 2002). Fathead minnow (FHM) epithelial cells were cultured according to a recommended method using Leibovitz's L-15 medium (ThermoFisher Scientific, USA) with 10 % fetal bovine serum (FBS) and 1 % penicillin and streptomycin. Initially, FHM cells were seeded at a concentration of $2 \times 10^5/\text{mL}$ in a 96-well plate. Seeded FHM cells were incubated at 25 $^{\circ}\text{C}$ for 24 h. The cells were pre-treated with different concentrations of rHaTXNDC17 (0, 25, 50, 75, and 100 $\mu\text{g/mL}$) and 1 mM dithiothreitol (DTT) and incubated for 30 min. H_2O_2 (100 μM) was added to the cell culture medium to induce oxidative stress followed by 24-h incubation. Control samples were prepared without adding 100 μM H_2O_2 to cells. Cellular viability was checked by using the standard 3-(4, 5-dimethylthiazol-2-yl)-2, 5-diphenyltetrazolium bromide (MTT) assay. After 24-h incubation,

50 μ L of 2 mg/mL MTT solution was added to each well (containing 200- μ L reaction mixture) and samples were incubated for 3 h. The supernatants were aspirated, and formazan crystals were dissolved by adding 150 μ L of DMSO into each well. Finally, the absorbance of the reaction mixtures were measured at 540 nm using the SYNERGY/HT™ microplate reader (Biotek, Korea). Microscopic observations of each treatment were recorded by using Leica DFC425C digital microscope. The extent of conversion of MTT into insoluble formazan was used to calculate the relative percentage of cell viability. The absorbance of control cells was considered as 100 % cell viability. Statistical analysis was performed by ANOVA with posthoc pairwise comparisons. All the samples were treated in triplicate (n=3) and mean percentages \pm SD were plotted compared to the control cells.

3. Results

Thioredoxin plays a major role in the maintenance of cellular homeostatic and redox balance, and it is involved in various biological processes of prokaryotes and eukaryotes (Glickman and Ciechanover, 2002; Li et al., 2017; Sarin and Sharma, 2006; Zhang et al., 2018). Degradation of malfunctioned oxidized proteins is one of the regulatory mechanisms to reduce oxidative stress within cells. In this study, TXNL1 and TXNDC17 proteins from seahorse *Hippocampus abdominalis* were characterized and thought to be involved in the maintenance of the redox balance.

3.1. Molecular characterization

The cDNA sequence of *HaTXNL1* and *HaTXNDC17* was identified from the seahorse transcriptome database, and the sequence was deposited in the NCBI GenBank. The ORF of *HaTXNL1* is 867 bp in length and encodes for 289 amino acids, and The ORF of *HaTXNDC17* was 369-bp long and comprised of 123 amino acids (aa). *In silico* analysis revealed that the

estimated molecular mass and predicted isoelectric point (*pI*) was HaTXNL1 is 32.2 kDa and 4.76 14.1 kDa and 5.04, respectively. HaTXNL1 and HaTXNDC17 did not possess signal peptide, and HaTXNL1 sequence displayed N-linked glycosylation sites at ⁷²NISA⁷⁵ and ¹³⁹NESD¹⁴², which are essential for the structure (Imperiali and O'Connor, 1999) and function (J., 2012). According to the Conserved Domain Database (NCBI) search results, TXN, and PITH domains are identified at 20–104 and 126–267 amino acid residues in HaTXNL1, respectively. A universally conserved CXXC motif, which is involved with the reversible oxidation of oxidized proteins, is observed in HaTXNL1. The residues X in CXXC motif may play different roles in different classes of the animal kingdom (Quan et al., 2007). For instance, fish species comprises CRPC, while mammals and amphibians display CGPC and CPPC, respectively (Figure 1). The presence of the CXXC motif is essential for the thiol-disulfide reduction in thioredoxin. PITH domain is a general 26S proteasome-interacting module (Andersen et al., 2009) and has no catalytic function.

The cDNA sequence of HaTXNDC17 was identified from the seahorse transcriptome database, and the sequence was deposited in the NCBI GenBank under the accession no: MH455283. The ORF of HaTXNDC17 was 369-bp long and comprised of 123 amino acids (aa). In silico analysis revealed that the estimated molecular mass and predicted isoelectric point (*pI*) was 14.1 kDa and 5.04, respectively. HaTXNDC17 did not possess signal peptide and N-linked glycosylation sites. According to the Conserved Domain Database (NCBI) search results, HaTXNDC17 contained thioredoxin domain between 4 and 121 aa residues and conserved redox-active motif (Cys-X-X-Cys) between 43 and 46 aa (Figure 1).

GAGCGCCTCACGAATAGACA -180

GCCGATTTGAGCTTACTTTTGACGCTAAGCTCAAACACACAACAAAATACTTTACAGTAA -120

TTAAGTGTAAATGTGTATCCAGGAATAATTATAACAAGGCCACGTCTCTCATTCTACC -60

ATGGTCGGTGTAAAGTGTATCGGGAGCGATCCGGAATTTCTACCGGAGCTAGCGGCCGC 60

M V G V K V I G S D P E F L P E L A A A

GGCTCGAGGCTCACGGTGGTAAAGTTCACAATGGCCGGGTGCCGGCCGTGTGTCAGAATA 120

G S R L T V V K F T M A G C R P C V R I

GCTCCAGCGTTCAACATGTTGAGTAATAAGTATCCACAGGTTGTCTTCCTTGAAGTTGAT 180

A P A F N M L S N K Y P Q V V F L E V D

GTCCATGTCTGTCCGACGACAAAGGAAGCCAACACATATCAGCCACACCACGTTCTTA 240

V H V C P T T K E A N N I S A T P T F L

TTCTTCAGGAACCGGGATCGGGTGGACCATCAAGGAGCAGATGCTGCGGGTCTGGAG 300

F F R N R D R V D Q Y Q G A D A A G L E

GACAAAATCAAACAGCTCACAGAGAATGATCCAGGAAACAGTGAGGACTCTGACATTCCA 360

D K I K Q L T E N D P G N S E D S D I P

AAGGATATATGGACCTCATGCCTTTTGTCAACAAAGCCGGCTGCGAGTGCCTCAACGAG 420

K G Y M D L M P F V N K A G C E C L N E

AGTGATGACTGTGGCTTTGACAACTGCTTACTGAAAGATTCTTCCTATCTGGAGTCAGAC 480

S D D C G F D N C L L K D S S Y L E S D

TGTGATGAACAGCTACTGATAACCATCGCCTTCAACCAGCCTGTGAAGCTTTTCCATG 540

C D E Q L L I T I A F N Q P V K L F S M

AAGCTACAGTCCCTCAGACTTTGCCAGGCTCCTAAAGTGGTAAAGATATTTATCAATCTC 600

K L Q S S D F A Q A P K V V K I F I N L

CCGCGCTCTATGGGTTTCGACGACGCCGAGCGAAACGAAGCCACCCAACTCTGGAAGT 660

P R S M G F D D A E R N E A T Q T L E L

GCAGAGGAAGACTACAAAGATGATGGAATCATTCCACTGCGCTATGTCAAGTTTCAGAAT 720

A E E D Y K D D G I I P L R Y V K F Q N

GTGCAGAGTGAACGTTGTTCATCAAATCAAACCATGGAGATGAGGAGACAAACAAAATA 780

V Q S V T L F I K S N H G D E E T T K I

AACTACCTGACCTTCATGGTAATCCTGTACAGGCCACCAACATGAATGACTTCAAAGG 840

N Y L T F I G N P V Q A T N M N D F K R

GTTGTTGGAAGAAAGGAGAGAGTCACTGA 870

V V G K K G E S H *

GTCAGGACAAATGGAGGGAAAGAGGAGACGACTGATATTTTGAAGGACTTTTCCCTTTGC 930

CAAAGCTGCCACACTTTAAGCAGACATTGTgACGCACCACaCACGTATACACACGTCAC 990

ACTGCTCAACTTCTGATTTCAAGAATTATCAGTGTCTGGGGACTCTCAGTCTATAAACAT 1050

TTGTATTGTAAGTCAAATTAATA 1073

TTGAAAACGATAATGACGTGTGTACAAACA -210

ACAACAAGAACATAACAATTAGATACGCATCTCTACTCCGGAAGTGCTCGTATGGCTTTT -180

TTGCAACTTGACATAAAGTGTTCCTGTCTTGGGAAATGCTATGTGAGCAGACAGCACAAA -120

CTGCAGGCTCCAGTTCTATCTTAATCATCTCCAAGCTACTGTTTCGCCGAACCGAACC -60

ATGGCCAGTACGAACAAGTGAACGTGCGTGGCTATAGTGAATTCTGCAAGGCTGTGGCA 60

M A Q Y E Q V N V R G Y S E F C K A V A

GACAGACCGGGCAAAGATATTTTGTCTACTTCTCTGGCGACAAAGACGAGAAAGGCAAT 120

D R P G K D I F A Y F S G D K D E K G N

AGCTGGTGTCCAGACTGTGTCAGAGCTGAGCCGATATAAAGGGAGCAATGAGCTCACCT 180

S W C P D C V R A E P I I K G A M S S L

CCCCAGGGCTCGGTCTTCATCTACTGTCAAGTTGGTGAAGGAACTATTGGAAGGATTCA 240

P Q G S V F I Y C Q V G E R N Y W K D S

AGCAATGAGTCAAGACAACACTCAAGCTGACTGGGGTCCCCACCCTCTGCGATACAAC 300

S N E F K T T L K L T G V P T L L R Y N

ACCCCTCAGAAACTGGTGGAGGAGGAAATGCTTCAAAGAGGATCTAGTGAGGATGATGTT 360

T P Q K L V E E E C F K E D L V R M M F

ACTGAAGATTGA 372

T E D *

GAGACATGTGCCTTCAGCCACTGTGGTGGATCAAGAAACACAATAAAACACTTCTTAA 432

TCACACTCAATATAGTGACAATGTGATGCTTTTATAATTATCCGTGTAAATGTCTTGT 492

CGTAGCATTTCATAAAGTCATGCCTGATCATGCAGATAATTGGGTCACTTCTTAAATTA 552

AAATTACAATTAAGA 568

A

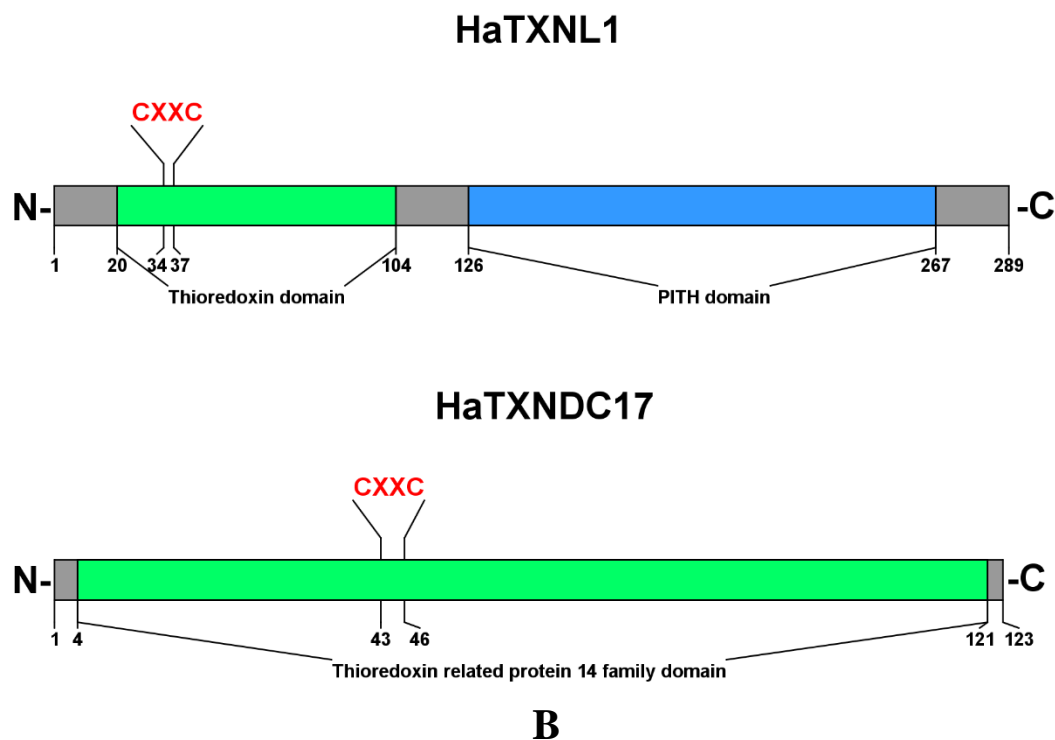


Figure 1: Sequence analysis figure of HaTXNL1 and HaTXNDC17 from big-belly seahorse and domain arrangement.

(A) Nucleotide and deduced amino acid sequences of HaTXNL1 and HaTXNDC17 from big-belly seahorse. Start and stop codons denoted by underlined bold black letters and conserved thioredoxin-related protein 14 family domain shaded in ash color. CPDC active site motif represented in blue color underlined letters. Stop signal of the protein denoted by an asterisk mark. (B) Structural representation of the big belly seahorse TXNL1 and TXNDC17. The CXXC motif is represented by red-colored letters and domains are shaded in light green and light blue. Maps and boundaries are based on the NCBI Conserved Domain Database (CDD). Numbers correspond to the first/last residues in each module.

3.1.1. Homology and phylogenetic analysis

The pairwise alignment of HaTXNL1 and TXNL1 from the members of the animal kingdom showed 99.0 % identity, and similarity with *Hippocampus comes* (Table 2). Multiple sequence alignment (MSA) shows that the evolutionary conserved CXXC motif was similar among all species. Furthermore, the amino acid residues at N-linked glycosylation, folding, and catalytic sites were highly conserved among all selected species (Figure 1). The unrooted phylogenetic tree was constructed using the neighbor-joining method to analyze the

evolutionary relationship between HaTXNL1 and other TXNL1 proteins. The results showed that TXNL1 proteins from different classes of the animal kingdom (Fish, Mammal, Aves, Reptiles, Amphibia, and Chondrichthyes) were clustered into their original taxonomic subgroups in the phylogenetic analysis (Figure 3). HaTXNL1 was positioned within the teleost group and showed the closest relationship with *Hippocampus comes*.

According to pairwise alignment, HaTXNDC17 showed the highest identity and similarity of 99.2 % with *Hippocampus comes* (Table 2). Multiple sequence alignment demonstrated that cysteine residues in WCXXC motif were conserved among the all selected species and represented as WCPDC in fish. Further, folding sites and catalytic sites were highly conserved across all species. There were five conserved cysteines in mammals while teleost had four (Figure 2). According to the phylogenetic tree, orthologs from different classes of the animal kingdom clustered to their original taxonomic subgroups, and positioned within the teleost group, showing the closest relationship with others (Figure 3).

Table 2: Pairwise identity and similarity percentages of HaTXNL1 and HaTXNDC17 with its ortholog amino acids.

Accession No (TXNL1)	Species Name	Identity (%)	Similarity (%)
XP_019749013.1	<i>Hippocampus comes</i> -Tiger tail seahorse	99.0	99.7
APP94554.1	<i>Sebastes schlegelii</i> - Korean rockfish	91.0	95.8
SBP16112.1	<i>Aphyosemion striatum</i> - Red-striped killifish	90.3	94.8
SBP44494.1	<i>Nothobranchius furzeri</i> - Turquoise killifish	90.0	94.5
NP_001187390.1	<i>Ictalurus punctatus</i> - Channel catfish	86.5	91.0
NP_001133152.1	<i>Salmo salar</i> - Atlantic salmon	85.8	93.4
AAI64656.1	<i>Danio rerio</i> - Zebrafish	84.5	94.5
KYO28928.1	<i>Alligator mississippiensis</i> - American alligator	79.6	87.2
OPJ71392.1	<i>Patagioenas fasciata</i> - Band-tailed pigeon	78.9	86.9
NP_001086748.1	<i>Xenopus laevis</i> - African clawed frog	78.2	86.2
NP_543163.1	<i>Rattus norvegicus</i> - Brown rat	77.5	87.2
NP_004777.1	<i>Homo sapiens</i> - Human	76.8	87.5
NP_001231205.1	<i>Sus scrofa</i> - Wild boar	76.8	87.2
NP_001071354.1	<i>Bos taurus</i> - Cattle	76.5	86.9
NP_001279832.1	<i>Callorhynchus milii</i> - Australian ghost shark	74.4	84.1
Accession No (TXNDC17)	Species Name	Identity (%)	Similarity (%)
XP_019748365.1	<i>Hippocampus comes</i> - Tiger tail seahorse	99.2	99.2
XP_004075376.1	<i>Oryzias latipes</i> - Japanese rice fish	78.0	87.0
XP_021443673.1	<i>Oncorhynchus mykiss</i> - Rainbow trout	77.2	87.8
AAI64925.1	<i>Danio rerio</i> - Zebrafish	76.4	88.6
XP_020784309.1	<i>Boleophthalmus pectinirostris</i> - Mudskipper	76.4	87.0
XP_012730006.1	<i>Fundulus heteroclitus</i> - Mummichog	74.8	89.4
XP_020476365.1	<i>Monopterus albus</i> - Asian swamp eel	74.0	90.2
NP_001089800.1	<i>Xenopus laevis</i> - African clawed frog	67.7	81.5
KYO32106.1	<i>Alligator mississippiensis</i> - American alligator	63.4	78.9
OPJ78416.1	<i>Patagioenas fasciata</i> - Band-tailed pigeon	61.8	74.8
XP_003131925.1	<i>Sus scrofa</i> - Wild boar	61.0	77.2
NP_001192750.1	<i>Bos taurus</i> - Cattle	59.3	75.6
NP_116120.1	<i>Homo sapiens</i> - Human	58.5	77.2
NP_001099275.1	<i>Rattus norvegicus</i> - Brown rat	58.5	76.4
NP_001279378.1	<i>Callorhynchus milii</i> - Australian ghost shark	52.8	74.0

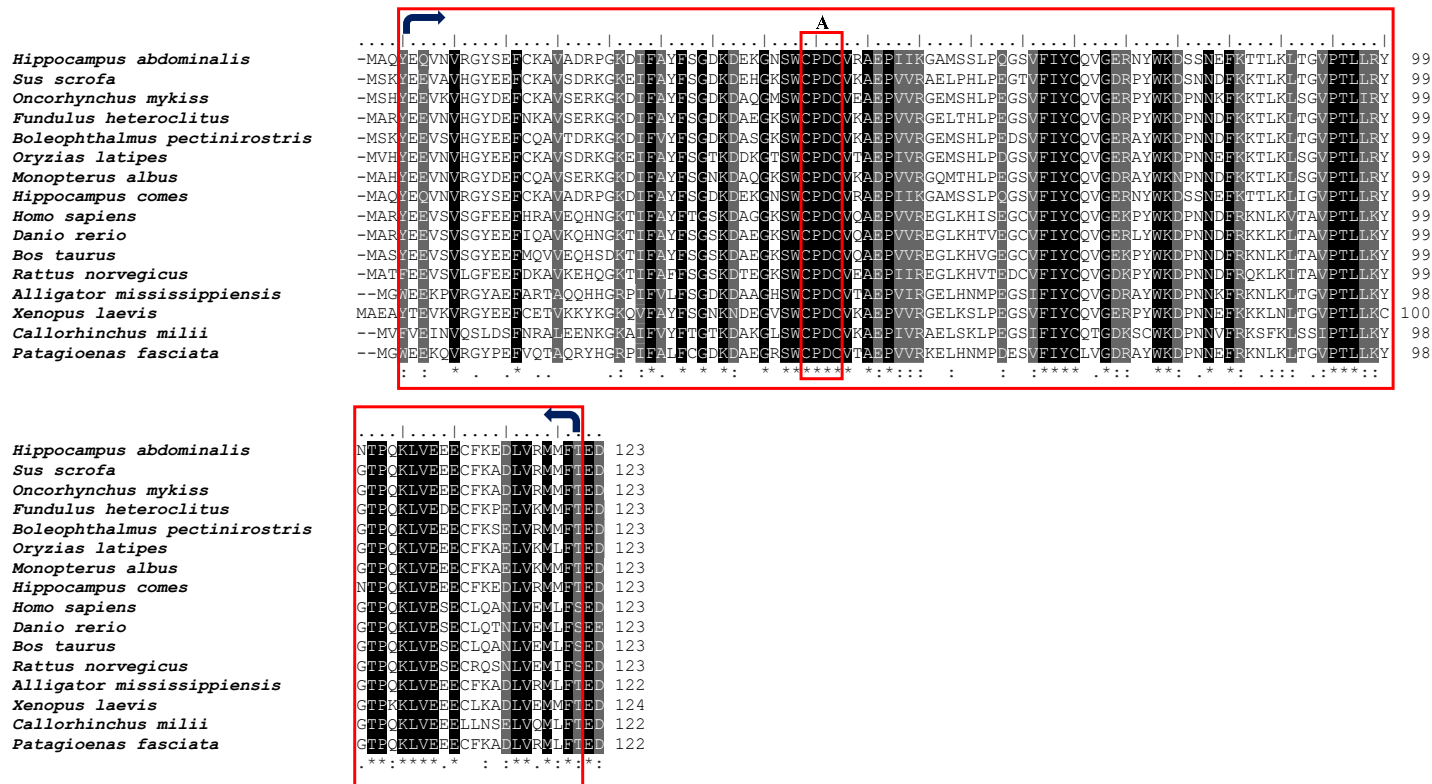
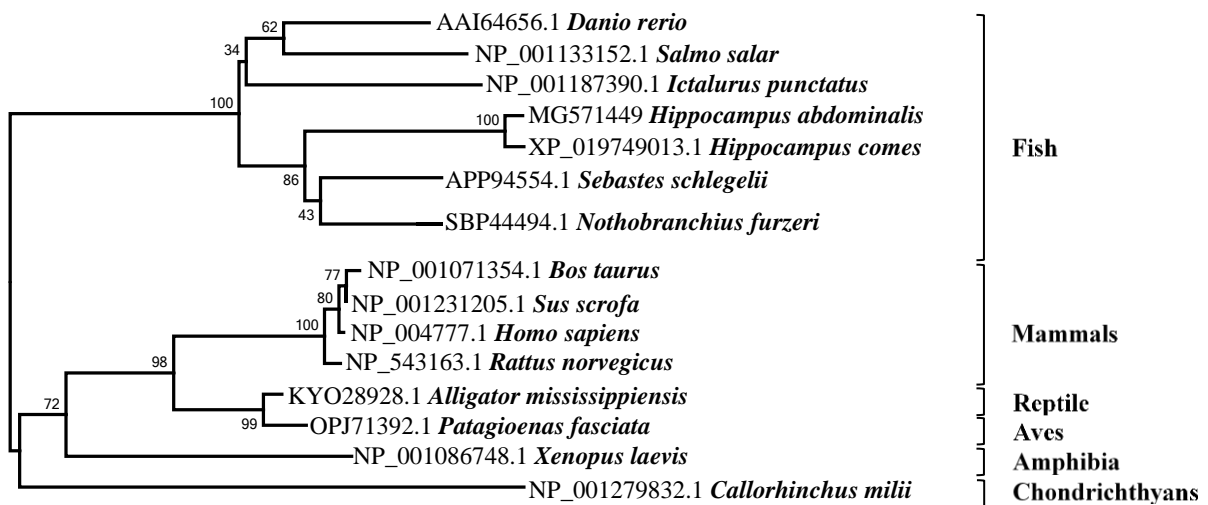
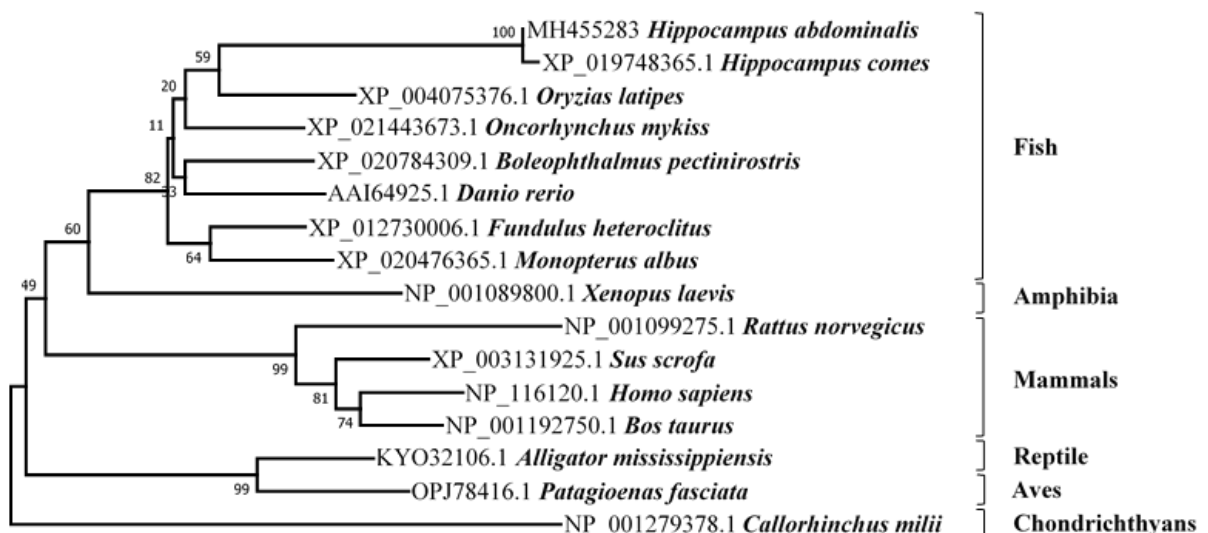


Figure 2: Multiple sequence alignment of HaTXNL1 and HaTXNDC17 with different ortholog amino acid sequences.

Multiple sequence alignment of (A) HaTXNL1 and (B) HaTXNDC17 with ortholog amino acid sequences of different classes of the animal kingdom. The active thiol-disulfide motif CXXC is indicated as A, N-linked glycosylation sites are indicated as B, and folding sites are indicated as C. An asterisk (*) indicates positions with a fully conserved residue. A colon (:) indicates conservation of strongly similar properties between groups. A period (.) indicates conservation of weakly similar properties between groups.



A



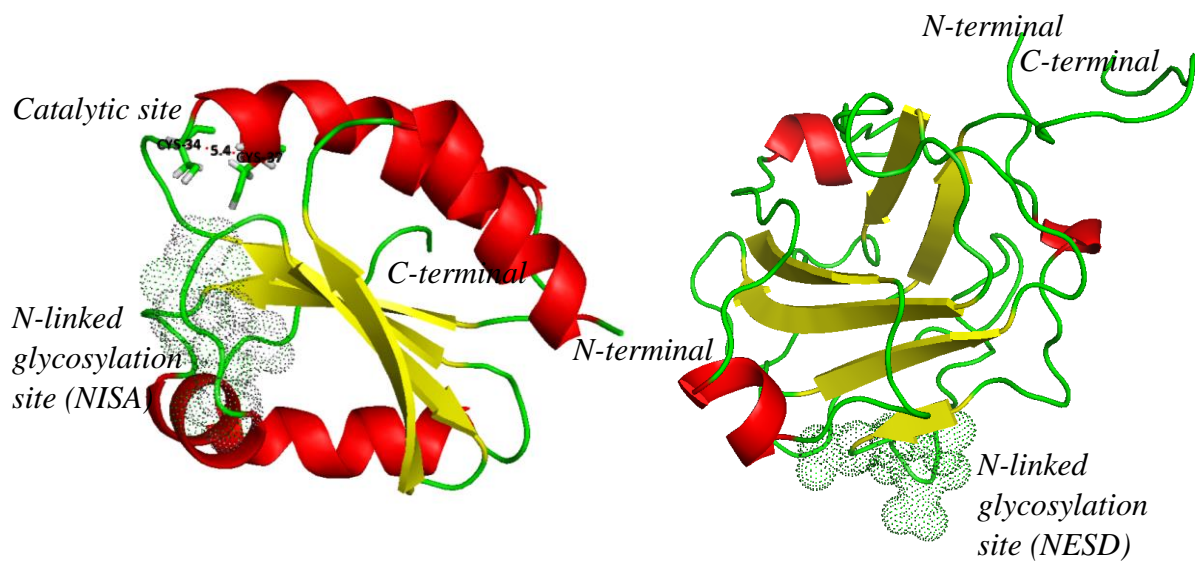
B

Figure 3: The phylogenetic tree of *HaTXNL1* and *HaTXNDC17* with other orthologs. Showing the phylogenetic tree of *HaTXNL1* and *HaTXNDC17* with different species of Fish, Mammal, Reptile, Aves, Amphibia, and Chondrichthyans, developed using MEGA 7 neighbor-joining method. The branches are validated with 5,000 replicates by bootstrap method, which is represented as the percentage values in each node. All sequences were retrieved from NCBI GenBank listed in Table 2.

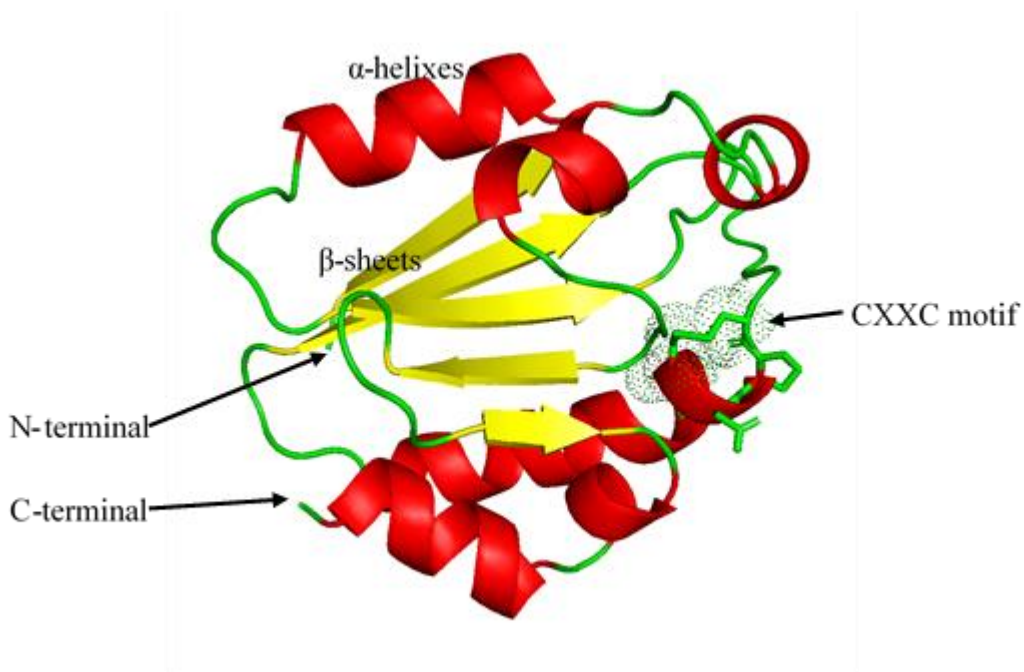
3.1.2. Protein structure

The predicted tertiary structure of HaTXNL1 was modeled using the structure of the PDB template 1gh2.1.A and 1wwy.1 with the best match (Figure 4). In comparison with the templates, HaTXNL1 gene showed 75.20 % accuracy. According to TXNL1 domain structure, the N-terminus displayed a thioredoxin domain, while the C-terminus carried a proteasome-interacting domain. The thioredoxin domain was composed of five β sheets and four α helices (Gleason and Holmgren, 1988; Holmgren, 1985). The predicted HaTXNL1 model represented the same structure as compared with the TXNL1. According to the predicted model, the distance between two Cys residues was 5.4 Å, and these residues formed a thiol-disulfide bond in the CXXC motif. The active site motif of thioredoxin domain was located at the beginning of the second β sheet. Furthermore, the tertiary structure of HaTXNL1 has a central core, which comprises four helices and five β sheets, resulting in a 3D structure similar to that of other TXNL1 with slight alterations. PITH domain identified at the C-terminus consists of seven β sheets and a domain dominated by the jelly-roll β sandwich structure. The β sandwich is formed by the face-to-face packing of two antiparallel β sheets and another two stranded β sheet seals of the one end of the β barrel (Goroncy et al., 2010; Song, 2005). According to PITH domain structure, HaTXNL1 showed a structure similar to the predicted model.

The tertiary structure of HaTXNDC17 was modeled by using the structure of closely matched PDB template 1wou.1 (Figure 4); HaTXNDC17 showed 77 % similarity with the template. Regarding domain structure, HaTXNDC17 consisted of thioredoxin domain, whose active site motif was located at the beginning of the second α -helix. Further, the tertiary structure of HaTXNDC17 had a central core consisting of five β -sheets surrounded by five α -helices. HaTXNDC17 showed very similar three-dimensional structure to human TXNDC17 with slight alterations.



A



B

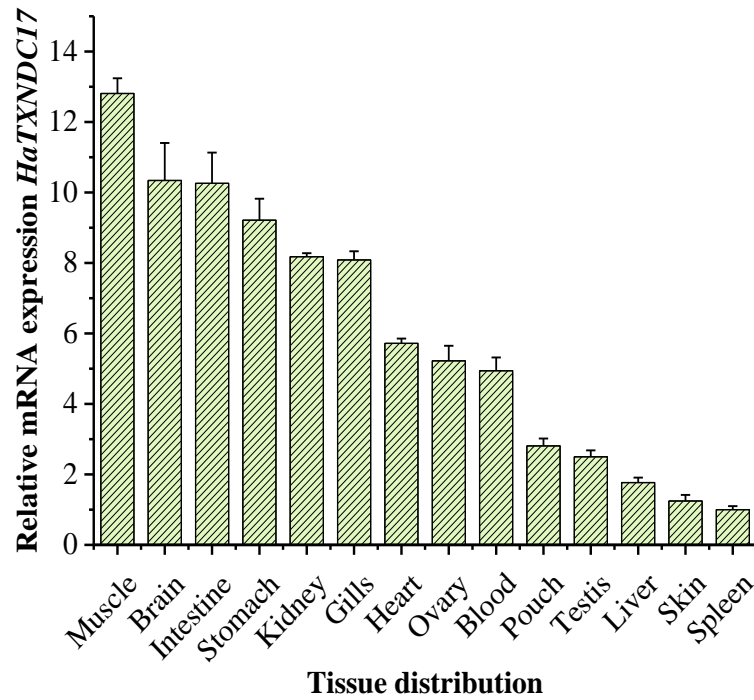
Figure 4: Predicted tertiary structure of HaTXNL1 and HaTXNDC17.

(A) Thioredoxin domain and proteasome- interacting thioredoxin domain of HaTXNL1, catalytic site residues represented by sticks and N-linked glycosylation site (NISA, NESD) represented by dotted spheres. (B) Predicted tertiary structure of thioredoxin-related protein 14 family domain of HaTXNDC17. Catalytic site residues are represented by dotted spheres.

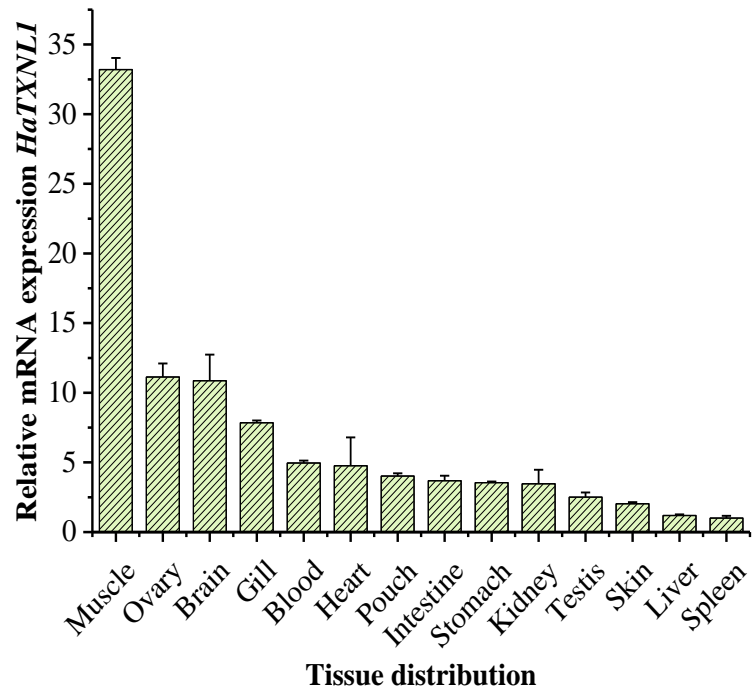
3.1.3. Analysis of mRNA expression

The spatial expression profile of *HaTXNL1* under normal physiological conditions was observed in 14 different tissues. The lowest mRNA expression level of *HaTXNL1* was detected in the spleen (one-fold); it was defined as the basal level. On the other hand, the highest expression level was observed in the muscle (33.20-fold). *HaTXNL1* was moderately expressed in the ovary (11.13-fold), brain (10.86-fold), gill (7.85-fold), and blood (4.96-fold) (Figure 5). TXNL1 exhibits typically a broad range of tissue distribution, owing to its role in the maintenance of cellular redox homeostasis. The highest TXNL1 availability usually occurs in the organs with the high antioxidant requirement, such as muscle (Cheng et al., 2016), ovary, brain, gill, and blood (Pacitti et al., 2014; Wang et al., 2015). In this study, *HaTXNL1* expression was detected in all tissues used for the transcriptional analysis.

Spatial expression profile of *HaTXNDC17* under normal physiological conditions was observed in 14 different tissues. The lowest mRNA expression level of *HaTXNDC17* was detected in spleen (1.00 ± 0.09 -fold) and the highest expression level was observed in muscle (12.80 ± 0.43 -fold); followed by the brain (10.33 ± 1.06 -fold), intestine (10.25 ± 0.87 -fold), stomach (9.21 ± 0.60 -fold), and trunk kidney (8.17 ± 0.09 -fold) (Figure 5). Immune-responsive transcriptional modulation of *HaTXNDC17* gene was monitored for two different immune-related tissues.



A



B

Figure 5: Relative mRNA expression (fold change) of HaTXNL1 and HaTXNDC17. Spatial mRNA expression of HaTXNL1 in fourteen different tissues of healthy seahorses under normal physiological conditions, with 40s ribosomal S7 protein used as a reference. The mRNA expression level of each tissue is indicated relative to the mRNA expression of spleen tissue. The data are represented as mean values (n=3) \pm standard deviation (SD) and $P < 0.05$.

For the pathogen challenges, LPS, Poly I:C, *E. tarda*, and *S. iniae* were used. Microbial products such as LPS or endotoxin are potent molecules that stimulate the immune system (Ki et al., 1994). Selected bacterial species, *Edwardsiella tarda* (as Gram-positive) and *Streptococcus iniae* (as Gram-negative) which are frequently known as infectious pathogens in aquaculture (Agnew and Barnes, 2007; Park et al., 2012). Poly I:C mimic the viral-like infections in the immune system (Fortier, 2004). The transcriptional modulation of *HaTXNL1* gene was monitored for two different immune-related tissues. In blood, *HaTXNL1* was significantly upregulated (5.29-fold) after 24–72 h post injection of *E. tarda*, while *S. iniae* injection resulted in a 5.20-fold increase in *HaTXNL1* expression after 72 h (Figure 6A). In the gill tissue, the *HaTXNL1* gene was significantly upregulated by 1.82-fold and 1.95-fold at 6 h and gradually decreased over the time in response to *E. tarda* and *S. iniae*, respectively (Figure 6B).

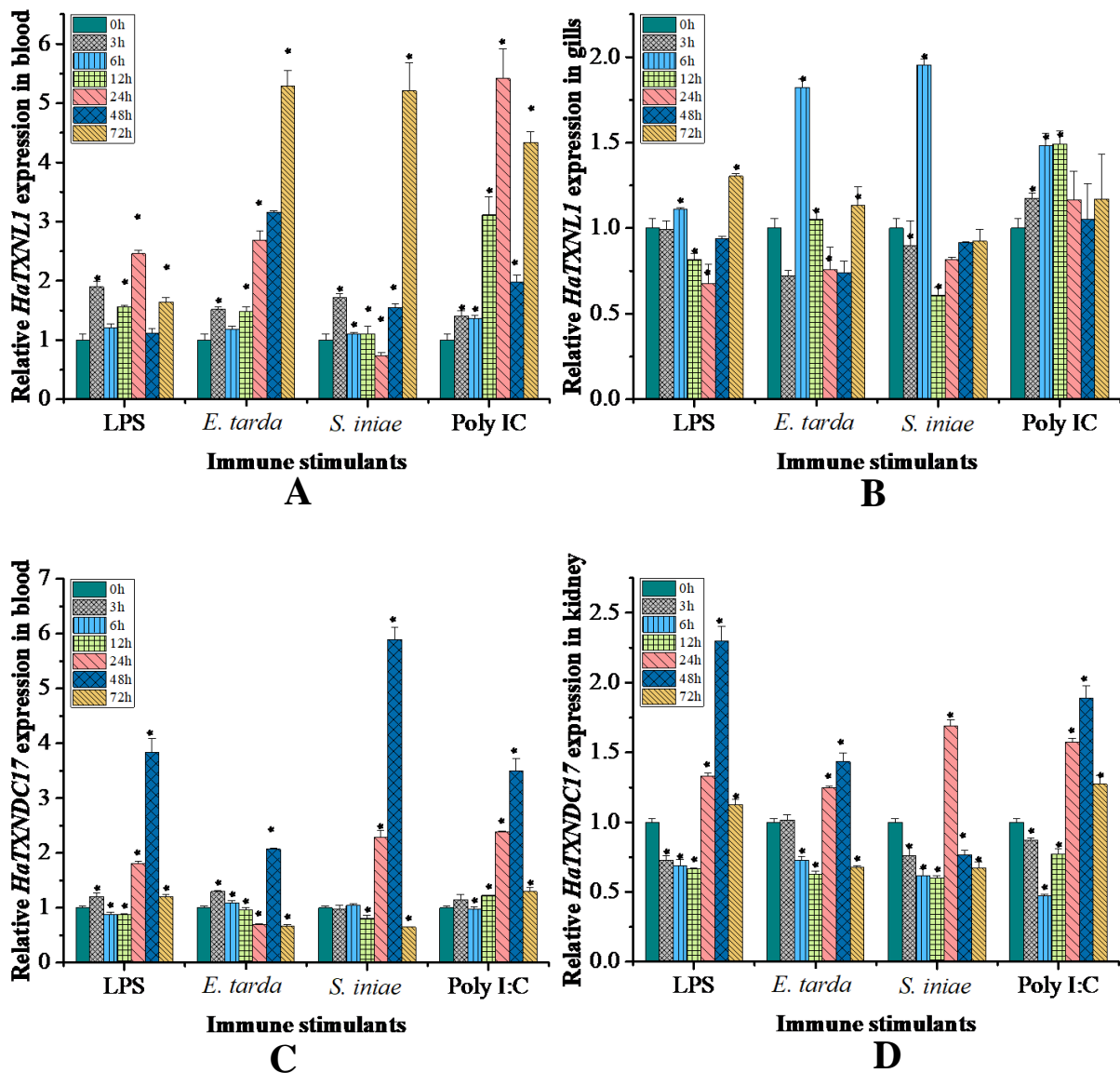


Figure 6: Temporal expression of HaTXNL1 and HaTXNDC17.

Temporal expression profiles of HaTXNL1 blood (A) gill (B) and HaTXNDC17 blood (C), spleen (D) tissues after LPS, *E. tarda*, *S. iniae*, and Poly (I:C) challenges. The relative fold changes in expression were compared with those of PBS-injected controls at different time points. The vertical bars represent the mean values ($n=3$) \pm SD. Significant differences are compared to the blank (0 h) with $P < 0.05$.

The temporal expression profile of *HaTXNDC17* in blood showed significant up-regulation after 24 h post injection (p.i.) to LPS, *S. iniae* and poly I:C stressors. Moreover, *HaTXNDC17* expression was significantly upregulated at 48 h p.i. towards the all bacterial and PAMPs. (Figure 6A). In the trunk kidney tissues, *HaTXNDC17* transcripts were significantly up-regulated up to 24-48 h p.i. in response to all the stressors except in *S. iniae*, LPS, *E. tarda* and poly I:C injected samples reached a peak at 48 h and downregulated during the experiential time, whereas *HaTXNDC17* expression in *S. iniae* treated samples started downregulation at 24 h p.i. interval and gradually decreasing thereafter over time (Figure 6B).

3.1.4. Expression and purification of rHaTXNL1 and rHaTXNDC17

The recombinant construct of HaTXNL1 and HaTXNDC17 has overexpressed in *E. coli* ER2523 cells with IPTG induction, followed by purification with MBP-fusion protein. Aliquots of different stages of purification steps were analyzed by SDS-PAGE. The gel image showed that rHaTXNL1 protein bands were at approximately 74.7 kDa as compared with the ladder, consistent with its predicted molecular weight (Figure 7).

The HaTXNDC17 protein molecular weight is approximately 14.1 kDa. Together with MBP fusion protein (~ 42.5 kDa), rHaTXNDC17 showed protein band at ~ 56.6 kDa in SDS-PAGE gel with compared to the protein ladder, which agreed with the expected molecular weight of rHaTXNDC17 (Figure 7).

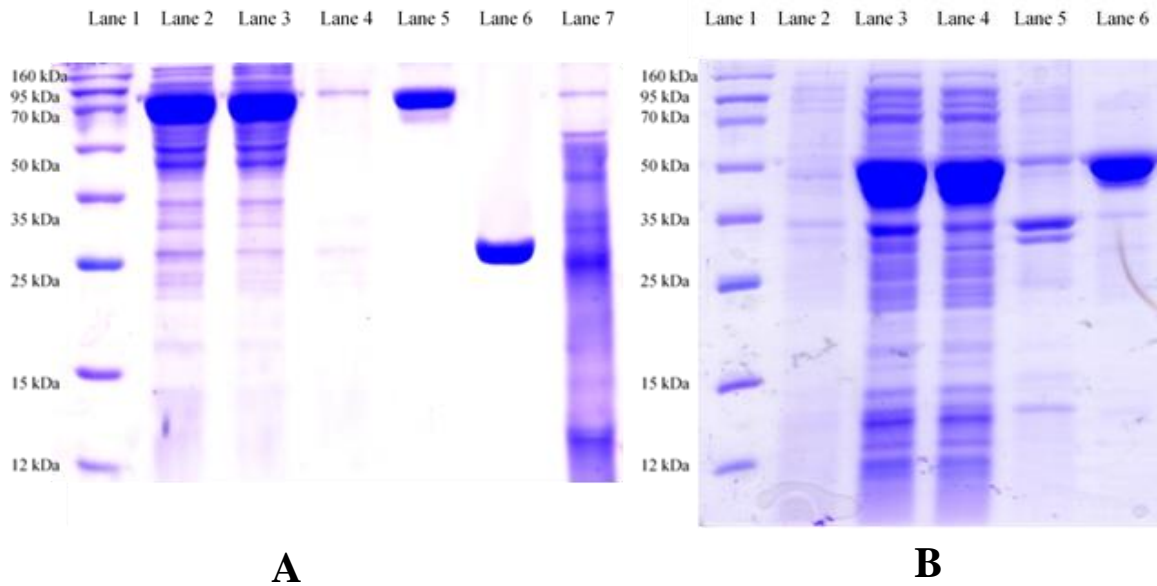


Figure 7: SDS-PAGE analysis of purified HaTXNL1 and HaTXNDC17.

(A) Lane 1: protein ladder, Lane 2: crude extract of induced *E. coli* ER2523 cells, Lane 3: supernatant after centrifugation, Lane 4: pellet, Lane 5: purified HaTXNL1 fusion protein, Lane 6: purified MBP Protein, Lane 7: crude extract of un-induced *E. coli* ER2523 cells.

(B) SDS-PAGE analysis of overexpressed and purified HaTXNDC17 as MBP-fusion protein. Lane 1: protein ladder, Lane 2: crude extract of un-induced *E. coli* ER2523 cells, Lane 3: crude extract of induced *E. coli* ER2523 cells, Lane 4: supernatant after centrifugation, Lane 5: pellet, Lane 6: purified HaTXNDC17 fusion protein.

3.2. Functional assays

3.2.1. DPPH assay

The compound DPPH is a highly stable radical-forming agent, which is used to measure the radical-scavenging ability and effectiveness of an antioxidant based on its H⁺ donating capacity. Figure 8 shows the percentage of DPPH radical-scavenging activity of rHaTXNL1 with reference to the ascorbic acid. A positively sloped relationship was observed between the calculated radical-scavenging activity and rHaTXNL1 concentrations. The recombinant protein showed maximum (73.01 %) inhibition of DPPH radicals within the assessed concentration range. A significant ($P < 0.05$) scavenging activity was evidenced at all the concentrations tested (45–120 $\mu\text{g}/\text{mL}$). rHaTXNL1 showed an IC₅₀ value at the concentration

of 56.01 $\mu\text{g/mL}$. These results indicate that the recombinant TXNL1 has antioxidant activity responses in a concentration dependent manner. Further, free radical scavenging ability of HaTXNL1 with DPPH may suggest the reaction of TXNL1 with ROS in the biological systems.

Figure 8 shows the percentage of DPPH radical scavenging activity of rHaTXNDC17 compared to that of ascorbic acid as a reference compound. A concentration-dependent relationship can be observed in the DPPH radical scavenging capacity that is increased with concentrations. The protein showed maximum inhibition of DPPH radicals (14.76 %) within the concentration range used. Significant scavenging ($P < 0.05$) of free radicals was evidenced at all the concentrations tested with rHaTXNDC17 and the reference (0–90 $\mu\text{g/mL}$). Further, rHaTXNDC17 showed IC_{50} value at the concentration of 23.94 $\mu\text{g/mL}$.

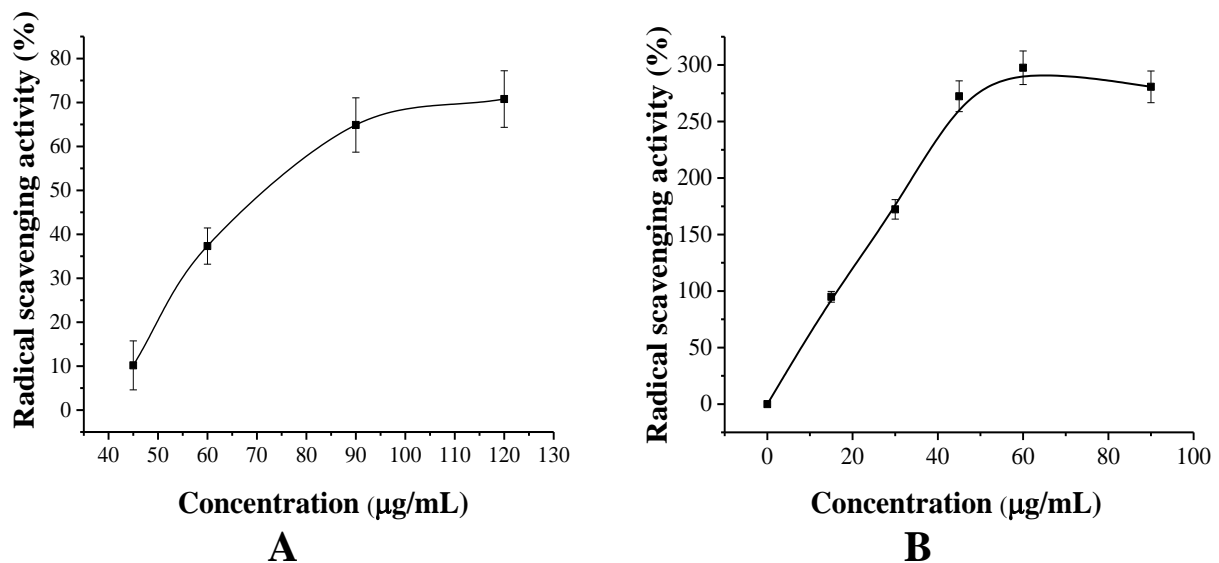


Figure 8: (A) DPPH radical-scavenging activity of rHaTXNL1 at different concentrations. Ascorbic acid was used as a standard in the experiment. Data are represented as the mean of triplicates with standard deviation ($P < 0.05$). (B) DPPH radical-scavenging activity of rHaTXNDC17 at different concentrations. Ascorbic acid was used as a standard in the experiment. Data are represented as the mean of triplicates with standard deviation ($P < 0.05$).

3.2.2. Insulin disulfide reduction assay

The biological activity of the rHaTXNL1 protein was evaluated using insulin disulfide reduction assay (Holmgren, 1979). DTT is a strong reducing agent and the reduction of typical disulfide bond occurs by the sequential thiol-disulfide exchange. Reduction of insulin was mediated by DTT to obtain a turbid reaction mixture. Thioredoxin promotes this precipitation while exchanging SH groups with insulin β chain. The assay was performed on a 96-well plate. No precipitation was observed in the negative control, while significant rapid precipitation was observed in samples in a concentration-dependent manner. In contrast, the presence of purified rHaTXNL1 increased the rate of insulin reduction, which was detectable after 15 min of incubation. The IC₅₀ values were measured to be of 41.42 ± 0.27 , 37.47 ± 0.20 , 31.35 ± 0.25 , and 26.15 ± 0.31 for 25, 50, 100, and 200 $\mu\text{g/mL}$ concentrations, respectively (Figure 9). Thus, an increase in rHaTXNL1 concentration resulted in a logarithmic increase in the precipitation of insulin. This assay demonstrated the functionality of rHaTXNL1 protein and suggested that the protein activity and redox feature play an important role in cellular defense against oxidative stress.

The biological activity of rHaTXNDC17 was evaluated using insulin disulfide reduction assay. Presence of rHaTXNDC17 increased the rate of insulin reduction that was detectable after 10 min of incubation. Results indicate the precipitation of insulin was increased with the incubation time in 25, 50, 100, 200 $\mu\text{g/mL}$ of rHaTXNDC17 treated samples. MBP treated sample showed the absorbance similar to the control (0 $\mu\text{g/mL}$ of rHaTXNDC17). DTT absent treatment did not give significant absorbance. The IC₅₀ values corresponding to 25 $\mu\text{g/mL}$, 50 $\mu\text{g/mL}$, 100 $\mu\text{g/mL}$, and 200 $\mu\text{g/mL}$ were 38.63 ± 0.63 , 37.47 ± 0.20 , 32.93 ± 0.51 , and 27.83 ± 0.21 , respectively (Figure 9). The specific activity was observed at 1.4, 1.9, 2.5, and 2.9 for 25, 50, 100 and 200 $\mu\text{g/mL}$ concentrations of rHaTXNDC17 protein respectively.

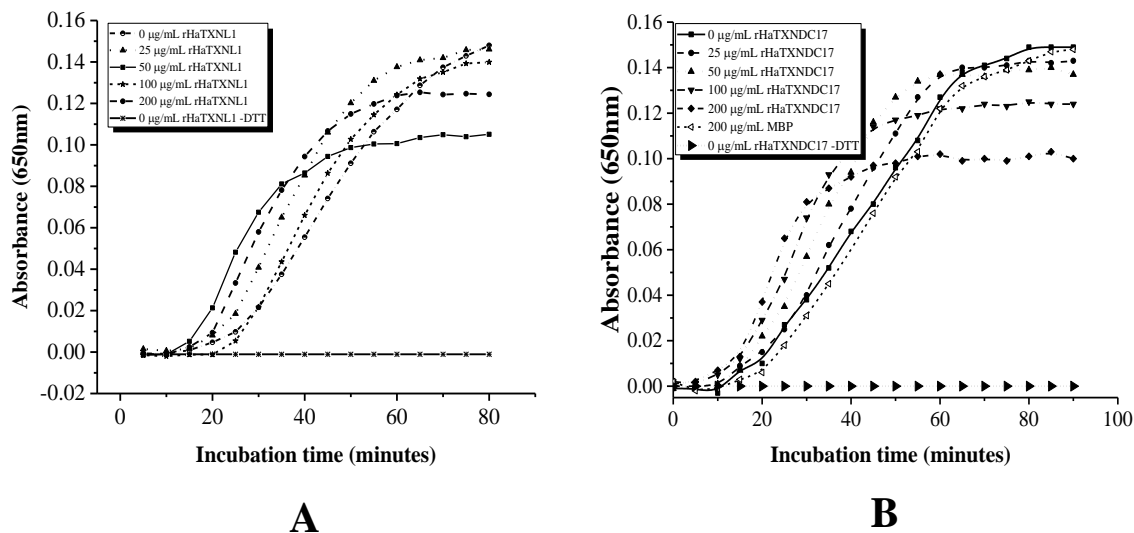


Figure 9: Insulin disulfide reduction activity assay for *HaTXNL1* and *HaTXNDC17*. (A) The reaction was performed with 0, 25, 50, 100, and 200 µg/mL *HaTXNL1* in the presence of DTT. The negative control was prepared in the absence of DTT. The turbidity was monitored at 650 nm and the difference in the absorbance was plotted against the incubation time. Data were presented as mean values (n=3). (B) Insulin disulfide reduction activity assay for *rHaTXNDC17*. The reaction was performed with 0, 25, 50, 100, and 200 µg/mL *rHaTXNDC17* in the presence of DTT. The negative control was prepared in the absence of DTT. The turbidity was monitored at 650 nm and the difference in the absorbance was plotted against the incubation time. Independent student t-test were used to compare the treatments. Standard deviation (SD) was calculated and significant differences were defined at $P < 0.05$. Data are presented as mean values (n=3).

3.2.3. The protective effect on the cultured cells under oxidative stress

Toxic effect of H_2O_2 on FHM cells was calculated by MTT assay. According to the results obtained, 88 % of live cells were detected among the H_2O_2 -treated cells with 0 µg/mL *rHaTXNDC17* (Figure 10). These results showed the peroxidase activity of *TXNDC17* and its contribution to cell viability upon oxidative stress. Microscopic observations confirmed the cellular protective ability of *HaTXNDC17* respect to different concentrations. H_2O_2 treated cells showed the highest cell damage compared to the untreated cells.

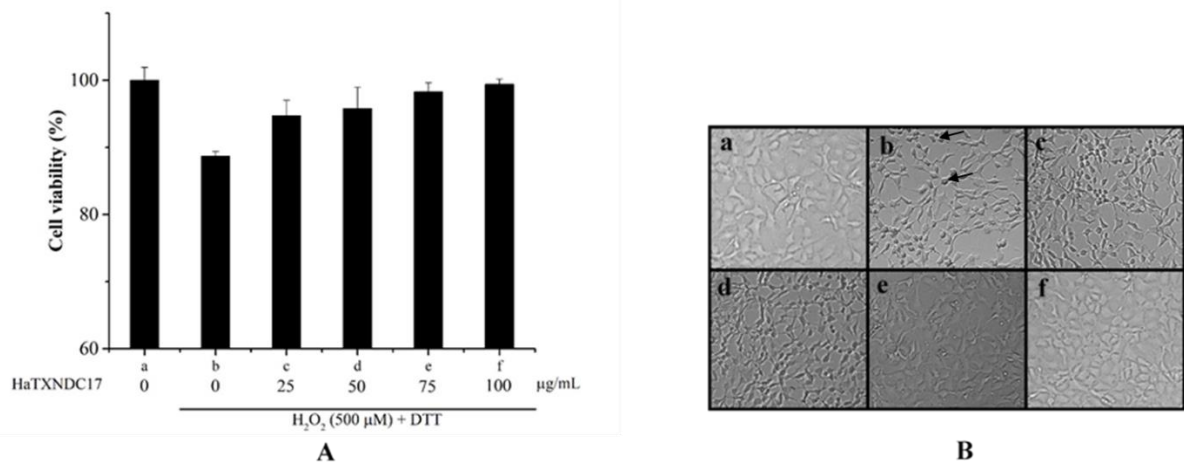


Figure 10: Effects of rHaTXNDC17 on the viability of fathead minnow epithelial cells
 (A) Effects of rHaTXNDC17 on the viability of fathead minnow epithelial cells (FHM) exposed to 100 μM H₂O₂. (B) Microscopic observations of FHM cells with related to each treatment and black arrows indicate damaged cells. Treatments: (a) control cells; (b) cells treated with H₂O₂ (100 μM), (c-f) cells pretreated with 25–100 μg/mL of rHaTXNDC17 and 1 mM of DTT followed by 100 μM of H₂O₂. Statistical analysis was performed by ANOVA with posthoc pairwise comparisons. All the samples were treated in triplicate (n=3) and mean percentages ±SD were plotted.

4. Discussion

Thioredoxin and glutathione are two major cellular components mediating the redox balance in cells *via* cysteine residues. The thioredoxin system includes several isoforms of thioredoxins, thioredoxin reductases, and thioredoxin-dependent proteins (Arnér and Holmgren, 2000). Thioredoxins are involved in various biological processes in prokaryotes as well as eukaryotes (Glickman and Ciechanover, 2002) and play an essential role in regulating the cellular environment by reducing oxidative stress. In this study, the TXNL1 and TXNDC17 homologs from the big belly seahorse was characterized, as it may be involved in maintaining redox balance in the seahorse. Several proteins are involved in cellular thiol-redox pathways, including thioredoxin, glutathione S transferase, GRX, and PDI, which are known to adopt a thioredoxin fold (Aslund et al., 1994; Holmgren, 1995; Kozlov et al., 2010). Previous subcellular localization studies revealed that TXNL1 and TXNDC17 are present in the

cytoplasm. Thioredoxins are involved in cellular processes like scavenging radicals in the cellular environment, repairing damaged proteins due to oxidative stress (FERNANDO et al., 1992), and regulating gene expression and apoptosis (Saitoh et al., 1998). It also modulates the gene expression of tumor necrosis factor and nuclear factor kappa B with dynein light chain LC8 (Jeong et al., 2004; Woo et al., 2004).

All organisms have different thioredoxin and thioredoxin related isoforms. Conserved CXXC common motif in the thioredoxin domain is essential for the thiol-disulfide reduction in thioredoxin and important in redox balancing in cells (Arnér and Holmgren, 2000; Miranda-Vizuete et al., 1997). It has CXXC motif, and those residues are conserved in all TXNL1 and TXNDC17 orthologs. Lack of N-terminal secretory signal indicated the localization of the HaTXNL1 and HaTXNDC17 in the cytosol and lack of *N*-linked glycosylation sites in HaTXNDC17 indicated the absence of protein modification by Asn residues in by the endoplasmic reticulum in the eukaryotic cells (Ranganathan et al., 2006). According to the protein structure, all thioredoxin isoforms have a similar 3D structure, which consists of five beta strands surrounded by four alpha helices [25]. The N terminal cysteine of CXXC motif in thioredoxin may be highly conserved and redox-sensitive [8].

HaTXNL1 and HaTXNDC17 are ubiquitously expressed in all tissues tested in this experiment as its major function is to maintain cellular redox homeostasis. ROS can interact with biomolecules and cause severe cell damage or cell death (Birben et al., 2012). According to the present tissue distribution results, TXNL1 and TXNDC17 may actively protect the cells from oxidative damage. Moreover, it helps organs to maintain cellular redox homeostasis and can be found in tissues that are more susceptible to oxidative stress. Muscles are susceptible to higher oxidative stresses due to active swimming in fish species than other tissues (Filho, 2007). Further, mitochondria produce higher energy to compensate for the energy requirement in brain tissues, which leads to ROS generation. Hence, TXNDC17 plays a crucial role in brain tissues

in response to regulate the redox balance (Meister, 1981). The intestine and stomach of the seahorses abundantly express TXNDC17, which may be due to the microbial flora and by-product accumulation in the digestive system (Bhattacharyya et al., 2014). Therefore, the tissue distribution results indicate the involvement of HaTXNL1 and *HaTXNDC17* in cellular defense mechanism.

The immune-related responses of *HaTXNLI* indicate the impact of pathological stimulation on the thioredoxin pathway. ROS may interact with the biomolecules, leading to severe cell damage or cell death. TXNL1 actively protects the cells from the damage via redox balance and is expressed in various tissues. Also, it helps the organs to maintain cellular redox homeostasis and may be found in tissues such as muscle, ovary, brain, gill, and blood that require higher antioxidant activity. In fish, muscles pose a higher requirement of antioxidants as compared with other tissues, owing to active swimming (Filho, 2007) and thioredoxin will protect the muscle fibers from the oxidative stress. Furthermore, ovaries are normally susceptible to microbial and parasitic infections (Di Cicco et al., 2013) and may produce higher TXNL1 to eliminate the generated ROS from harmful invaders. The higher energy requirement of the brain tissue necessitates the production of the high amount of energy by mitochondria that results in the production of ROS as a byproduct (Meister, 1981). Moreover, immune tissues like blood, kidney, spleen involving the phagocytic activities lead to eliminating the invading microbes by producing the TXNL1. As a consequence, TXNL1 is produced to regulate the redox balance. The presence of a higher amount of oxygen radicals in a blood and gill tissues (Pandey and Rizvi, 2011) results in the higher expression of TXNL1. Altogether, the tissue distribution results indicate the involvement of *HaTXNLI* in activities related to cellular redox balance.

The gill tissue showed immediate *HaTXNLI* mRNA expression at 3 to 6 h after immune challenge with a bacterial pathogen. This observation may be attributed to the oxidative burst

and severe membrane damage, which may lead to lipid peroxidation. The blood tissue showed upregulated *HaTXNLI* mRNA expression from 3 to 72 h after bacterial challenge, owing to an increase in ROS to suppress the invading bacteria. A large amount of thioredoxin expression was observed in the blood due to higher redox stress in red blood cells which are involved in carrying oxygen in many organisms (Wahid et al., 2017) and macrophages in blood involving in engulfing bacterial invaders. Thus, the *HaTXNLI* gene may be used as an immunologically important gene for seahorses.

Considering the immune-related activities of *HaTXNDC17*, the thioredoxin pathway is activated upon pathological stimulation. The upregulation of *HaTXNDC17* expression after 24–48 h in the peripheral blood cells may be due to an increase in ROS to suppress the invading bacteria like *E. tarda* and *S. iniae*. LPS triggered the immune system via the LPS receptors and activated the downstream signaling cascades of macrophages (Ki et al., 1994). Poly I:C is a viral mimic that activates the immune responses in peripheral blood leukocytes (Zhou et al., 2014) and in response to that *HaTXNDC17* may be expressed highly to balance redox stress. Moreover, high oxidative stress occurs in the erythrocytes due to direct interaction with oxygen that leads to ROS generation, and TXNDC17 is actively involved in regulating oxidative stress in the blood (Mills, 1957). Kidney tissues are one of the main hematopoietic tissues (Catton, 2012; Roberts and Ellis, 2012) and the increased expression of *HaTXNDC17* after 24–48 h may be due to the high amount of ROS produced during hematopoiesis due to the rapid loss of cells in the host immune system (Sattler et al., 1999) due to bacteria like *E. tarda* and *S. iniae*, and it's main function is to regulate cell proliferation (Ghaffari, 2008). Due to the acute endotoxin stress produced by LPS in trunk kidney, high number of immune signaling and apoptosis-related genes were expressed (Forn-Cuní et al., 2017) and that leads to producing a large amount of ROS in the cells. In order to regulate the redox stress, *HaTXNDC17* was expressed

highly. Further poly I:C can activate the immune responses in kidney macrophages leads to activation of downstream signaling cascades (Zhou et al., 2014).

Though members of the thioredoxin family are well known to promote redox homeostasis. Hence, we performed the DPPH radical scavenging assay to evaluate the function of HaTXNL1 and HaTXNDC17. DPPH assay is quite popular assay to measure the biological samples (Antolovich et al., 2002; Dejian Huang et al., 2005) and DPPH is a highly stable radical-forming agent used to measure the scavenging ability. The color of DPPH changes from purple to yellow according to the antioxidant activity of the compound. Using of ascorbic acid as a reference provides the ability to get the absolute value of IC₅₀ value. IC₅₀ of recombinant protein for DPPH can be defined as the concentration of recombinant protein required to inhibit 50% of DPPH radical and provides the information regarding the potency of recombinant protein in DPPH radical scavenging activity.

The insulin reduction assay is used to measure the antioxidant ability of proteins where the precipitation of insulin depends on the time of incubation (Holmgren, 1979). DTT is a robust reducing agent, and the reduction of the typical disulfide bond is mediated by the sequential thiol-disulfide exchange. Reduction of insulin is facilitated by adding DTT to the mixture, and it forms a turbid solution, which can be quantified using spectrophotometry. Thioredoxin promotes the precipitation of insulin while exchanging SH groups with the insulin β chain. Increasing concentration of rHaTXNL1 and rHaTXNDC17 concentration logarithmically increases the precipitation of insulin.

The protective ability of rHaTXNDC17 was tested on FHM cells by the MTT assay. Previous studies suggest that TXNDC17 has peroxidase activity (Hirota et al., 2002). Peroxidases are thiol dependent proteins which require an electron donor. TXNDC17 has thiol-active cysteine residues that can be activated by electron donors like thioredoxin, GRX, or DTT. The thiol-active CXXC motif undergoes oxidation and reduction in the presence of DTT and

H₂O₂. Since TXNDC17 is not a specific enzyme to mediate the cellular peroxidase activity, increasing the concentration of TXNDC17 may not increase cell survival, and a linear relationship cannot be observed. The cellular protective ability of peroxiredoxin to the H₂O₂ was previously studied in *Scophthalmus maximus* (Zheng et al., 2010) and *Haliotis discus discus* (Nikapitiya et al., 2009) to observe peroxidase activity. Microscopic images revealed cell growth reduced and damaged due to H₂O₂. The HaTXNDC17 treated cells got the ability to survive under oxidative stress conditions. The previous study on mice peroxiredoxin 6 showed significant resistant to H₂O₂ on keratinocytes (Kümin et al., 2006). In summary, Cellular ROS level increased during the pathological conditions or oxidative stresses. Hence, the observed results revealed that rHaTXNDC17 might play a significant role in protecting the cellular organelles from H₂O₂-mediated oxidative damage.

4. Conclusion

In conclusion, the TXNL1 and TXNDC17 gene from *H. abdominalis* was analyzed using various *in silico* tools, and molecular properties were examined. The *HaTXNL1* and *HaTXNDC17* gene was ubiquitously expressed in all the tissues examined. Modulation of *HaTXNL1* and *HaTXNDC17* transcripts in blood, gill and trunk kidney revealed the significant upregulation against the bacterial and PAMP infections. Further, functional properties such as antioxidant activity using DPPH assay, thiol reductase activity using insulin reductase assay, and peroxidase activity of rHaTXNDC17 using cell viability assay were observed. These assays showed that rHaTXNL1 and rHaTXNDC17 protein served to reduce oxidative stress and suggested that this protein plays a significant role in maintaining a cellular defense against oxidative stress. Moreover, TXNL1 and TXNDC17 from *H. abdominalis* assessing first time in this study and provide a better understanding of the functional and molecular properties of the *HaTXNL1* and *HaTXNDC17* gene.

CHAPTER 2

Membrane attack complex-associated molecules from redlip mullet (*Liza haematocheila*): Molecular characterization and transcriptional evidence of C6, C7, C8 β , and C9 in innate immunity

1. Introduction

The immune system plays a vital role in protecting organisms against pathogens by activating innate and adaptive immune responses. Innate immunity has an earlier evolutionary history compared to adaptive immunity, which arose in early vertebrate development between the divergence of jawless fish and cartilaginous fish (Fujita et al., 2004); innate immunity evolved before the emergence of adaptive immunity (Hoffmann et al., 1999). The complement system is composed of a series of soluble proteins, including circulating plasma proteins, membrane-bound receptors, and regulatory factors (Markiewski et al., 2009), which are key modulators of both innate and adaptive immunity (Gasque, 2004; Morgan et al., 2005). These proteins are related to innate immunity, and they have vital functions in the host's immune response by purging foreign bodies such as cell debris, apoptotic cells, antigen-antibody complexes and microorganisms (Tschopp, 1984). In mammals, the complement system bridges the innate and adaptive immune systems (Aybar et al., 2009; Wei et al., 2009). The complement system's role as a humoral effector system during inflammation and infection is activated and regulated through three different pathways – the classical, the lectin, and the alternative pathways (Carroll and Isenman, 2012). The complement system can be activated by a variety of stimuli, such as the hydrolysis of complement component 3 (C3), foreign bodies, pathogens, or injured cells (Kimura and Nonaka, 2009; Nonaka, 2011). C3 is the main molecule of the complement system that triggers the classical and alternative pathways. (Tschopp, 1984). The sixth, seventh, eighth, and ninth complement components are the late-acting complement proteins involved in the development of the membrane attack complex (MAC) (Bayly-Jones et al., 2017). The complex produces pores in the cell membrane and causes lysis (Bhakdi and Tranum-Jensen, 1991). Once C5 is activated by the classical, alternative, or lectin pathways, C5b is produced and it contains a binding site for C6. C6 interacts with C5b to form a soluble C5b-C6 dimer (Tegla et al., 2011). C7 binds to the C5b-C6 dimer, and this trimolecular

complex alters its conformation to allow the attachment of the hydrophobic site of C7 to the lipid bilayer of opsonized cells (Würzner, 2000). After the C5b-C6-C7 trimolecular complex associates with the binding site, C8 is exposed, and it promotes the complex to insert into the cell membrane. The C8 β protein attaches to C5b, and the attachment of C8 β to the membrane-bound C5b-C6-C7 complex permits the hydrophobic domain of C8 α -C8 γ to enter into the lipid bilayer (Lovelace et al., 2011). Finally, the C8 α -C8 γ complex induces the polymerization of C9 into the MAC (Bhakdi and Trandum-Jensen, 1991). MAC components include the terminal complement components (TCC) C6, C7, C8 α , C8 β , and C9 that create a cluster of perforins, the lytic proteins of natural killer (NK) cells, and cytotoxic lymphocytes of a similar gene family (Plumb and Sodetz, 2000). The MAC can form pores on the cell surface of the pathogen and act as an essential effector complex of the innate immune system (Bayly-Jones et al., 2017). TCCs and perforins share a membrane attack complex/perforin-like domain (MACPF) (Shinkai et al., 1988) that may have evolved from the same ancestral gene but were differentiated by genome arrangement. It has a more complex domain structure in C6, while it has a simple arrangement in C9 (Mondragón-Palomino et al., 1999; Shinkai, 1989). In general, the complement pathway identifies and kills the pathogens, as well as stimulates other mechanisms of innate immunity. In mammals, the complement system may enhance phagocytosis by modulating macrophage-activating cytokines (Collins and Bancroft, 1992). In teleost fish, C6 from large yellow croaker, rainbow trout, and grass carp (Chondrou et al., 2006; Liu et al., 2016; Shen et al., 2012b); C7 from trout and rock bream (Wickramaarachchi et al., 2013a; Zarkadis et al., 2005); C8 α and C8 β from rock bream and catfish (Qin et al., 2017; Wickramaarachchi et al., 2013b); C8 and C9 from carp (Uemura et al., 1996); C9 from rock bream and bamboo shark (Wang et al., 2013; Wickramaarachchi et al., 2012) and other major complement genes (Sun et al., 2013; Xu et al., 2018) have been documented in previous studies.

However, there has been no reported comprehensive comparison of TCC molecules with immune challenge experiments in fish.

The redlip mullet (*Liza haematocheila*) is a saltwater fish distributed worldwide and is mainly used as food in different places of the world. According to the statistics published by the Korean Ministry of Maritime Affairs and Fisheries, all species of mullets account for 8% of the total consumption and cultivation in Korea. Furthermore, the redlip mullet is one of the most treasured species in the aquaculture sector, and they are mostly cultivated in the south coastal area of Korea. In culture, they are susceptible to infection by *Lactococcus garvieae* (*L. garvieae*). In this study, we aimed to characterize the mullet C6 (MuC6), C7 (MuC7), C8 β (MuC8 β), and C9 (MuC9) genes at the molecular level. Moreover, we assessed the expression levels of each gene in the spleen and head kidney after infection with lipopolysaccharides (LPS), polyinosinic:polycytidylic acid (poly I:C), and *L. garvieae*.

2. Materials and Methods

2.1. Database construction and isolation of the MuC6, MuC7, MuC8 β , and MuC9

sequences

The mullet transcriptomic database was constructed using PacBio sequencing technology. Total RNA was isolated from the skin, liver, intestine, stomach, heart, eye, brain, kidney, spleen, muscle, head kidney, gill, and blood of five healthy mullets. The RNA was sent to Insilicogen, Korea for sequencing. cDNA library construction was carried out by the service provider. In brief, concentration and the quality of the RNA sample were measured before the sequencing preparation. Then library preparation was performed using the IsoSeq method. RNA is converted into first strand cDNA using the Clontech SMRTer PCR cDNA Synthesis Kit. Amplified cDNA is fractioned according to the size and converted into SMRTbell templates for sequencing on PacBio. After base calling, adapter trimming, and barcode

removing, identify the full length reads based on the 5' terminal cDNA primers and 3' terminal polyA tail signal. Assembly classification will recognize and remove polyA/T tails, remove primers, and identify reads with full-length and non-full-length. Finally, generated the high-quality, full-length, transcript isoform sequences and subjected to annotation using Blast2Go software. The cDNA sequences with the highest homology to the TCC genes (MuC6 (Accession No: MG980610), MuC7 (Accession No: MG980611), MuC8 β (Accession No: MG980612), and MuC9 (Accession No: MG980613) were identified from the mullet cDNA library.

2.2. Sequence characterization

The MuC6, MuC7, MuC8 β , and MuC9 sequences were crosschecked with databases using NCBI blastx and blastp (Agarwala et al., 2016). Multiple sequence alignment was performed using Clustal Omega (<http://www.ebi.ac.uk/Tools/msa/clustalo/>). A phylogenetic tree was constructed using the neighbor-joining algorithm with 5000 bootstrap replicates using MEGA 7 (Kumar et al., 2016), where human perforin was used as an outgroup. Prediction of domains and motifs of genes was carried out using the NCBI Conserved Domain Database (CDD) (<https://www.ncbi.nlm.nih.gov/Structure/cdd/wrpsb.cgi>), ExPASy PROSITE (<http://prosite.expasy.org/>), and SMART (<http://smart.embl-heidelberg.de/>). Sequence similarities and identities of different orthologs were identified using the EMBOSS Needle pairwise sequence alignment software (http://www.ebi.ac.uk/Tools/psa/emboss_needle/). Signal peptides were identified using the SignalP 4.1 online server (<http://www.cbs.dtu.dk/services/SignalP/>). N-linked glycosylation sites were identified using NetNGlyc 1.0 Server (<http://www.cbs.dtu.dk/services/NetNGlyc/>). Illustration of the domains, signature motifs, and sequence characteristics were done using IBS 1.0.3 (Liu et al., 2015).

2.3. Fish rearing, immune challenge, and collection of tissues

Healthy mullets with an average body weight of 100 g were obtained from the Sangdeok fishery in Hadong, Korea, and they were maintained under a controlled environment at 20 °C in 300-L tanks one week prior to experimentation. In order to determine the health conditions of the mullets, we followed the guidelines for health and welfare monitoring of fish in the experiments (Johansen Needham, J.R., Colquhoun, D.J., 2006). Normal fish anesthetics were used (Tricaine mesylate-MS222; 40 mg/L). For the tissue-specific spatial mRNA expression analysis, five healthy mullets were dissected and the head kidney, spleen, liver, gill, intestine, kidney, brain, muscle, skin, heart, and stomach were carefully removed; and isolated tissues were stored in -80 °C until they were used for RNA extraction. Blood was collected using syringes coated with heparin sodium salt (USB, USA). The blood was immediately centrifuged at $3000 \times g$ at 4 °C for 10 min to collect the peripheral blood cells.

To understand the temporal mRNA expression of TCC genes in response to pathogenic stimulation, LPS, poly I:C and *L. garvieae* were used as immunostimulants. Recommended culture procedures were used to prepare *Lactococcus garvieae* cultures. In brief, brain heart infusion (BHI) media supplemented with 1.5% salt was used to culture the bacteria, with incubation at 37°C. Purified LPS (1.25 µg/g; Sigma, USA), poly I:C (1.5 µg/g; Sigma, USA), and *L. garvieae* (1×10^3 CFU/µL) were dissolved in 100 µL of PBS separately and injected intraperitoneally; the control group was injected with 100 µL of PBS. Mullet head kidney and spleen tissues were collected from five immune-challenged fish and five fish injected with PBS at 0, 6, 24, 48, and 72 h post-injection.

2.4. RNA isolation and cDNA library construction

Total RNA was extracted from a pool of tissues (N=5 for tissue distribution and immune challenge) using RNAiso Plus (TaKaRa, Japan) and RNeasy spin column (Qiagen,

USA) following the manufacturer's protocol. The concentration (260/280 nm) and the quality of the extracted RNA was measured using a spectrophotometer and samples were subsequently electrophoresed using a 1.5% agarose gel. The isolated RNA was diluted to a concentration of 1 mg/mL, and cDNA was subsequently synthesized in a 20- μ l reaction mixture using the PrimeScript™ II 1st strand cDNA synthesis kit (TaKaRa, Japan) using 2.5 μ g of RNA. The cDNA was diluted 40-fold and stored at -80 °C.

2.5. Tissue distribution and Immune challenge expression analysis of TCC genes

The spatial and temporal expression of TCC genes were measured using the TaKaRa Thermal Cycler Dice Real Time System III. The synthesized cDNA was used as the template for qPCR with the following gene-specific primers: MuC6 (Forward (F): 5'-TCAACTGTCGGCCTGATGGAAC-3' / Reverse (R): 5'-CCCACTGATTCGCCCACTCTGTAT-3'), MuC7 (F: 5'-GTCATAGGCACACCCACCAAAGC-3' / R: 5'-GGCAGGAGAAGGAGACCACTGAA-3'), MuC8 β (F: 5'-ACCCAAGCTGCCATCCTGAAAC-3' / R: 5'-ACAGGACACACACAGTCACACCT-3'), and MuC9 (F: 5'-CCTGTCAGAACGGAGGCACTCTTA-3' / R: 5'-GCACGACTGGTGGTCTTGTCTTTG-3'). Mullet elongation factor 1 α (EF1 α) gene (Accession No: MH017208) (F: 5'-CCCTGGTCAGATCAGTGCTGGTTAT-3' and R: 5'-AGCGTCGCCAGACTTTAGGGATTT-3') was used as the internal control for qPCR. A 10 μ L reaction containing 3 μ L of the template, 5 μ L of Ex Taq™ SYBR premix (TaKaRa, Japan), and 4 pmol of forward and reverse primers for each gene was prepared. The thermal cycling profile used was as follows: initial denaturation at 95 °C for 10 s, followed by 45 cycles of denaturation, annealing and extension at 95 °C for 5 s, 58 °C for 10 s, and 72 °C for 20 s, respectively. The dissociation of TCC genes expression programmed for the final cycle at 95 °C

for 15 s, 60 °C for 30 s, and 95 °C for 15 s. The immune-stimulated head kidney and spleen cDNAs obtained at different time intervals were used for analyzing the mRNA expression changes of the TCC genes. All the reactions were performed in triplicate. Ct values were calculated and expressed in terms of fold-change following the Livak ($2^{-\Delta\Delta CT}$) method described previously (Livak and Schmittgen, 2001). All the samples were normalized to the Ct values of the MuEF1 α gene. For the spatial distribution of mRNA in healthy mullets, the relative mRNA level for each gene was calculated and compared to the sample with the lowest average Ct value. For the temporal expression profiles of head kidney and spleen tissues, the expression in PBS-injected mullets was used to calculate the relative fold-change difference in expression of TCC genes upon LPS, poly I:C, and *L. garvieae* injection. The data were calculated as the mean \pm standard deviation (SD) at significance level $P < 0.05$.

3. Results

3.1. Isolation and sequence analysis of full-length TCC genes from mullet cDNA

Full-length TCC genes were isolated from redlip mullet cDNA and were analyzed through sequencing. The fragment lengths of 5' untranslated region (UTR), open reading frame (ORF), 3' UTR, encoding amino acids length, molecular mass and theoretical isoelectric point were shown in Table 1. MuC6 comprised of two thrombospondin type 1 repeats (TSP1), a low-density lipoprotein receptor class A domain (LDLa), a MAC/Perforin domain (MACPF), a complement control protein domain (CCP), and a factor I membrane attack complex domain (FIMAC). MuC7 consisted of a TSP1 repeat, a LDLa domain, a MACPF domain, two CCP domains, and two FIMAC domains. MuC8 β comprised of two TSP1 repeats, a LDLa domain, and a MACPF domain. MuC9 consisted of two TSP1 repeats, a LDLa domain, and a MACPF domain (Figure 11). Sequence of each gene and the domain arrangement were shown in Figure 12. Amino acid sequence analysis of TCC genes revealed that MuC6, MuC8 β , and MuC9 have

a signal peptide cleavage site at residues 22–23, 37–38, and 26–27, respectively, while MuC7 does not have a signal peptide. N-linked glycosylation sites were found in MuC6 (¹⁵⁵NSTL¹⁵⁸, ⁹⁰⁴NLTR⁹⁰⁷), MuC7 (⁶⁸¹NPSL⁶⁸⁴), and MuC9 (³⁵⁸NLTE³⁶¹, ²⁵⁰NATV²⁵³).

Table 3: cDNA fragment information, gene length in amino acids, molecular mass, theoretical isoelectric point and domain positions of the redlip mullet C6, C7, C8 β and C9.

Gene	MuC6	MuC7	MuC8β	MuC9
Fragment length	3733 bp	3407 bp	2050 bp	2194 bp
5' UTR	400 bp	53 bp	81 bp	309 bp
3' UTR	510 bp	804 bp	226 bp	112 bp
Gene length	940 aa	849 aa	580 aa	590 aa
Molecular mass	106 kDa	93.6 kDa	64.6 kDa	64.8 kDa
pI	6.33	6.34	6.21	5.43

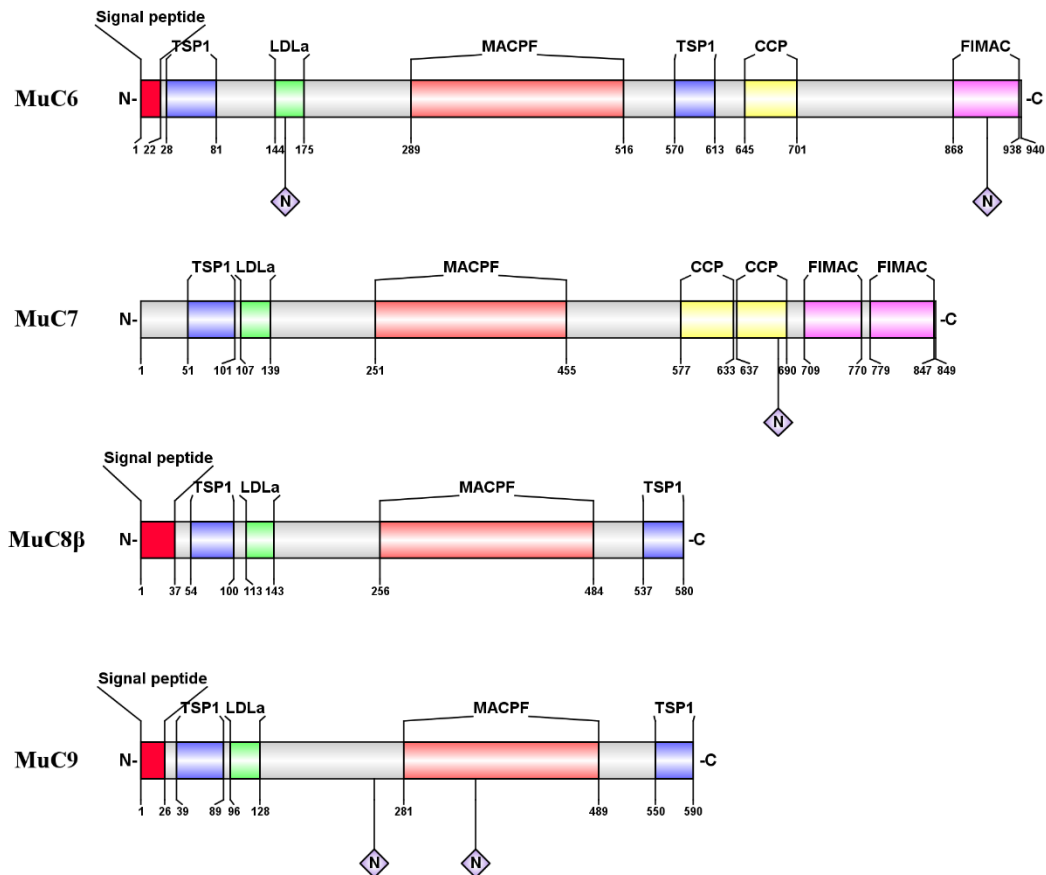


Figure 11: Structural representation of the redlip mullet terminal complement components (C6-C9): C6 (MuC6), C7 (MuC7), C8 β (MuC8 β), and C9 (MuC9). Maps and boundaries are based on the NCBI Conserved Domain Database (CDD). Abbreviations are corresponding to thrombospondin type 1 repeats (TSP1), low-density lipoprotein receptor class A domain (LDLa), MAC/Perforin domain (MACPF), complement control protein (CCP), and factor I membrane attack complex (FIMAC). Numbers correspond to the first/last residues in each module. Diamond shaped symbols are designated as Asn residues that have a potential to form N-linked glycosylation sites.

C6

ATTTGCATTCCGGAAACTCCACAGCTCTTTGCTCCCGTA -420
ACAAGAGAGTTATGCAAGAACTTTATTTTTATAAATCTGAATATAGTTTATTTTGAA -360
GTACTTTGGACACTGATGGTAAAATAGTGGAGAAAGAAAGGGTGGATCTTTGTTGG -300
GATGGGAAATACTGCTGGAGGCTTATATTCCTGCTCTCAATTCAGCCTCAGACCCAGC -240
AATCCACTTCAGCTCTGCCTGCAGTGCAGAGGCCACTAATCCACTTGTATCTTTTAGAA -180
GATTCTCAGCTGCCTAAACATTTAGCCAAACACGGAAAGGCACATATTTGTCGTTTGGT -120
GTCTGCTGAAGAGGACCTCAGTTCATGTGAGAAGGTGAAACAGCTGAGGACCCCGCTG -60
ATGGCCCTTGCAGCAGTCTGGTCTGGTCTGCAGCTCCTGGCTGCATATCTGTCCAGC 60
M A P C S S L V L V L Q L L G C I S V S
CTGGCTGTTTCTGTGACCGATACCTTGGAGCTCCTGGTGGTCTGTTCCAGCACATGC 120
L A C F C D R Y F W S S W S V C S S T C
AACTATGGGACGCAACAAGAGAGAGGATATTTAACTACAACGACAATTAATCTGGAAG 180
N Y G T Q Q R E R I F N Y N D N Y Y W K
AGCAGTTGCCCTCAGCTGTGTCGACATACGACCGGAGGGCTTGTTCACGCAGCCCTGT 240
S S E R Q L C F T Y D R R A C F T Q P C
CCAGTTAATGCCTGCTGACGGGTATGGGCCGGTGGTCCGACTGCTCCGCTGTGCCAGG 300
V N C L L T G Y G F W S D C S F C A R
AAACAGTTTCGGACCCCTCGGTGCGAGGGCCCTCCAGTTCGGTGGATCAGAGTGCAGC 360
K O F R T R S V Q R F S Q F G G S
CGGAGCTGSCAGAGGAGAGGCCCTCATCCCTCCAGAGAGTCCAGTTCAGCAGCGT 420
A E L A E E R P C H P S R E C Q L A P V
GACTGCAGAGCAGCTTAAGTGTGATAACGGGGCTGCATCAACTGCAGCACTAATCTGC 480
D C R D P E L D D S S C C I N S S L T
AACAGACAGAAGCTGTGGTGAATCTGATGAGAGGGACTGTCCAACCTCAAAT 540
N E N D D D D D S D E E L S N F K I
GTGTGTCGGCCGAGAAGAGAGTGGCCCGGGGGCTGATCTGGTGGGAAACGGGTTTGAT 600
V C P A E K R V A P G A D L V G N G F D
GTTCTAGCCAACGAGCCGAGGGGGGGCTCTGGACATCATGTTTCATGGGAGGACCTGC 660
V L A N E P R G A V L D I M F M G G T C
AAATCAGGAGACCTCAGAGCACCACACTTACCATCGAGTCCCTCATAACTTTGAGAAG 720
N I R R P Q S T T L Y H R V P H N F E K
TTTGACATCAAGGTAGGAACACTGGAAGACTTCAACACAGAGCCCAACCTCTGCGGACA 780
F D I K V G T L E D F N N E P H P L R T
GAAACCTGAGTGTAAAACACCCACTACAGAACGACAGAGCGGTAGCCAACAAGGCGAG 840
E T L S V K T F T T E R Q S G S Q Q G S
ATGTTCTCTCCCATCTTTACTTCTCAGGGTCATCTCAGTCCGAGCTCACTTCAAC 900
M F L F E Y
AAGGAAGCTTTGAAGCATCAAAGCAAAGGACTTAAATTTTCAGAGTGCATCAGGT 960
CTTCTGTGTCACGTTCAAGGTGAGGGACCCGGGGACCTCGTCTTGTCTGCCTTTC 1020
CTCCAGTTCCTCCATGCTCTTCTCTCGAGTACAATACGCCCTGTACAGGGACATCTTC 1080
CAGCGCTCCGGACACACTACTACAGCTCAGGGACGCTGGGAGGCCACTATGACTTGGTC 1140
TATCAGTACAGCCGAGAAGAGATCAAAGTTTCAGGTGTAACAGAAGGCATTTCAAAGGC 1200
TGCTGAGCCGAGACACCCTGGACCGTCATCCTCTACCCGAAACCCGTAGTGAACC 1260
CGATGCCATGATGACAGGATGACTGAGAAATATGAAGGCTCGTACATTAAAGGCATCAGAG 1320
AAGTCTTCTCCAAAGTGAAGGGCGGTGAACCCAGAGAAGCAGCAGCTCTGGCCTGGGAA 1380
AGCAGGGCCCTTCTCCGAGCCGGCATCCTACAAGAATGGGACAGTCTGTCTCTGGAC 1440
AAGCCAGCTGTGGTCAAGAGAGAAGTCTCCCATCATAGATCTGTCAGGGGATTCCT 1500
TGCGCTGCCACAAAGAGGAGGCCACTGAGGAAGGCCCTGCTGACGACTCCTGGATGAATTT 1560
L D E F
GATACCTGCAAGTGTCTCTTGTCCCAACAAGGGCAGGCCATTTCTCTCCGGCAGTGG 1620
D T C K C A P C P N N G R P F L S G T E
TGCAAGTGTGTTGTGCACTGGCACATTTGGCACCTACTGTGAGAAACGGGGCTCCTGAC 1680
C K C V C Q T G T F G T Y C E K R A P D
TACACTCAGAGGCGGTGGATGGTACTGGAGTGTGGGGTCCGTGGAGTCCGTGTGGGA 1740
Y T S E A V D G Y W S C W G F W S R C G
GCCTCCATGAAGAGACGAGGACGAGGGCGGTGTGATAACCTCCACCCCTCGCGGGAGGC 1800
A S M K R R R T R K C D N P P P L A G S
CAACCGTGGATGGTCTGACAAAACAGGAGGATCCATGTTACATCTCCATTTTCAAAA 1860
D P C D D P D R Q E D F C Y I S I F Q K
CAGGAGCCTGGCAATGACGAAGACTTCATGAAGGATGGGTAGATGAGCTGCCTCT 1920
Q E N D E D F I E G W V D E L F
GTTGGGAAGTCTCCGAGGCCGAAAGGGCTGACAACGGCTTCTCAGAAAGCCGAA 1980
G V E G C R R F K R P D N G E F L R K A K
CAGTATTACCTTACCGTGAAGGAGGAGATCCTGTGCTTCACTGGATTGAACAGAG 2040
Q Y Y L Y G E E E E I L C F T G F E Q E
GGTCCAGTTCATCACTTCCGCTGATGGAACCTGGACTGAAACAGCTGTAATAATGC 2100
G H O F I N C R P D G T W T E T R V K C
ATCAGAAATATGCTTCCGCTGATCTCCTGATGACATGACGCCGTTCGGAACAAA 2160
I R K L C L P P D L P D D M T P F P N K
GACCAATACAGAGTGGGCAATCAGTGGTTTGGATTGCAATGACAGGGGCTGAAACCG 2220
D Q Y R V G E S V G L D C N D T G L E P
CAGCCAGGAGCCCTACAGATGCTCCACAGTCTCCTGGAGCCCTCCGTTACCTGCT 2280
Q P G G L Y R C S N S L S W E P P L P A
GACCTCCGCTGTGCCGCTATAAATACTGATGAACCGGTGTTCTCTGACCCCTCAGTGGT 2340
D L R C A A I N T D E P V V P D P Q C G
CCAGGAAGAAGCGTCAGGGCTCCGACTGTGTCTGCTCCGAGGGGAGACCTGTCTTCA 2400
P G K K R Q G S D C V C L R R E T C L S
CAACCAGCGTGTATGTCTGATGATGAGAGTGGCGCCATCGTGTCAATCCCTC 2460
Q P D G V C V L N V D V G A I V S M S L
TGCTCTTCCACTTGGCCGTTGCCATGGTATCCACTTCTTCTGTTAGCGATGGTGTG 2520
C S F H S G R C H G D P L F F V S D G V
TGTGACCCAGCAGATTACGGCAAAGTGGAGTGGGCAAGTTCAGAGCTGCAATCTCCTC 2580
C D P A D S G K L E W A K F R A A M S S
AAGAGCTCCGTTCCAGGTGCCTTCCGAGCATGACACCTGCTACGAATGGGAGACCTGCT 2640
K S S V Q V P E H D P C Y E W E E C
GACGCTCAGAGGTGTGAATGCAAGGCCGCTCGGGACTCGCGCAAACCTTGATAACCCATG 2700
I A D D D P A R P D C K L E N D
TTCTGTGAACCTGACGAGGAATCAGAGGACCCGAGCATGAACCTCTGTTCCATGGCC 2760
I A A T T E N D P F S M L S S M
GCCCTCAAATGCGCCAGCTATGAGTTTGAATTTGCAAGTGAAGTGCCTGTGCGTCCAGA 2820
I R R A S T E F F I V S E E A A S R
TGA 2823
E
TCCTGCCAAAGCCTTCTGCTGCATCACACTTAACTTCTGCACTCATGAAAAGTGGTGT 2883
GTTTCACCACTGTTGAAATATGCTGATTAATAATGTTGTTTACCATCAAATGCTT 2943
AGACTTTAGCACATGTTGCAATAGAATACTATGCAACATGTTTACATGTGAATACTAAA 3003
AGCTACACTTAGCAGATTTAGCTGATCTCTGCTTACATCAAAGAGCAGCGAGGACAGCA 3063
ACCTGGTCTGAAATGATCAATTCAGCTCATAGGAATGAATAATGGGAAAAATAAAAT 3123
GATCTAACAAAATAAATTTTCAGTCACTCAGTGAATGAGTGAAGCTCAATGCTGATTGA 3183
TATACTATAGCAGGCACTATGGTATTGATGATGATGTTGTTATCAGAAATCAGAAATC 3243
TTTATACTCTCACTGCTTGTGCTCTTTCTCCATAAAATAGCAAGGTGACAGAG 3303
TCAAATGCAATAGAAATAAAAGTAAATA 3333

A.



C7

CCTGGACTCTGTTGAGTAATCACTCGCCACCTCCTCAACCTGCTGATTAT -53
ATGACTCCGAGAGTTACCGTGCAGGACCAAGAGGGCTGAACCGTGAGGAACACATC 60
M T P R V T V P D Q T R G L N A E E H I
ATGAAGTTGAATTGGTATGCACTCTGCCTCTTTGGTGCCTGTCACCTTTTGGTACCA 120
M K L N W Y A A L P S L V L S L F L S P
GTTTGGTGTGACGAGCTGTAACCTCCAACTGGGACCTTATGGAGAGTGGTCTGAGTGT 180
V W C Q Q P V N C Q **N C P Y G E W S E G**
GATGGCTGCACAAGGACAAAGGTACGAACCTGCCACGTGGATGTTATGCCAGTATGGT 240
D G C T R T K V R T R H V D V Y A Q Y G
GGCATGCCATGTTGAGAGAAGCCACAAAACGAGTCTGTGTCTCAGAGAAGCAATGC 300
E M E C S G E A T Q T Q S C V S Q K A G
CCCTGGAAACAGGTTGTGAAGACAGGTTCCGCTGGCCCTCAGTCAAGTATCAGCCAG 360
H L E T G C
TCTCTGGTATGTAACGGAGACAGGACTGTGAGGATGGATTGGATGAGCGACACTGTGCC 420
S L V C N R D N D E D L D L D F R B B A
CAAGACAGCAGCCAGTATATGTGACAATGACAAAACACCTCCTAACTGACTTCACA 480
Q D S S Q Y I C D N D K T P P N S D F T
GGCAGAGGTACGAGCTTCAACAGGAAACTGAGGGCAGGTGTGATCAACACTTAAGC 540
G R G Y D V L T G K L R A G V I N T L S
TTCGGAGGTGAGTGGAGAAAGTGTTCAGGGCCGACATAAGTCTACTACAGACTGCCA 600
F G G Q C R K V F S G D H K V Y Y R L P
CAGAACATCCTGAGATACAACCTTGGAGTAAAGTGGACAATGAAGACAGCGATGAATCC 660
Q N I L R Y N F E V K V D N E D S D E S
TACGAGAGCTTGGTCTATGTGACGACATCCAGTCCAACGATGCTGGGGCAGCAC 720
Y E S S W S Y V Q H I Q S N A L L G H D
CGTCGCACCTCCACAAGAGCTCACTGACAACAAGGAGTACAACCTTATAATCTGAAG 780
R R T F H K E L T D
AATAAAGTGGAGCTGGCCAGTTTCAAACTCTGCCCCAGTATCTGACTCTGTCCGAA 840
GGCTTCTGGAAGGCTTGTCTCACTCCCTACACATATGACTACTCGGCCTACGCCAG 900
CTGTTGCAGACATATGGCACACACTATCTCTGAAGGCTCACTTGGAGGCGAATACCAG 960
GGATTGTTGGAGTTGACCATCAAGCGCTCGCCTCAACAGTACCAGATATAGAGTAC 1020
CAGAGGTGTTGGAGAAAAGTAAAGCGTCTGTTCTTCAAGAAAAGTCAAACTGTGTGT 1080
GAAAAATTAATAAATCCTTATCATCGAGCTATGCAAAATGTACACAAGATGCCATC 1140
AAGGTCAATGTCTTCGGAGGAGATCCAGCCTTAATAAGCGGTTGACTCTCTGGATTG 1200
GACAACCCAGAGGTTAACGGAGAGCTCTATGACAACCTGGCCCTGCTCTGCAAGATTTT 1260
CTTGAAGTATAGACCAGAAGCTGCGACCCCTGTATGAGCTGGTGAAGAGGTGCAGTGT 1320
GCGGGTTTGAAGAAGCTCCACCTGAAAAGGGCCACTGAGGAGTACCTGGCTGAGGAGAT 1380
L A E E H
CCCTGTCACTGCCGCCCTGCCAGAACAACGGTCAAGCCACTGCTGGCAGGACCCAGTGT 1440
P C H C R P C Q N N G O P L L A G T E C
CGCTGTATTTGCCGSCAGGAACGTGAGGAAAGCCTGCGAGAGGGGAGCTGTGATTGGA 1500
R C I C R P G T S G K A C E R G A V I G
GAGCAACCGAGGATGATACATGGCAGTTGGAGCTGCTGGTCTTCTGGGGATCCGCTCT 1560
E Q P G V I H G S W S C W S S W G S C S
GGAGGTCAAATGTCAAGGACCAAGAGCTGCAACAACCCCGCTCCAGAGGAGGTGCCAC 1620
G G Q M S R T R S C N N P A P R G G R H
TGCAATGGACCGCAGGTGGAAGGAAAGCCTTGTGAAGACCCAGACATCCAGCACTACAG 1680
C I G P Q V E G K P C E D P D I Q H L Q
ATGATGAACTCAGTCTCAGTCTTTCTATACCTCCACAAAACCTGTTGGGGTGGCT 1740
M M E P Q C F S L S I P P P K T **C G L P**
CCAAGCCTCAGGAATGATTATTTCTGGATCCAAAGATTTCTACCTGGTTGGGAACAG 1800
F S L R N G F I L D P K D F Y L V G N T
GTGCGTTACTCCTGCATAGACGGGTATATATCAGTGGAAACGCTGTGCCAGGTGCAT 1860
V R Y S C I D G Y Y I S G N A V A R C T
GAAAAATCAGATGTTGAGCACAAGTGGAGGTTTGTAAAAGTCCACATGTTGGAGTCCC 1920
E N Q M W S T E V R V Q K S S T **C G S P**
TCCCTTAATAGTTTAGTCATAGGCACACCCACCAAGTGCCTACCAGATTTGGAGAAAG 1980
S L N S L V I G T P T K A A Y Q I G E T
GTGTTCTGTCTGTCACCAAGGGTCTGTGCTGGACGGTGAAGTGCAGAGATCATATGC 2040
V F L S C P K G S V L D G E M S E I I C
AATCCAGCTTTCAGTGGTCTCCTTCTCCTGCCAGTGTCTATTGTAAGCAGAGCCACA 2100
N P S L Q W S P S E A S A H C K A E P T
GCTCACTCTCCTCGGCCAACCTGAAGTGTAAAGTGTGGAAACTGTAGGAAGAACTCGG 2160
A H S P P A N L
TGTGTTTGAATAATGCCATTTCACTGTCCGACTTCTCTGAGTGTGTGTGTCAGACTGGGC 2220
TCAATCCAAACCCGTTATTAGTGTGTTGTCAGCTCGGAGCTCTGCAGTGCATGGGCCGG 2280
AGCTTACGTTGGCCAGCGACAGTACTGTGATCGGCCAGAGAAGCGTTCAGCGCTTGC 2340
AAGGACTGCCAGCCGGGACAACCTGCGAAGAAATCAGCAAGACAGTCCGATGCCAAAT 2400
ACATCAGACTGCCCTAAGGACTCTGCCCGCTGTGCGTTAGCTCTGGTGCCGGCGGTGCT 2460
TCCGTTACTATGAGCGAATGTGAGGTGGGGCCAGGAGGTGCGGGGAGCAGGTCAAT 2520
GTGATCAGTATTGAGCCTTGTCCAGAA**TAA** 2550
C P E
AATGACCTGAACCTGAATAAGAAAACGCTTATTTTATATTTGTCATAAAAAGACTGATG 2610
ATTGAAGCAATTTGTTCTCAGATACTGAAATGCTTAGTATTTTGAATAAGAAAAT 2670
TAATAAAATGTTTTCAGAAATTTTGTGTCATTGTTGACAATGTCAGTGAATTT 2730
GATGATTTAGAAATGTTTATTTGTGAAATGCTTCCCTTTGGCAATTTCCAAAGCAG 2790
CAGTATTTTCGGGGGATTTGGAGAAATCTCACTTGTTTTGAAGCTTTGAATACACTTT 2850
TATTCATAGAGATGGCATTGAGAGTACATGCTAAGCAAGAGATGATGATAAATGAA 2910
AAGATTTTATTTTCATGATGAGTACATTAATTCACCCCTGACCTGATTTAGCTGAT 2970
GGACTGTCGCGCCTTCTATGGAATGTCAGGAGTAAAGAAACAGGGGTTTCTGTTTTC 3030
ACTCATTAAACACTTAAATCATGTGCTTCCGACATATCAGTTTGAATCATTTTGGAG 3090
CTAGTCCCATATGAACAGTTGATATGCCAATCCAGTTCATGCCATTGGATGCCTAGCA 3150
CTAGACTTAAACCTTTTCTGTAAGCCCATAGGTGTCTGACCATTTTACATGCTTAAA 3210
ATACTAAAATTTCTTTTATAATAAAAATAAATACTTTTAAACACAGGCTTTGGGC 3270
CTTTAAATATGGAGTAATGTGTCTTAACCAAGATGCATCCATCCAGGGAACTTCA 3330
CAAAGTGGCTAAAACATCTCACT 3354

B.

3.2. Alignment of TCC amino acid sequences and phylogenetic analysis

The amino acid sequences of the TCC genes were aligned with corresponding orthologs, and results showed the highest sequence identity of MuC6 with *Siniperca chuatsi* (85.8%), MuC7 with *Monopterus albus* (89.2%), MuC8 β with *Monopterus albus* (89.8%), and MuC9 with *Stegastes partitus* (82.2%) (Table 2). The phylogenetic tree was generated from the amino acid sequence alignment with orthologs and it showed each gene clustered into their original taxonomic positions in separate clades (Figure 13). Moreover, mullet TCC genes were evolutionarily positioned with their corresponding highest sequence identity orthologs. Multiple sequence alignment of TCC genes showed a high conservation of domains; most cysteine residues were highly conserved in their corresponding orthologs (Figure 14).

Table 4: Percent identity and similarity of C6, C7, C8 β and C9 orthologs from different species compared to MuC6, MuC7, MuC8 β and MuC9

Scientific Name	Accession	Species	Similarity (%)	Identity (%)
<i>Siniperca chuatsi</i>	AKA66307.1	Mandarin fish C6	85.8	76.0
<i>Oncorhynchus mykiss</i>	NP_001118093.1	Rainbow trout C6	75.4	59.7
<i>Salmo salar</i>	NP_001167046.1	Atlantic salmon C6	74.6	58.9
<i>Danio rerio</i>	NP_956932.1	Zebrafish C6	65.4	49.5
<i>Homo sapiens</i>	AAA59668.1	Human C6	59.0	43.8
<i>Monopterus albus</i>	XP_020479067.1	Asian swamp eel C7	89.2	80.0
<i>Oncorhynchus mykiss</i>	NP_001118090.1	Rainbow trout C7	74.8	63.0
<i>Danio rerio</i>	XP_021329099.1	Zebra fish C7	68.4	53.5
<i>Salmo salar</i>	NP_001133245.1	Atlantic salmon C7	63.9	49.5
<i>Homo sapiens</i>	NP_000578.2	Human C7	56.8	43.6
<i>Monopterus albus</i>	XP_020474047.1	Asian swamp eel C8 β	89.8	83.0
<i>Salmo salar</i>	XP_014047216.1	Atlantic salmon C8 β	82.0	70.8
<i>Oncorhynchus mykiss</i>	AAL16647.1	Rainbow trout C8 β	78.9	68.8
<i>Danio rerio</i>	NP_001243652.1	Zebra fish C8 β	72.1	57.1
<i>Homo sapiens</i>	NP_000057.2	Human C8 β	64.6	47.2
<i>Stegastes partitus</i>	XP_008274386.1	Bicolor damselfish C9	82.2	71.4
<i>Salmo salar</i>	XP_013994122.1	Atlantic salmon C9	74.5	59.8
<i>Oncorhynchus mykiss</i>	NP_001117898.1	Rainbow trout C9	74.1	59.5
<i>Danio rerio</i>	NP_001314855.1	Zebra fish C9	56.7	41.4
<i>Homo sapiens</i>	AAH20721.1	Human C9	50.2	34.6

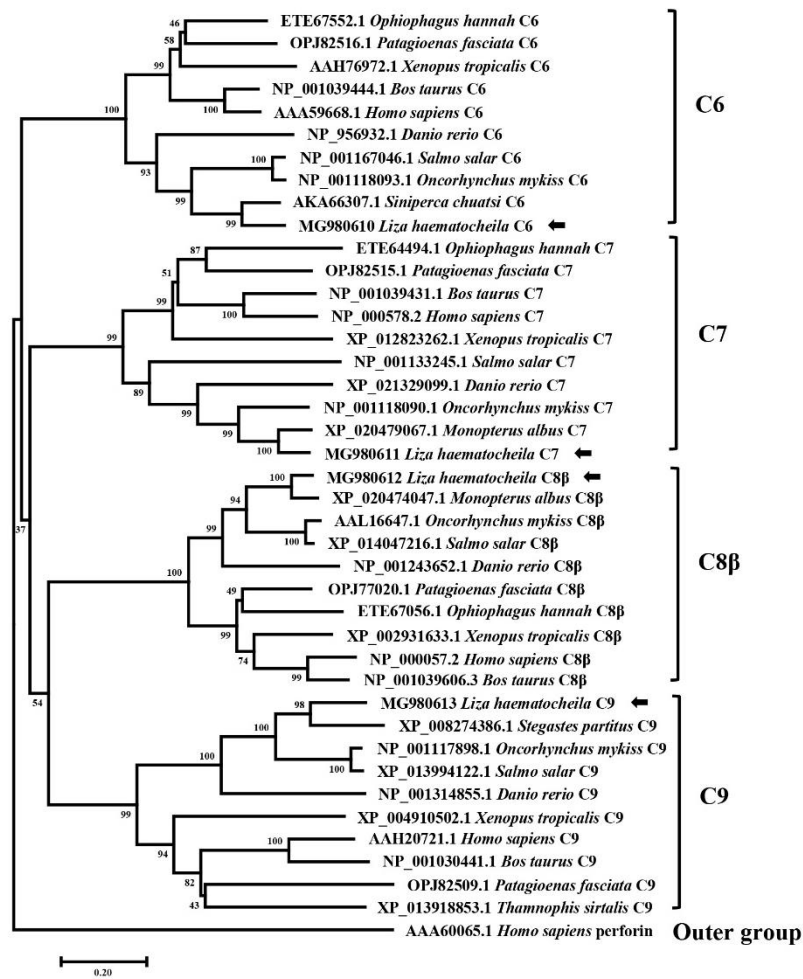


Figure 13: Phylogenetic tree of Mullet TCC genes.

The evolutionary development of each gene was analyzed with its different homologs under different taxonomic groups based on the multiple alignment profile of the protein sequences generated by the neighbor-joining method using MEGA 7.0 software with 5000 bootstraps.

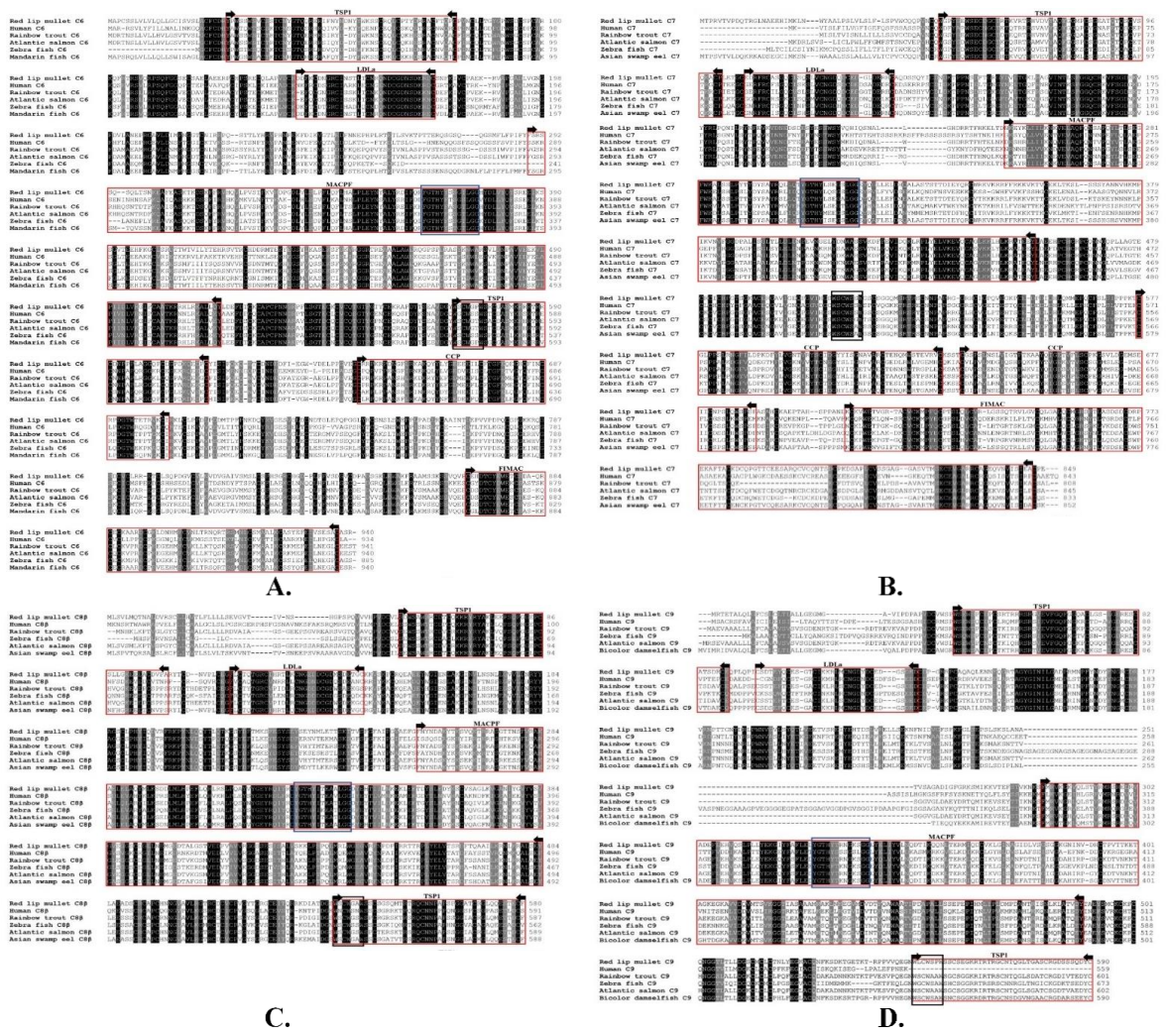


Figure 14: Multiple-sequence alignment of MuC6 (A); MuC7 (B.); MuC8 β (C.); and MuC9 (D.); and its orthologs from selected organisms. Sequence alignments were obtained using Clustal omega tool. The conserved domains are marked with red boxes and C-mannosylation motif (WX₂WX₂W), in the C-terminal TSP1 domain is marked with a black box, and ((Y/W/F)G(T/S)H(F/Y)X₆GG) signature motif marked in the blue box. A black arrow indicating the start and end of the specific domain. Fully conserved residues shaded in black, amino acids with similar properties shaded in ash color.

3.3. Spatial mRNA expression of TCC

MuC6, MuC7, MuC8 β , and MuC9 were found to be ubiquitously expressed in twelve different tissues assessed in this study (Figure. 15). MuC6 showed the highest expression in the heart (47.48-fold), spleen (24.56-fold), and muscle (22.97-fold) tissues; however, it was least expressed in the brain (Figure 15A). MuC7 was highly expressed in the liver (1312.49-

fold) and in muscle (175.36-fold); however, it was least expressed in the gill (Figure 15B). MuC8 β showed the highest expression in liver (147868.81-fold) and stomach (3881.97-fold) tissues; in contrast, least expression of MuC8 β was observed in the blood (Figure 15C). MuC9 was showed the highest expression in the liver (8082.05-fold), whereas the lowest in the kidney (Figure 15D).

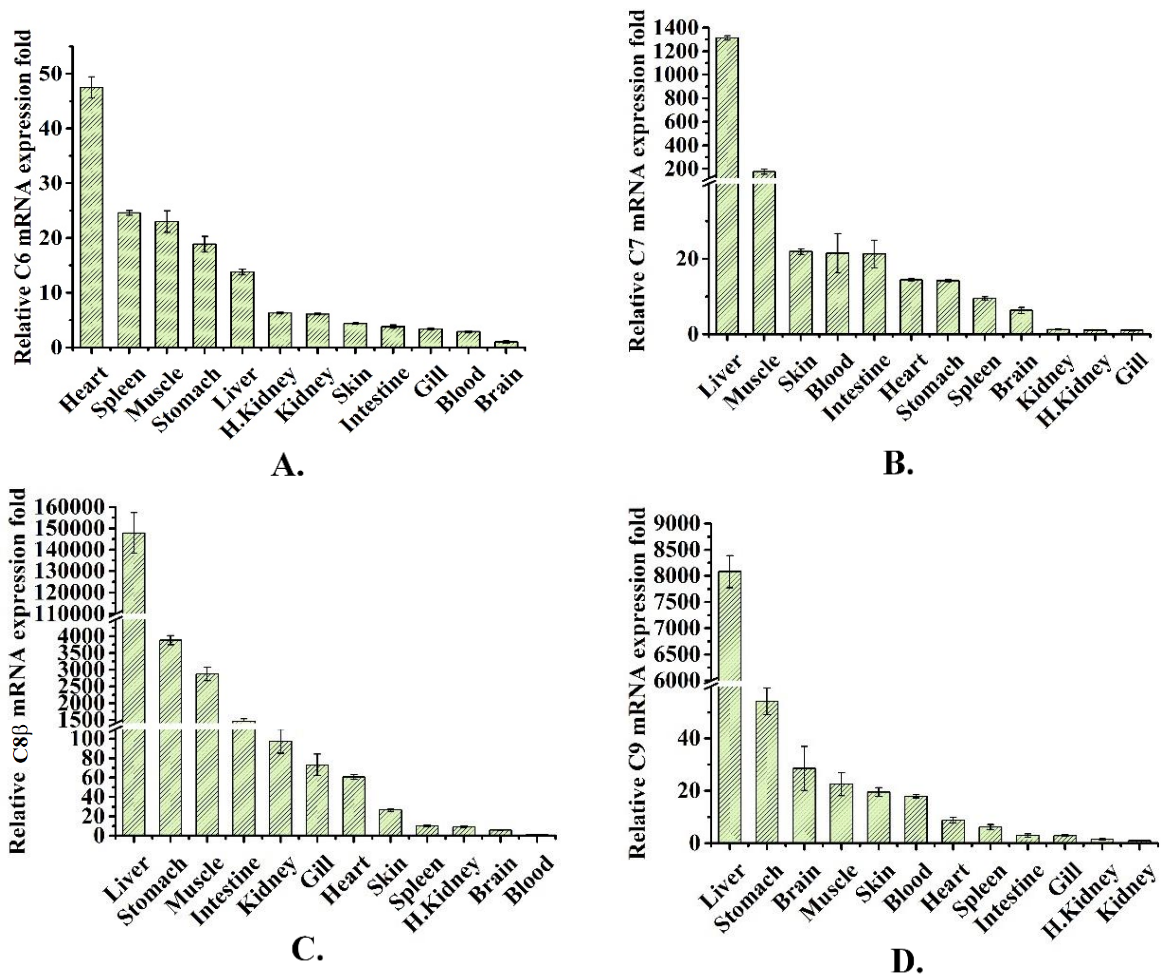


Figure 15: MuC6 (A), MuC7 (B), MuC8 β (C), and MuC9 (D) tissue-specific transcript expression analysis of healthy mullets under normal physiological conditions.

The Livak method was used to calculate the relative mRNA expression of each tissue and Mullet elongation factor 1 α (EF1 α) gene was used as the reference gene in the quantitative real-time polymerase chain reaction (qPCR) experiment. The data represented as mean values (n=3) \pm standard deviation (SD).

3.4. Induced expression of TCC genes after infection with LPS, Poly I:C, and *L. garvieae*

TCC gene transcripts in the head kidney and the spleen tissues were significantly upregulated after immune challenge with LPS, poly I:C, and *L. garvieae*. The head kidney showed significant upregulation of MuC6 expression at 72 h after infection with *L. garvieae* (Figure 16A). The spleen showed upregulation of MuC6 expression at 24 h after infection with either LPS or *L. garvieae* (Figure 16B). The highest expression of MuC7 was observed in both head kidney and spleen at 72 h post-injection of *L. garvieae*. LPS and poly I:C injections revealed the significant upregulation of MuC7 in both head kidney and spleen at 6 h post-infection (Figure 16C-D). MuC8 β showed the highest expression in the head kidney 48 h after injection with poly I:C and *L. garvieae* (Figure 16E). Moreover, spleen tissue showed prominent upregulation of MuC8 β expression after 24 h, 48 h, and 72 h in response to injection with LPS, poly I:C, and *L. garvieae*, respectively (Figure 16F). MuC9 expression was upregulated in the head kidney at 48 h after injection with poly I:C and *L. garvieae* (Figure 16G). MuC9 expression also showed significant upregulation in the spleen at 48 h and 72 h time points after injection with *L. garvieae* (Figure 16H).

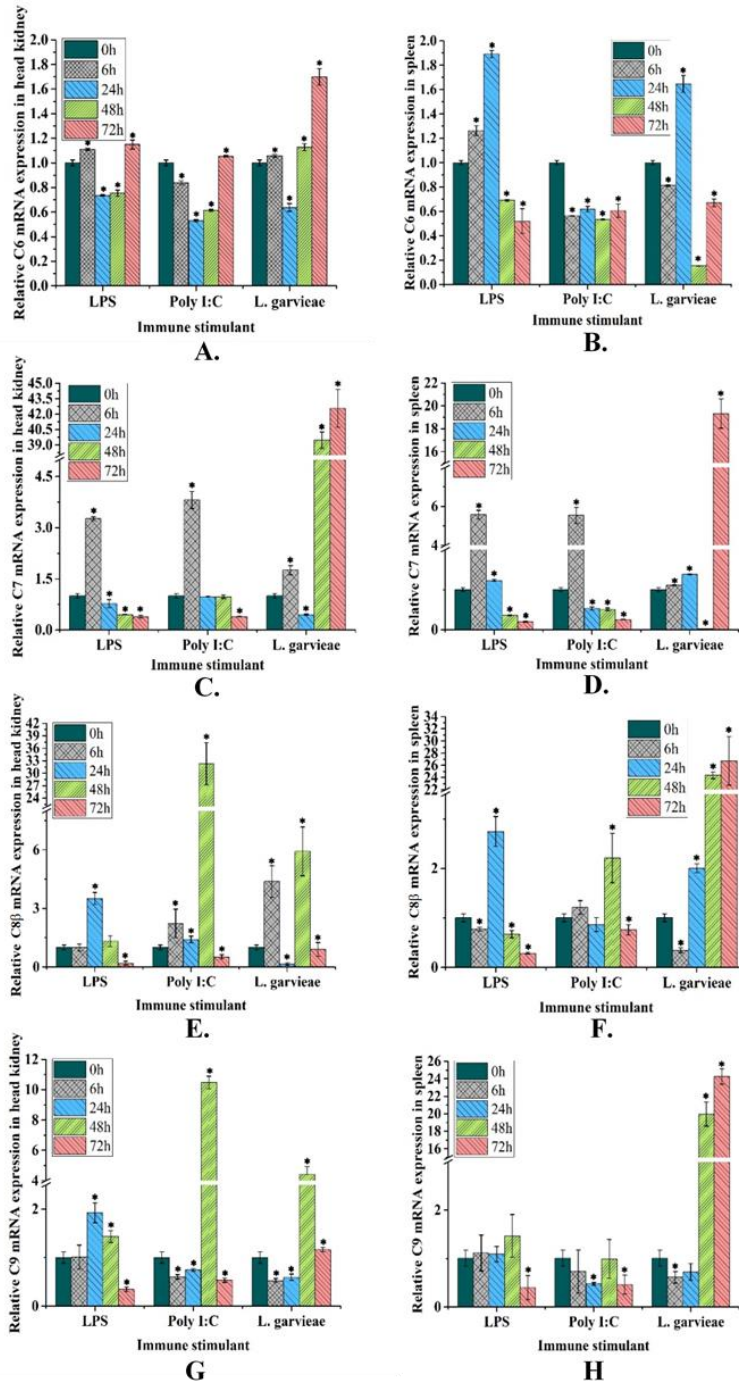


Figure 16: Temporal expression profiles of *MuC6*, *MuC7*, *MuC8 β* , and *MuC9*.

Expression in head kidney (A, C, E, G) and spleen tissues (B, D, F, H) after pathogen-associated molecular patterns (PAMP) (LPS and Poly I:C) and pathogenic (*L. garvieae*) challenges. The Livak method was used to calculate the fold changes in mRNA expression and Mullet elongation factor 1 α (EF1 α) gene was used as a reference gene in the quantitative real-time polymerase chain reaction (qPCR) experiment. The relative fold changes in expression were compared with those of PBS injected control at different time points. The vertical bars represent the mean values ($n=3$) \pm SD. Significant differences compared to the blank (0 h) with $P < 0.05$.

4. Discussion

TCC components gather to form the MAC that produces pores in the plasma membrane of pathogenic cells, leading to lysis disrupting the membrane structure. The assembly of the MAC is initiated by the proteolytic cleavage of C5 into C5a and C5b. C5b binds sequentially with C6, C7, C8, and multiple copies of the MAC pore-forming subunit C9. Factor I is responsible for cleaving the alpha chains of C4 β and C3 β in the presence of C4-binding protein and factor H, respectively (Blom et al., 2003). Mammalian TCC molecules, C6, C7, C8, and C9, share many common structural motifs and domains, including the TSP domain, the LDLR class A domain, the MACPF domain, and the EGF-like domain; moreover, C6 and C7 consist additional CCP and FIM domains at their C terminal. All TCC components are present in mammalian, avian, amphibian, teleost, and cartilaginous fish genomes, with the exception of C9 being absent in the avian genome (Nonaka, 2014). The evolution of the TCC genes can be identified at the differentiation of phylum Chordata to subphyla Urochordata, Cephalochordata, and Vertebrata. The duplications of the C6, C7, C8, and C9 genes appeared in the occurrence of the vertebrate lineage after its divergence from the urochordates and the cephalochordates. There have also been no reports about TCC genes in the genomes of sharks and lampreys. Additionally, there are proteins that contain the MACPF domain but lack the other TCC-specific domains, that have been found in many organisms, including invertebrates (Haag et al., 1999; Mah et al., 2004), protozoans (Kaiser et al., 2004), plants (Morita-Yamamuro et al., 2005), and bacteria (Ponting, 1999). Other TCC-specific domains such as TSP1, LDLa, CCP, and FIMAC regulate the interactions of the complement components. TSP1 domains are involved in cell-cell interactions, inhibition of angiogenesis, and apoptosis (Guo et al., 1997; Iruela-Arispe et al., 1999). Cysteine-rich repeats in the LDLa domain play a central role in mammalian cholesterol metabolism. The N-terminal LDLa domain binds lipoproteins (Yamamoto et al., 1984). Other homologous domains in TCCs and in related receptors are

functionally unrelated. The CCP or sushi domain is involved in many recognition processes, including the binding of several complement factors to fragments of complement proteins (Blom et al., 2003; Reid and Day, 1989). The FIMAC domain is involved in multiple interactions critical for the function of Factor I. FIMAC directly contacts with the active site of specificity protein 1 (SP1) domain, though it adopts a fold found in serine protease inhibitors. FIMAC domain mostly induces the SP1 transcription factor by structural changes (Sanchez-Gallego et al., 2012).

Teleosts appear to have a functionally active complement system activated by three pathways. According to previous studies, complement proteins occur in different isoforms that are encoded by multiple copies of the same gene (Mutsuro et al., 2005; Zarkadis et al., 2001). In this study, we elucidated the lytic process of TCCs based on nucleotide and protein sequences, as well as on analyses of the temporal and spatial expression of MuC6, MuC7, MuC8 β , and MuC9. MuC6 carries two copies of the TSP1 domain, which may help in regulating protein interactions with other MAC molecules (Iruela-Arispe et al., 1999). MuC7 consisted of two CCP domains and two FIMAC domains, which have been implicated in the capacity of C7 to interact with the C5b-C6 complex. Previous studies have shown that teleost TCCs have similar motifs as those found in lytic components of complement system (Kazantzi et al., 2003). Furthermore, in mammals, C8 β is involved in at least two binding interactions at the time of MAC formation, and the MACPF domain binding site was found to be indispensable to the formation of the MAC (Brannen and Sodetz, 2007). C9 is important in creating a cylindrical transmembrane hole to weaken the membrane integrity of the target cell (Lovelace et al., 2011). C9 shares common structural and functional behaviors to the perforins which are effector molecules secreted by cytotoxic T cells and natural killer (NK) cells (Shinkai, 1989). All the mullet TCC genes contained a C-mannosylation motif (WX₂WX₂W) within the C terminal TSP1 domain which is important in the folding or targeting of substrate proteins

(Hofsteenge et al., 1999; Ihara et al., 2011). TCCs share a common signature motif ((Y/W/F)G(T/S)H(F/Y)X₆GG) identified in the middle of the MACPF domain, which is highly conserved in the MACPF superfamily of proteins. Furthermore, potential N-glycosylation sites in the sequences may suggest that glycosylation is important in the function of proteins (Imperiali and O'Connor, 1999). All the conserved cysteine residues are important for the correct folding of the TCC genes (Miseta and Csutora, 2000).

Expressions of C7, C8 β , and C9 are high in the liver as it is the primary site for production of the complement components. It controls innate immunity by producing 80–90% of complement components and pattern recognition receptors (PRRs), which are important in immune defense mechanisms against bacterial agents and in complement activation (Gao et al., 2008). Similarly, high C6 expression in heart tissues might be due to its involvement in the clearance of blood-borne substances in fish (Press and Evensen, 1999). Mullet TCCs are similar to other complement components that are acute phase proteins of hepatic origin (Witzel-Schlömp et al., 2001). Upregulated expression of TCCs in the stomach may be due to the host bacterial and parasite interactions in the fish intestinal ecosystem (Wu et al., 2016). High expression of TCCs in muscle tissue may be due to the activation of early complement pathway genes. In mammals, anaphylatoxin receptors have been found on muscle cells and they stimulate various inflammatory responses, contraction of smooth muscle cells, and an increase of vascular permeability (Wetsel, 1995).

Classical immune organs such as head kidney and spleen are recommended to study the immune modulated transcriptional response in teleosts (Foey and Picchiatti, 2014). Moreover, spleen and head kidney are the main immune responsive tissues that removes pathogens in host organism. According to the temporal expression results, *L. garvieae* can trigger the immune tissues like head kidney and spleen. Previous studies also suggest that the expression of TCCs significantly changes in the head kidney and spleen of grass carp in

response to the immune challenge with *Aeromonas hydrophila* (Shen et al., 2012a); in the head kidney of rock bream in response to infection with *Edwardsiella tarda*, *Streptococcus iniae*, LPS, and rock bream iridovirus (Wickramaarachchi et al., 2013a); and in the head kidney of large yellow croaker in response to the immune challenge with *Vibrio alginolyticus* (Guo et al., 2016). TCC gene expression was significantly upregulated in the head kidney and spleen of redlip mullets, suggesting their involvement in the innate immunity of the fish against pathogenic bacterial infection. Different expression patterns between the head kidney and spleen could be due to the difference in tissue of origin and the differences of cell composition. The leukocytes in these tissues contain different cell types (T cells, B cells, macrophages, monocytes, dendritic cells, etc.). Additionally, each individual cell type is responsible for secreting different kinds of complement molecules (Lubbers et al., 2017). Therefore, the expression patterns of these cells accounted for the expression pattern differences. Previous experimental tests observed that the incubation period of the disease is very short in case of bacteria with high virulence (Vendrell et al., 2006). Therefore, the expressions 72 h post infection with *L. garvieae* is high possibly due to the activation of the bacteria in the host after 2–3 days (Vendrell et al., 2006); it may be downregulated later. Significant upregulation of MuC7, MuC8 β , and MuC9 expression upon injection with poly I:C suggest that the complement pathway might be activated upon viral infections (Tegla et al., 2011). Since some complement genes showed non-significant expression upon the poly I:C stimulation, the expressions of complement molecules may not be consistent (Tam, n.d.). Reasons like excessive early pathway activation in some complement molecules, and various inhibitors and regulators in complement activation are involved with such inconsistencies (Lubbers et al., 2017). Downregulation of the expression of TCCs may indicate that excessive early pathway activation, and various inhibitors and regulators in the complement system regulate the expression of complement components (Lubbers et al., 2017). Furthermore, CD59-like

molecules can be mimicked, or their conformation can be altered by foreign invaders to protect them from the host immune system (Klerk, 2009). These results indicate that the TCCs of the redlip mullet may be involved in immunity against Gram-positive bacteria and enveloped viruses. However, the regulatory mechanisms underlying these genes in the context of the complement system have not yet been fully elucidated.

In summary, we isolated and identified full-length TCC genes from the cDNA of redlip mullet and characterized them with various bioinformatic tools to get a comprehensive understanding of the molecular arrangement of TCCs. Moreover, MuC6, MuC7, MuC8 β , and MuC9 expression was measured using qPCR to identify spatial and temporal expression patterns upon injection with different immune stimulants. Results revealed the highest expression of TCC genes in the liver and heart of a healthy mullet. Expression of TCCs in head kidney and the spleen tissues showed their potential role in immunity against pathogenic infections. The findings from this study provide new and comprehensive knowledge about the terminal complement components of redlip mullet, as well as provide insights into the lytic complement pathway of teleosts.

References

- Agarwala, R., Barrett, T., Beck, J., Benson, D.A., Bollin, C., Bolton, E., Bourexis, D., Brister, J.R., Bryant, S.H., Canese, K., Charowhas, C., Clark, K., Dicuccio, M., Dondoshansky, I., Federhen, S., Feolo, M., Funk, K., Geer, L.Y., Gorenkov, V., Hoepfner, M., Holmes, B., Johnson, M., Khotomlianski, V., Kimchi, A., Kimelman, M., Kitts, P., Klimke, W., Krasnov, S., Kuznetsov, A., Landrum, M.J., Landsman, D., Lee, J.M., Lipman, D.J., Lu, Z., Madden, T.L., Madej, T., Marchler-Bauer, A., Karsch-Mizrachi, I., Murphy, T., Orris, R., Ostell, J., O'sullivan, C., Panchenko, A., Phan, L., Preuss, D., Pruitt, K.D., Rodarmer, K., Rubinstein, W., Sayers, E., Schneider, V., Schuler, G.D., Sherry, S.T., Sirotkin, K., Siyan, K., Slotta, D., Soboleva, A., Sousov, V., Starchenko, G., Tatusova, T.A., Todorov, K., Trawick, B.W., Vakarov, D., Wang, Y., Ward, M., Wilbur, W.J., Yaschenko, E., Zbicz, K., 2016. Database resources of the National Center for Biotechnology Information. *Nucleic Acids Res.* 44, D7–D19. <https://doi.org/10.1093/nar/gkv1290>
- Agnew, W., Barnes, A.C., 2007. *Streptococcus iniae*: An aquatic pathogen of global veterinary significance and a challenging candidate for reliable vaccination. *Vet. Microbiol.* 122, 1–15. <https://doi.org/10.1016/j.vetmic.2007.03.002>
- Andersen, K.M., Madsen, L., Prag, S., Johnsen, A.H., Semple, C.A., Hendil, K.B., Hartmann-Petersen, R., 2009. Thioredoxin Txn11/TRP32 is a redox-active cofactor of the 26 S proteasome. *J. Biol. Chem.* 284, 15246–15254. <https://doi.org/10.1074/jbc.M900016200>
- Antolovich, M., Prenzler, P.D., Patsalides, E., McDonald, S., Robards, K., 2002. Methods for testing antioxidant activity. *Analyst* 127, 183–98.
- Arnér, E.S.J., Holmgren, A., 2000. Physiological functions of thioredoxin and thioredoxin reductase. *Eur. J. Biochem.* 267, 6102–6109. <https://doi.org/10.1046/j.1432-1327.2000.01701.x>
- Aslund, F., Ehn, B., Miranda-Vizuete, A., Pueyo, C., Holmgren, A., 1994. Two additional glutaredoxins exist in *Escherichia coli*: glutaredoxin 3 is a hydrogen donor for ribonucleotide reductase in a thioredoxin/glutaredoxin 1 double mutant. *Proc. Natl. Acad. Sci. USA* 91, 9813–9817. <https://doi.org/10.1073/pnas.91.21.9813>
- Aybar, L., Shin, D.H., Smith, S.L., 2009. Molecular characterization of the alpha subunit of complement component C8 (GcC8 α) in the nurse shark (*Ginglymostoma cirratum*). *Fish Shellfish Immunol.* 27, 397–406. <https://doi.org/10.1016/j.fsi.2009.05.020>
- Bajpai, V.K., Sharma, A., Kang, S.C., Baek, K.H., 2014. Antioxidant, lipid peroxidation inhibition and free radical scavenging efficacy of a diterpenoid compound sugiol isolated from *Metasequoia glyptostroboides*. *Asian Pac. J. Trop. Med.* 7, 9–15. [https://doi.org/10.1016/S1995-7645\(13\)60183-2](https://doi.org/10.1016/S1995-7645(13)60183-2)
- Balcázar, J.L., Gallo-Bueno, A., Planas, M., Pintado, J., 2010. Isolation of *Vibrio alginolyticus* and *Vibrio splendidus* from captive-bred seahorses with disease symptoms. *Antonie van Leeuwenhoek, Int. J. Gen. Mol. Microbiol.* 97, 207–210. <https://doi.org/10.1007/s10482-009-9398-4>
- Bayly-Jones, C., Bubeck, D., Dunstone, M.A., 2017. The mystery behind membrane insertion: a review of the complement membrane attack complex. *Philos. Trans. R. Soc. Lond. B. Biol. Sci.* 372, 20160221. <https://doi.org/10.1098/rstb.2016.0221>

- Berlett, B.S., Stadtman, E.R., 1997. Protein oxidation in aging, disease, and oxidative stress. *J. Biol. Chem.* 272, 20313–20316. <https://doi.org/10.1074/jbc.272.33.20313>
- Bhakdi, S., Tranum-Jensen, J., 1991. Complement lysis: a hole is a hole. *Immunol. Today* 12, 318–320. [https://doi.org/10.1016/0167-5699\(91\)90007-G](https://doi.org/10.1016/0167-5699(91)90007-G)
- Bhattacharyya, A., Chattopadhyay, R., Mitra, S., Crowe, S.E., 2014. Oxidative Stress: An Essential Factor in the Pathogenesis of Gastrointestinal Mucosal Diseases. *Physiol. Rev.* 94, 329–354. <https://doi.org/10.1152/physrev.00040.2012>
- Birben, E., Sahiner, U.M., Sackesen, C., Erzurum, S., Kalayci, O., 2012. Oxidative Stress and Antioxidant Defense. *World Allergy Organ. J.* 5, 9–19. <https://doi.org/10.1097/WOX.0b013e3182439613>
- Blom, A.M., Kask, L., Dahlbäck, B., 2003. CCP1-4 of the C4b-binding protein α -chain are required for factor I mediated cleavage of complement factor C3b. *Mol. Immunol.* 39, 547–556. [https://doi.org/10.1016/S0161-5890\(02\)00213-4](https://doi.org/10.1016/S0161-5890(02)00213-4)
- Brannen, C.L., Sodetz, J.M., 2007. Incorporation of human complement C8 into the membrane attack complex is mediated by a binding site located within the C8 β MACPF domain. *Mol. Immunol.* 44, 960–965. <https://doi.org/10.1016/j.molimm.2006.03.012>
- Carroll, M.C., Isenman, D.E., 2012. Regulation of Humoral Immunity by Complement. *Immunity* 37, 199–207. <https://doi.org/10.1016/J.IMMUNI.2012.08.002>
- Catton, W.T., 2012. Blood Cell Formation in Certain Teleost Fishes. *Blood* 6, 39–60.
- Chang, C.H., Jang-Liaw, N.H., Lin, Y.S., Fang, Y.C., Shao, K.T., 2013. Authenticating the use of dried seahorses in the traditional Chinese medicine market in Taiwan using molecular forensics. *J. Food Drug Anal.* 21, 310–316. <https://doi.org/10.1016/j.jfda.2013.07.010>
- Cheng, S., Li, C., Wang, Y., Yang, L., Chang, Y., 2016. Characterization and expression analysis of a thioredoxin-like protein gene in the sea cucumber *Apostichopus japonicus*. *Fish Shellfish Immunol.* 58, 165–173. <https://doi.org/10.1016/j.fsi.2016.08.061>
- Chondrou, M.P., Mastellos, D., Zarkadis, I.K., 2006. cDNA cloning and phylogenetic analysis of the sixth complement component in rainbow trout. *Mol. Immunol.* 43, 1080–1087. <https://doi.org/10.1016/j.molimm.2005.07.036>
- Cintra, L.C., Domingos, F.C., Lima, Y.A.R., Barbosa, M.S., Santos, R.S., Faria, F.P., Jesuino, R.S.A., 2017. Molecular cloning, expression and insulin reduction activity of a thioredoxin 1 homologue (TRX1) from the pathogenic fungus *Paracoccidioides lutzii*. *Int. J. Biol. Macromol.* 103, 683–691. <https://doi.org/10.1016/j.ijbiomac.2017.05.114>
- Circu, M.L., Aw, T.Y., 2010. Reactive oxygen species, cellular redox systems, and apoptosis. *Free Radic. Biol. Med.* 48, 749–762. <https://doi.org/10.1016/j.freeradbiomed.2009.12.022>
- Collins, H.L., Bancroft, G.J., 1992. Cytokine enhancement of complement-dependent phagocytosis by macrophages: synergy of tumor necrosis factor- α and granulocyte-macrophage colony-stimulating factor for phagocytosis of *Cryptococcus neoformans*. *Eur. J. Immunol.* 22, 1447–1454. <https://doi.org/10.1002/eji.1830220617>
- Dejian Huang, *, †, Boxin Ou, § and, Prior#, R.L., 2005. The Chemistry behind Antioxidant

Capacity Assays. <https://doi.org/10.1021/JF030723C>

- Di Cicco, E., Paradis, E., Stephen, C., Turba, M.E., Rossi, G., 2013. SCUTICOCILIATID CILIATE OUTBREAK IN AUSTRALIAN POT-BELLIED SEAHORSE, *HIPPOCAMPUS ABDOMINALIS* (LESSON, 1827): CLINICAL SIGNS, HISTOPATHOLOGIC FINDINGS, AND TREATMENT WITH METRONIDAZOLE. *J. Zoo Wildl. Med.* 44, 435–440. <https://doi.org/10.1638/2012-127R1.1>
- FERNANDO, M.R., NANRI, H., YOSHITAKE, S., NAGATA-KUNO, K., MINAKAMI, S., 1992. Thioredoxin regenerates proteins inactivated by oxidative stress in endothelial cells. *Eur. J. Biochem.* 209, 917–922. <https://doi.org/10.1111/j.1432-1033.1992.tb17363.x>
- Filho, D.W., 2007. Reactive oxygen species, antioxidants and fish mitochondria. *Front. Biosci.* 12, 1229. <https://doi.org/10.2741/2141>
- Foey, A., Picchietti, S., 2014. Immune Defences of Teleost Fish, in: *Aquaculture Nutrition*. John Wiley & Sons, Ltd, Chichester, UK, pp. 14–52. <https://doi.org/10.1002/9781118897263.ch2>
- Forn-Cuní, G., Varela, M., Pereiro, P., Novoa, B., Figueras, A., 2017. Conserved gene regulation during acute inflammation between zebrafish and mammals. *Sci. Rep.* 7. <https://doi.org/10.1038/SREP41905>
- Fortier, M.-E., 2004. The viral mimic, polyinosinic:polycytidylic acid, induces fever in rats via an interleukin-1-dependent mechanism. *AJP Regul. Integr. Comp. Physiol.* 287, R759–R766. <https://doi.org/10.1152/ajpregu.00293.2004>
- Fujita, T., Matsushita, M., Endo, Y., 2004. The lectin-complement pathway - Its role in innate immunity and evolution. *Immunol. Rev.* 198, 185–202. <https://doi.org/10.1111/j.0105-2896.2004.0123.x>
- Gao, B., Jeong, W. Il, Tian, Z., 2008. Liver: An organ with predominant innate immunity. *Hepatology* 47, 729–736. <https://doi.org/10.1002/hep.22034>
- Gasque, P., 2004. Complement: A unique innate immune sensor for danger signals. *Mol. Immunol.* <https://doi.org/10.1016/j.molimm.2004.06.011>
- Ghaffari, S., 2008. Oxidative Stress in the Regulation of Normal and Neoplastic Hematopoiesis. *Antioxid. Redox Signal.* 10, 1923–1940. <https://doi.org/10.1089/ars.2008.2142>
- Gleason, F.K., Holmgren, A., 1988. Thioredoxin and related proteins in procaryotes. *FEMS Microbiol. Lett.* 54, 271–297. [https://doi.org/10.1016/0378-1097\(88\)90247-9](https://doi.org/10.1016/0378-1097(88)90247-9)
- Glickman, M.H., Ciechanover, A., 2002. The Ubiquitin-Proteasome Proteolytic Pathway: Destruction for the Sake of Construction. *Physiol. Rev.* 82, 373–428. <https://doi.org/10.1152/physrev.00027.2001>
- Goroncy, A.K., Koshiba, S., Tochio, N., Tomizawa, T., Inoue, M., Tanaka, A., Sugano, S., Kigawa, T., Yokoyama, S., 2010. Solution structure of the C-terminal DUF I000 domain of the human thioredoxin-like 1 protein. *Proteins Struct. Funct. Bioinforma.* 78, 2176–2180. <https://doi.org/10.1002/prot.22719>
- Guo, B., Wu, C., Lv, Z., Liu, C., 2016. Characterisation and expression analysis of two

- terminal complement components: C7 and C9 from large yellow croaker, *Larimichthys crocea*. *Fish Shellfish Immunol.* 51, 211–219. <https://doi.org/10.1016/j.fsi.2016.01.015>
- Guo, N.H., Krutzsch, H.C., Inman, J.K., Roberts, D.D., 1997. Thrombospondin 1 and type I repeat peptides of thrombospondin 1 specifically induce apoptosis of endothelial cells. *Cancer Res.* 57, 1735–1742.
- Haag, E.S., Sly, B.J., Andrews, M.E., Raff, R.A., 1999. Apexrin, a novel extracellular protein associated with larval ectoderm evolution in *Heliocidaris erythrogramma*. *Dev. Biol.* 211, 77–87. <https://doi.org/10.1006/dbio.1999.9283>
- Hippocampus* spp (Seahorses) | CITES [WWW Document], n.d. URL <https://cites.org/eng/taxonomy/term/331> (accessed 3.31.18).
- Hirota, K., Nakamura, H., Masutani, H., Yodoi, J., 2002. Thioredoxin superfamily and thioredoxin-inducing agents. *Ann. N. Y. Acad. Sci.* 957, 189–199. <https://doi.org/10.1111/j.1749-6632.2002.tb02916.x>
- Hoffmann, J.A., Kafatos, F.C., Janeway, C.A., Ezekowitz, R.A.B., 1999. Phylogenetic perspectives in innate immunity. *Science* (80-.). 284, 1313–1318. <https://doi.org/10.1126/science.284.5418.1313>
- Hofsteenge, J., Blommers, M., Hess, D., Furmanek, A., Miroshnichenko, O., 1999. The four terminal components of the complement system are C-mannosylated on multiple tryptophan residues. *J. Biol. Chem.* 274, 32786–32794. <https://doi.org/10.1074/jbc.274.46.32786>
- Holmgren, A., 1995. Thioredoxin structure and mechanism: conformational changes on oxidation of the active-site sulfhydryls to a disulfide. *Structure* 3, 239–243. [https://doi.org/10.1016/S0969-2126\(01\)00153-8](https://doi.org/10.1016/S0969-2126(01)00153-8)
- Holmgren, A., 1985. Thioredoxin. *Annu. Rev. Biochem.* 54, 237–271. <https://doi.org/10.1146/annurev.bi.54.070185.001321>
- Holmgren, A., 1979. Thioredoxin catalyzes the reduction of insulin disulfides by dithiothreitol and dihydrolipoamide. *J. Biol. Chem.* 254, 9627–9632. <https://doi.org/10.1079>
- Holmgren, A., Bjornstedt, M., 1995. Thioredoxin and thioredoxin reductase. *Methods Enzymol.* 252, 199–208. [https://doi.org/10.1016/0076-6879\(95\)52023-6](https://doi.org/10.1016/0076-6879(95)52023-6)
- Ihara, Y., Inai, Y., Ikezaki, M., 2011. Protein C-Mannosylation and Its Prospective Functions in the Cell. *Trends Glycosci. Glycotechnol.* 23, 1–13. <https://doi.org/10.4052/tigg.23.1>
- Imperiali, B., O'Connor, S.E., 1999. Effect of N-linked glycosylation on glycopeptide and glycoprotein structure. *Curr. Opin. Chem. Biol.* 3, 643–649. [https://doi.org/10.1016/S1367-5931\(99\)00021-6](https://doi.org/10.1016/S1367-5931(99)00021-6)
- Iruela-Arispe, M.L., Lombardo, M., Krutzsch, H.C., Lawler, J., Roberts, D.D., 1999. Inhibition of angiogenesis by thrombospondin-1 is mediated by 2 independent regions within the type 1 repeats. *Circulation* 100, 1423–1431. <https://doi.org/10.1161/01.CIR.100.13.1423>
- J., B., 2012. The Role of Glycosylation in Receptor Signaling, in: *Glycosylation*. InTech, pp. 273–286. <https://doi.org/10.5772/50262>

- Jeong, W., Chang, T.S., Boja, E.S., Fales, H.M., Rhee, S.G., 2004. Roles of TRP14, a Thioredoxin-related Protein in Tumor Necrosis Factor- α Signaling Pathways. *J. Biol. Chem.* 279, 3151–3159. <https://doi.org/10.1074/jbc.M307959200>
- Jo, E., Elvitigala, D.A.S., Wan, Q., Oh, M., Oh, C., Lee, J., 2017. Identification and molecular profiling of DC-SIGN-like from big belly seahorse (*Hippocampus abdominalis*) inferring its potential relevancy in host immunity. *Dev. Comp. Immunol.* 77, 270–279. <https://doi.org/10.1016/j.dci.2017.08.017>
- Johansen Needham, J.R., Colquhoun, D.J., R., 2006. Guidelines for health and welfare monitoring of fish used in research. *Lab. Anim.* 40, 323–340.
- Kaiser, K., Camargo, N., Coppens, I., Morrisey, J.M., Vaidya, A.B., Kappe, S.H.I., 2004. A member of a conserved Plasmodium protein family with membrane-attack complex/perforin (MACPF)-like domains localizes to the micronemes of sporozoites. *Mol. Biochem. Parasitol.* 133, 15–26. <https://doi.org/10.1016/j.molbiopara.2003.08.009>
- Kazantzi, A., Sfyroera, G., Holland, M.C.H., Lambris, J.D., Zarkadis, I.K., 2003. Molecular cloning of the β subunit of complement component eight of rainbow trout. *Dev. Comp. Immunol.* 27, 167–174. [https://doi.org/10.1016/S0145-305X\(02\)00092-7](https://doi.org/10.1016/S0145-305X(02)00092-7)
- Kern, R., Malki, A., Holmgren, A., Richarme, G., 2003. Chaperone properties of *Escherichia coli* thioredoxin and thioredoxin reductase. *Biochem. J.* 371, 965–972. <https://doi.org/10.1042/bj20030093>
- Ki, T., Hade, T.S., Mamai, U.W.E., Nter, G., Brade, H., Loepno, H., Pava, F.O.D.I., 1994. activity endotoxin : mOle ..: ar ships of struetui to and fction ; LOM. *FASEB J.* 8, 217–225.
- Kimura, A., Nonaka, M., 2009. Molecular cloning of the terminal complement components C6 and C8 β of cartilaginous fish. *Fish Shellfish Immunol.* 27, 768–772. <https://doi.org/10.1016/j.fsi.2009.08.008>
- Klerk, N. de, 2009. Evasion of the terminal complement pathway by human pathogens. Master thesis.
- Kozlov, G., Määttänen, P., Thomas, D.Y., Gehring, K., 2010. A structural overview of the PDI family of proteins. *FEBS J.* 277, 3924–3936. <https://doi.org/10.1111/j.1742-4658.2010.07793.x>
- Kumar, S., Stecher, G., Tamura, K., 2016. MEGA7: Molecular Evolutionary Genetics Analysis Version 7.0 for Bigger Datasets. *Mol. Biol. Evol.* 33, 1870–1874. <https://doi.org/10.1093/molbev/msw054>
- Kümin, A., Huber, C., Rüllicke, T., Wolf, E., Werner, S., 2006. Peroxiredoxin 6 is a potent cytoprotective enzyme in the epidermis. *Am. J. Pathol.* 169, 1194–1205. <https://doi.org/10.2353/ajpath.2006.060119>
- Landino, L.M., Skreslet, T.E., Alston, J.A., 2004. Cysteine oxidation of tau and microtubule-associated protein-2 by peroxynitrite: Modulation of microtubule assembly kinetics by the thioredoxin reductase system. *J. Biol. Chem.* 279, 35101–35105. <https://doi.org/10.1074/jbc.M405471200>
- Li, F., Ma, L., Zhang, H., Xu, L., Zhu, Q., 2017. A thioredoxin from antarctic microcrustacean (*Euphausia superba*): Cloning and functional characterization. *Fish*

- Shellfish Immunol. 63, 376–383. <https://doi.org/10.1016/j.fsi.2017.02.035>
- Liu, W., Jiang, L., Dong, X., Liu, X., Kang, L., Wu, C., 2016. Molecular characterization and expression analysis of the large yellow croaker (*Larimichthys crocea*) complement component C6 after bacteria challenge. *Aquaculture* 458, 107–112. <https://doi.org/10.1016/j.aquaculture.2016.03.003>
- Liu, W., Xie, Y., Ma, J., Luo, X., Nie, P., Zuo, Z., Lahrmann, U., Zhao, Q., Zheng, Y., Zhao, Y., Xue, Y., Ren, J., 2015. IBS: An illustrator for the presentation and visualization of biological sequences. *Bioinformatics* 31, 3359–3361. <https://doi.org/10.1093/bioinformatics/btv362>
- Livak, K.J., Schmittgen, T.D., 2001. Analysis of relative gene expression data using real-time quantitative PCR and the 2- $\Delta\Delta$ CT method. *Methods* 25, 402–408. <https://doi.org/10.1006/meth.2001.1262>
- Lovelace, L.L., Cooper, C.L., Sodetz, J.M., Lebioda, L., 2011. Structure of human C8 protein provides mechanistic insight into membrane pore formation by complement. *J. Biol. Chem.* 286, 17585–17592. <https://doi.org/10.1074/jbc.M111.219766>
- Lubbers, R., van Essen, M.F., van Kooten, C., Trouw, L.A., 2017. Production of complement components by cells of the immune system. *Clin. Exp. Immunol.* 188, 183–194. <https://doi.org/10.1111/cei.12952>
- Mah, S.A., Moy, G.W., Swanson, W.J., Vacquier, V.D., 2004. A perforin-like protein from a marine mollusk. *Biochem. Biophys. Res. Commun.* 316, 468–475. <https://doi.org/10.1016/j.bbrc.2004.02.073>
- Markiewski, M.M., DeAngelis, R.A., Strey, C.W., Foukas, P.G., Gerard, C., Gerard, N., Wetsel, R.A., Lambris, J.D., 2009. The Regulation of Liver Cell Survival by Complement. *J. Immunol.* 182, 5412–5418. <https://doi.org/10.4049/jimmunol.0804179>
- Meister, A., 1981. Metabolism and functions of glutathione. *Trends Biochem. Sci.* 6, 231–234. [https://doi.org/10.1016/0968-0004\(81\)90084-0](https://doi.org/10.1016/0968-0004(81)90084-0)
- Messens, J., Silver, S., 2006. Arsenate Reduction: Thiol Cascade Chemistry with Convergent Evolution. *J. Mol. Biol.* 362, 1–17. <https://doi.org/10.1016/j.jmb.2006.07.002>
- Mills, G.C., 1957. HEMOGLOBIN CATABOLISM. *J. Biol. Chem.* 229, 189–197.
- Miranda-Vizuete, A., Damdimopoulos, A.E., Gustafsson, J.-Å., Spyrou, G., 1997. Cloning, Expression, and Characterization of a Novel *Escherichia coli* Thioredoxin. *J. Biol. Chem.* 272, 30841–30847. <https://doi.org/10.1074/jbc.272.49.30841>
- Miseta, A., Csutora, P., 2000. Relationship between the occurrence of cysteine in proteins and the complexity of organisms. *Mol. Biol. Evol.* 17, 1232–1239. <https://doi.org/10.1093/oxfordjournals.molbev.a026406>
- Mondragón-Palomino, M., Piñero, D., Nicholson-Weller, A., Lacleste, J.P., 1999. Phylogenetic analysis of the homologous proteins of the terminal complement complex supports the emergence of C6 and C7 followed by C8 and C9. *J. Mol. Evol.* 49, 282–289. <https://doi.org/10.1007/PL00006550>
- Morgan, B.P., Marchbank, K.J., Longhi, M.P., Harris, C.L., Gallimore, A.M., 2005. Complement: Central to innate immunity and bridging to adaptive responses, in:

- Immunology Letters. Elsevier, pp. 171–179. <https://doi.org/10.1016/j.imlet.2004.11.010>
- Morita-Yamamuro, C., Tsutsui, T., Sato, M., Yoshioka, H., Tamaoki, M., Ogawa, D., Matsuura, H., Yoshihara, T., Ikeda, A., Uyeda, I., Yamaguchi, J., 2005. The Arabidopsis gene CAD1 controls programmed cell death in the plant immune system and encodes a protein containing a MACPF domain. *Plant Cell Physiol.* 46, 902–912. <https://doi.org/10.1093/pcp/pci095>
- Mutsuro, J., Tanaka, N., Kato, Y., Dodds, A.W., Yano, T., Nakao, M., 2005. Two Divergent Isotypes of the Fourth Complement Component from a Bony Fish, the Common Carp (*Cyprinus carpio*). *J. Immunol.* 175, 4508–4517. <https://doi.org/10.4049/jimmunol.175.7.4508>
- Nakamura, H., 2005. Thioredoxin and its related molecules: update 2005. *Antioxid. Redox Signal.* 7, 823–828. <https://doi.org/10.1089/ars.2005.7.823>
- Nakamura, T., Nakamura, H., Hoshino, T., Ueda, S., Wada, H., Yodoi, J., 2005. Redox Regulation of Lung Inflammation by Thioredoxin. *Antioxid. Redox Signal.* 7, 60–71. <https://doi.org/10.1089/ars.2005.7.60>
- Nikapitiya, C., De Zoysa, M., Whang, I., Kim, C.G., Lee, Y.H., Kim, S.J., Lee, J., 2009. Molecular cloning, characterization and expression analysis of peroxiredoxin 6 from disk abalone *Haliotis discus discus* and the antioxidant activity of its recombinant protein. *Fish Shellfish Immunol.* 27, 239–249. <https://doi.org/10.1016/j.fsi.2009.05.002>
- Nonaka, M., 2014. Evolution of the complement system. *Subcell. Biochem.* 80, 31–43. https://doi.org/10.1007/978-94-017-8881-6_3
- Nonaka, M., 2011. The complement C3 protein family in invertebrates. *ISJ-Invertebrate Surviv. J.* 8, 21–32.
- Oh, M., Umasuthan, N., Elvitigala, D.A.S., Wan, Q., Jo, E., Ko, J., Noh, G.E., Shin, S., Rho, S., Lee, J., 2016. First comparative characterization of three distinct ferritin subunits from a teleost: Evidence for immune-responsive mRNA expression and iron depriving activity of seahorse (*Hippocampus abdominalis*) ferritins. *Fish Shellfish Immunol.* 49, 450–460. <https://doi.org/10.1016/j.fsi.2015.12.039>
- Pacitti, D., Wang, T., Martin, S.A.M., Sweetman, J., Secombes, C.J., 2014. Insights into the fish thioredoxin system: Expression profile of thioredoxin and thioredoxin reductase in rainbow trout (*Oncorhynchus mykiss*) during infection and in vitro stimulation. *Dev. Comp. Immunol.* 42, 261–277. <https://doi.org/10.1016/j.dci.2013.09.013>
- Pandey, K.B., Rizvi, S.I., 2011. Biomarkers of oxidative stress in red blood cells. *Biomed. Pap.* 155, 131–136. <https://doi.org/10.5507/bp.2011.027>
- Park, S. Bin, Aoki, T., Jung, T.S., 2012. Pathogenesis of and strategies for preventing *Edwardsiella tarda* infection in fish. *Vet. Res.* 43, 67. <https://doi.org/10.1186/1297-9716-43-67>
- Plumb, M.E., Sodetz, J.M., 2000. An indel within the C8 α subunit of human complement C8 mediates intracellular binding of C8 γ and formation of C8 α - γ . *Biochemistry* 39, 13078–13083. <https://doi.org/10.1021/bi001451z>
- Ponting, C.P., 1999. Chlamydial homologues of the MACPF (MAC / perforin) domain. *Curr. Biol.* 9, 911–913. [https://doi.org/10.1016/S0960-9822\(00\)80102-5](https://doi.org/10.1016/S0960-9822(00)80102-5)

- Press, C.M., Evensen, Ø., 1999. The morphology of the immune system in teleost fishes. *Fish Shellfish Immunol.* 9, 309–318. <https://doi.org/10.1006/FSIM.1998.0181>
- Priyathilaka, T.T., Oh, M., Bathige, S.D.N.K., De Zoysa, M., Lee, J., 2017. Two distinct CXC chemokine receptors (CXCR3 and CXCR4) from the big-belly seahorse *Hippocampus abdominalis*: Molecular perspectives and immune defensive role upon pathogenic stress. *Fish Shellfish Immunol.* 65, 59–70. <https://doi.org/10.1016/j.fsi.2017.03.038>
- Qi, S., Zhao, B., Zhou, B., Jiang, X., 2017. An electrochemical immunosensor based on pristine graphene for rapid determination of ractopamine. *Chem. Phys. Lett.* 685, 146–150. <https://doi.org/10.1016/j.cplett.2017.07.055>
- Qin, C., Shao, T., Zhao, D., Duan, H., Wen, Z., Yuan, D., Li, H., Qi, Z., 2017. Effect of ammonia-N and pathogen challenge on complement component 8α and 8β expression in the darkbarbel catfish *Pelteobagrus vachellii*. *Fish Shellfish Immunol.* 62, 107–115. <https://doi.org/10.1016/j.fsi.2016.12.031>
- Quan, S., Schneider, I., Pan, J., Von Hacht, A., Bardwell, J.C.A., 2007. The CXXC motif is more than a redox rheostat. *J. Biol. Chem.* 282, 28823–28833. <https://doi.org/10.1074/jbc.M705291200>
- Ranganathan, S., Wongsai, S., Nevalainen, K.M.H., 2006. Comparative Genomic Analysis of Glycoylation Pathways in Yeast, Plants and Higher eukaryotes. *Appl. Mycol. Biotechnol.* 6, 227–248. [https://doi.org/10.1016/S1874-5334\(06\)80013-4](https://doi.org/10.1016/S1874-5334(06)80013-4)
- Ravi, D., Muniyappa, H., Das, K.C., 2005. Endogenous thioredoxin is required for redox cycling of anthracyclines and p53-dependent apoptosis in cancer cells. *J. Biol. Chem.* 280, 40084–40096. <https://doi.org/10.1074/jbc.M507192200>
- Reid, K.B.M., Day, A.J., 1989. Structure-function relationships of the complement components. *Immunol. Today* 10, 177–180. [https://doi.org/10.1016/0167-5699\(89\)90317-4](https://doi.org/10.1016/0167-5699(89)90317-4)
- Ren, G., Stephan, D., Xu, Z., Zheng, Y., Tang, D., Harrison, R.S., Kurz, M., Jarott, R., Shouldice, S.R., Hiniker, A., Martin, J.L., Heras, B., Bardwell, J.C.A., 2009. Properties of the thioredoxin fold superfamily are modulated by a single amino acid residue. *J. Biol. Chem.* 284, 10150–10159. <https://doi.org/10.1074/jbc.M809509200>
- Roberts, R.J., Ellis, A.E., 2012. The Anatomy and Physiology of Teleosts, in: *Fish Pathology: Fourth Edition*. Wiley-Blackwell, Oxford, UK, pp. 17–61. <https://doi.org/10.1002/9781118222942.ch2>
- Saitoh, M., Nishitoh, H., Fujii, M., Takeda, K., Tobiume, K., Sawada, Y., Kawabata, M., Miyazono, K., Ichijo, H., 1998. Mammalian thioredoxin is a direct inhibitor of apoptosis signal-regulating kinase (ASK) 1. *EMBO J.* 17, 2596–2606. <https://doi.org/10.1093/emboj/17.9.2596>
- Sanchez-Gallego, J.I., Groeneveld, T.W.L., Krentz, S., Nilsson, S.C., Villoutreix, B.O., Blom, A.M., 2012. Analysis of Binding Sites on Complement Factor I Using Artificial N-Linked Glycosylation. *J. Biol. Chem.* 287, 13572–13583. <https://doi.org/10.1074/jbc.M111.326298>
- Sarin, R., Sharma, Y.D., 2006. Thioredoxin system in obligate anaerobe *Desulfovibrio*

- desulfuricans: Identification and characterization of a novel thioredoxin 2. *Gene* 376, 107–115. <https://doi.org/10.1016/j.gene.2006.02.012>
- Sattler, M., Winkler, T., Verma, S., Byrne, C.H., Shrikhande, G., Salgia, R., Griffin, J.D., 1999. Hematopoietic growth factors signal through the formation of reactive oxygen species. *Blood* 93, 2928–2935.
- Sebaugh, J.L., 2011. Guidelines for accurate EC50/IC50 estimation. *Pharm. Stat.* 10, 128–134. <https://doi.org/10.1002/pst.426>
- Shen, Y., Zhang, J., Xu, X., Fu, J., Li, J., 2012a. Expression of complement component C7 and involvement in innate immune responses to bacteria in grass carp. *Fish Shellfish Immunol.* 33, 448–454. <https://doi.org/10.1016/j.fsi.2012.05.016>
- Shen, Y., Zhang, J., Xu, X., Fu, J., Liu, F., Li, J., 2012b. Molecular cloning, characterization and expression of the complement component Bf/C2 gene in grass carp. *Fish Shellfish Immunol.* 32, 789–795. <https://doi.org/10.1016/j.fsi.2012.01.032>
- Shinkai, Y., 1989. Structure and function of perforin, in: *Seikagaku. The Journal of Japanese Biochemical Society*. Springer, Berlin, Heidelberg, pp. 709–712. https://doi.org/10.1007/978-3-642-73911-8_2
- Shinkai, Y., Takio, K., Okumura, K., 1988. Homology of perforin to the ninth component of complement (C9). *Nature* 334, 525–527. <https://doi.org/10.1038/334525a0>
- Song, J., 2005. Solution structure of At3g04780.1-des15, an Arabidopsis thaliana ortholog of the C-terminal domain of human thioredoxin-like protein. *Protein Sci.* 14, 1059–1063. <https://doi.org/10.1110/ps.041246805>
- Sun, Y., Wang, R., Xu, T., 2013. Conserved structural complement component C3 in miiuy croaker *Miichthys miiuy* and their involvement in pathogenic bacteria induced immunity. *Fish Shellfish Immunol.* 35, 184–187. <https://doi.org/10.1016/j.fsi.2013.04.028>
- Tam, K., n.d. Expression Responses of the Complement Components in Zebrafish Organs after Stimulation with Poly I : C , *Mimicry of Viral Infection* 54, 389–395.
- Tegla, C.A., Cudrici, C., Patel, S., Trippe, R., Rus, V., Niculescu, F., Rus, H., 2011. Membrane attack by complement: The assembly and biology of terminal complement complexes. *Immunol. Res.* 51, 45–60. <https://doi.org/10.1007/s12026-011-8239-5>
- Tschopp, J., 1984. Ultrastructure of the membrane attack complex of complement. Heterogeneity of the complex caused by different degree of C9 polymerization. *J. Biol. Chem.* 259, 7857–7863. <https://doi.org/10.1146/annurev.iy.04.040186.002443>
- Uemura, T., Yano, T., Shiraishi, H., Nakao, M., 1996. Purification and characterization of the eighth and ninth components of carp complement. *Mol. Immunol.* 33, 925–932. [https://doi.org/10.1016/S0161-5890\(96\)00054-5](https://doi.org/10.1016/S0161-5890(96)00054-5)
- Vendrell, D., Balcázar, J.L., Ruiz-Zarzuola, I., de Blas, I., Gironés, O., Múzquiz, J.L., 2006. *Lactococcus garvieae* in fish: A review. *Comp. Immunol. Microbiol. Infect. Dis.* 29, 177–198. <https://doi.org/10.1016/J.CIMID.2006.06.003>
- Vincent, A.C.J., Clifton-Hadley, R.S., 1989. Parasitic Infection of the Seahorse (*Hippocampus erectus*)— A Case Report. *J. Wildl. Dis.* 25, 404–406.

<https://doi.org/10.7589/0090-3558-25.3.404>

- Vincent, A.C.J., Foster, S.J., Koldewey, H.J., 2011. Conservation and management of seahorses and other Syngnathidae. *J. Fish Biol.* 78, 1681–1724. <https://doi.org/10.1111/j.1095-8649.2011.03003.x>
- Wahid, H., Ahmad, S., Nor, M.A.M., Rashid, M.A., 2017. Prestasi kecekapan pengurusan kewangan dan agihan zakat: perbandingan antara majlis agama islam negeri di Malaysia. *J. Ekon. Malaysia* 51, 39–54. <https://doi.org/10.1017/CBO9781107415324.004>
- Wang, L., Guo, H., zhang, N., Ma, Z., Jiang, S., Zhang, D., 2015. Thioredoxin of golden pompano involved in the immune response to *Photobacterium damsela*. *Fish Shellfish Immunol.* 45, 808–816. <https://doi.org/10.1016/j.fsi.2015.05.044>
- Wang, Q., Ning, X., Chen, L., Pei, D., Zhao, J., Zhang, L., Liu, X., Wu, H., 2011. Responses of thioredoxin 1 and thioredoxin-related protein 14 mRNAs to cadmium and copper stresses in *Venerupis philippinarum*. *Comp. Biochem. Physiol. - C Toxicol. Pharmacol.* 154, 154–160. <https://doi.org/10.1016/j.cbpc.2011.04.009>
- Wang, Y., Xu, S., Su, Y., Ye, B., Hua, Z., 2013. Molecular characterization and expression analysis of complement component C9 gene in the whitespotted bambooshark, *Chiloscyllium plagiosum*. *Fish Shellfish Immunol.* 35, 599–606. <https://doi.org/10.1016/j.fsi.2013.04.042>
- Wei, W., Wu, H., Xu, H., Xu, T., Zhang, X., Chang, K., Zhang, Y., 2009. Cloning and molecular characterization of two complement Bf/C2 genes in large yellow croaker (*Pseudosciaena crocea*). *Fish Shellfish Immunol.* 27, 285–295. <https://doi.org/10.1016/j.fsi.2009.05.011>
- Weinstein, M.R., Litt, M., Kertesz, D.A., Wyper, P., Rose, D., Coulter, M., McGeer, A., Facklam, R., Ostach, C., Willey, B.M., Borczyk, A., Low, D.E., 1997. Invasive Infections Due to a Fish Pathogen, *Streptococcus iniae*. *N. Engl. J. Med.* 337, 589–594. <https://doi.org/10.1056/NEJM199708283370902>
- Wetsel, R.A., 1995. Structure, function and cellular expression of complement anaphylatoxin receptors. *Curr. Opin. Immunol.* 7, 48–53. [https://doi.org/10.1016/0952-7915\(95\)80028-X](https://doi.org/10.1016/0952-7915(95)80028-X)
- Wickramaarachchi, W.D.N., Wan, Q., Lee, Y., Lim, B.S., De Zoysa, M., Oh, M.J., Jung, S.J., Kim, H.C., Whang, I., Lee, J., 2012. Genomic characterization and expression analysis of complement component 9 in rock bream (*Oplegnathus fasciatus*). *Fish Shellfish Immunol.* 33, 707–717. <https://doi.org/10.1016/j.fsi.2012.06.019>
- Wickramaarachchi, W.D.N., Whang, I., Kim, E., Lim, B.S., Jeong, H.B., De Zoysa, M., Oh, M.J., Jung, S.J., Yeo, S.Y., Yeon Kim, S., Park, H.C., Lee, J., 2013a. Genomic characterization and transcriptional evidence for the involvement of complement component 7 in immune response of rock bream (*Oplegnathus fasciatus*). *Dev. Comp. Immunol.* 41, 44–49. <https://doi.org/10.1016/j.dci.2013.04.007>
- Wickramaarachchi, W.D.N., Whang, I., Wan, Q., Bathige, S.D.N.K., De Zoysa, M., Lim, B.S., Yeo, S.Y., Park, M.A., Lee, J., 2013b. Genomic characterization and expression analysis of complement component 8 α and 8 β in rock bream (*Oplegnathus fasciatus*). *Dev. Comp. Immunol.* 39, 279–292. <https://doi.org/10.1016/j.dci.2012.09.005>

- Witzel-Schlömp, K., Rittner, C., Schneider, P.M., 2001. The human complement C9 gene: structural analysis of the 5' gene region and genetic polymorphism studies. *Eur. J. Immunogenet.* 28, 515–522. <https://doi.org/10.1046/j.0960-7420.2001.00248.x>
- Woo, J.R., Kim, S.J., Jeong, W., Cho, Y.H., Lee, S.C., Chung, Y.J., Rhee, S.G., Ryu, S.E., 2004. Structural basis of cellular redox regulation by human TRP14. *J. Biol. Chem.* 279, 48120–48125. <https://doi.org/10.1074/jbc.M407079200>
- Wu, N., Song, Y.L., Wang, B., Zhang, X.Y., Zhang, X.J., Wang, Y.L., Cheng, Y.Y., Chen, D.D., Xia, X.Q., Lu, Y.S., Zhang, Y.A., 2016. Fish gut-liver immunity during homeostasis or inflammation revealed by integrative transcriptome and proteome studies. *Sci. Rep.* 6, 36048. <https://doi.org/10.1038/srep36048>
- Würzner, R., 2000. Modulation of complement membrane attack by local C7 synthesis. *Clin. Exp. Immunol.* 121, 8–10. <https://doi.org/10.1046/j.1365-2249.2000.01263.x>
- Xu, Y., Yu, Y., Zhang, X., Huang, Z., Li, H., Dong, S., Liu, Y., Dong, F., Xu, Z., 2018. Molecular characterization and expression analysis of complement component 3 in dojo loach (*Misgurnus anguillicaudatus*). *Fish Shellfish Immunol.* 72, 484–493. <https://doi.org/10.1016/j.fsi.2017.11.022>
- Yamamoto, T., Davis, C.G., Brown, M.S., Schneider, W.J., Casey, M.L., Goldstein, J.L., Russell, D.W., 1984. The human LDL receptor: A cysteine-rich protein with multiple Alu sequences in its mRNA. *Cell* 39, 27–38. [https://doi.org/10.1016/0092-8674\(84\)90188-0](https://doi.org/10.1016/0092-8674(84)90188-0)
- Zarkadis, I.K., Duraj, S., Chondrou, M., 2005. Molecular cloning of the seventh component of complement in rainbow trout. *Dev. Comp. Immunol.* 29, 95–102. <https://doi.org/10.1016/j.dci.2004.06.006>
- Zarkadis, I.K., Sarrias, M.R., Sfyroera, G., Sunyer, J.O., Lambris, J.D., 2001. Cloning and structure of three rainbow trout C3 molecules: A plausible explanation for their functional diversity. *Dev. Comp. Immunol.* 25, 11–24. [https://doi.org/10.1016/S0145-305X\(00\)00039-2](https://doi.org/10.1016/S0145-305X(00)00039-2)
- Zhang, H., Cheng, D., Liu, H., Zheng, H., 2018. Differential responses of a thioredoxin-like protein gene to *Vibrio parahaemolyticus* challenge in the noble scallop *Chlamys nobilis* with different total carotenoids content. *Fish Shellfish Immunol.* 72, 377–382. <https://doi.org/10.1016/j.fsi.2017.11.020>
- Zheng, W.J., Hu, Y.H., Zhang, M., Sun, L., 2010. Analysis of the expression and antioxidative property of a peroxiredoxin 6 from *Scophthalmus maximus*. *Fish Shellfish Immunol.* 29, 305–311. <https://doi.org/10.1016/j.fsi.2010.04.008>
- Zhou, Z., Zhang, B., Sun, L., 2014. Poly(I:C) Induces Antiviral Immune Responses in Japanese Flounder (*Paralichthys olivaceus*) That Require TLR3 and MDA5 and Is Negatively Regulated by Myd88. *PLoS One* 9, e112918. <https://doi.org/10.1371/journal.pone.0112918>